Analysis of Laminated Sediments from Lake DV09, Northern Devon Island, Nunavut, Canada

Colin John Courtney Mustaphi
Master's of Science in Geography candidate

Supervisor:

Dr. Konrad Gajewski
Department of Geography, University of Ottawa

Committee Members:

Dr. Luke Copland
Department of Geography, University of Ottawa

Dr. Mike Sawada
Department of Geography, University of Ottawa

A thesis submitted to the Faculty of Graduate Studies and Postdoctoral Studies in partial fulfillment of the requirements for a Master's of Science in Geography

December 2008

Abstract

A 147cm sediment core from Lake DV09, northern Devon Island, Nunavut, Canada (75° 34’34”N, 89° 18’55”W) contains annually-laminated (varved) sediments, providing a 1600-year record of climate variability. A minerogenic lamina deposited during the annual thaw period and a thin deposit of organic matter deposited during the summer and through the winter, together form a clastic-organic couplet each year. The thinnest varves occur from AD800-1050, and the thickest from AD1100-1300, during the Medieval Warm Period. The relative sediment density is also highest during this period suggesting increased sediment transport energy. The coldest period of the Little Ice Age appears to be during the AD1600s. Varve widths over the past century indicate climate warming in the region.

Document Format and Structure

This document presents the results from the analysis of several sediment cores from Lake DV09, located on northern Devon Island, Canada. It has been divided into 6 chapters, each of which builds upon the previous in order to logically present all of the information. Tables and figures are found at the end of each chapter in the order they appear within the text.

Chapter 1 begins by describing the methods and results of the currently available literature pertaining to studies of varved lake sediments in the Canadian Arctic, and finishes with a detailed geographic description of the study site, Lake DV09.

Chapter 2 details the methods used to obtain and study the sediment cores from the lake.

Chapter 3, entitled "**Post-glacial sedimentology of Lake DV09, northern Devon Island, Nunavut, Canada**" describes the results from the analysis of several sediment cores and is aimed at establishing an overall sediment history of the lake.

Chapter 4, entitled "**A 1600-year climate-proxy record inferred from the annually-laminated sediments of Lake DV09, northern Devon Island, Nunavut, Canada**" investigates the most recent sediment of the stratigraphy, in particular, it aims to describe and interpret the annually-laminated (varved) sequence that has been preserved in the sediments of Core B. The thickness of these varves is then used to infer the paleoclimate of northern Devon Island. The record is then compared to numerous other Arctic proxy and climate records to look at the climate dynamics of the past 1600 years. This chapter was combined with Chapter 3 to form a paper that will be submitted to an academic journal; but in this document they are separated to allow for an extensive description of methods, results and discussion, as well as to establish a stratigraphic context to the varve study.

Chapter 5, "**A preliminary exploration of the red-noise spectra of DV09 varve series in the context of other annual series from northern Canada and Greenland**" appears as a separate chapter. It is an extension of the description of the DV09 varve width series and comparison to other proxy-climate records found in the previous chapter. It is described as a preliminary exploration because interpretation of the results at this time is difficult due to the current lack of an understanding of the fundamental mechanisms and processes that may be causing cyclicity in the records.

Chapter 6 summarizes the discussion from each of the three results chapters (Chapters 3-5) and is followed by a reference list for this document and a series of pertinent appendices, which are referred to in the text.

Acknowledgements

This research program was funded by the Natural Sciences and Engineering Research Council of Canada (NSERC), and the Canadian Foundation for Climate and Atmospheric Sciences (CFCAS). A tuition bursary from Ultramar Inc. also helped in making this research possible. Logistical support was provided by the Polar Continental Shelf Project (PCSP Contribution number 04508).

We thank P.B. Hamilton and T. Malik for help in the field; M. Frappier, C. Prince, M.-C. Roch, B. O'Neil, T. Paull, and J. McGuinness for help in the laboratory; A. Trudel for supervising the x-radiography; and J. Bunbury for ostracode identifications.

A huge thank you to K. Gajewski for supporting and guiding me through the world of academic research, and to my committee members L. Copland and M. Sawada for their helpful suggestions along the way.

I am indebted to all of those who are mentioned throughout the cited works in this paper and I further thank those researchers who have provided me with paleoclimatic datasets.

Of course this would not be possible without the support of my family and friends, and that of the members of the LPC.

Results (1) Post-glacial sedimentology of Lake DV09, northern Devon Island, Nunavut, Canada

Results (2) A 1600-year climate-proxy record inferred from the annually-laminated sediments of Lake DV09, northern Devon Island, Nunavut, Canada

Results (3) A preliminary exploration of the red-noise spectra of DV09 varve series in the context of other annual series from northern Canada and Greenland

List of Figures

List of Tables

List of Equations

List of Appendices

1 Introduction

The purpose of this study is to investigate the sediment history of a small and deep freshwater lake located on the northern coast of Devon Island, Nunavut, Canada (DV09; 75° 34'34"N, 89° 18'55"W), and to examine the relation between climate variability and the depositional characteristics of the sediments. The lake sediments are layered, and the laminations of the uppermost 14cm were shown to be annually laminated (varved), making this site particularly important for paleoclimatic study (Gajewski *et al*, 1997).

The depositional character of sediments reflects variations in hydrological factors, which in turn, are influenced by climate variability at various scales. Because sediments are constantly accumulating on the lake bottom, this information can then be used to produce a paleoclimate reconstruction for the site. Understanding past Arctic climatic trends enables us to place the current climate warming in a longer-term context, which can aid in distinguishing between natural and anthropogenic influences.

The study of natural paleoclimate proxies is important to climate studies of the Canadian Arctic because the instrumental record dates only to the post-World War II period and coverage is quite sparse. By extending the climate record back through time, and obtaining information from new sites not represented by the current climate data, paleoclimate studies aid in understanding regional manifestations of climate variability. A stronger understanding of past climatic conditions can be used to differentiate natural and anthropogenic influences on the climate (Fritts, 1991) and serves future sustainable development by supplying additional environmental data. As humanity continues to focus and intensify activities in cold regions, the importance of understanding these

environments becomes more critical if we wish to conserve and responsibly manage one of Canada's most pristine regions.

1.1 Literature Review

1.1.1 Varved Sediments

Annually-laminated lake sediments (varves) are found in various lakes throughout the world and can be used to create high-resolution climate reconstructions of the late Holocene (Lowe and Walker, 1997; Brauer and Negendank, 2002), and occasionally beyond if found preserved in sedimentary rock strata. Varves are often fine-grained, and are often found in the deep, distal areas of lakes, away from inflows and steep hypsographic gradients that can cause extensive reworking of sediments (Gale and Hoare, 1991). Lake morphometry is an important factor for promoting varve formation and preservation in many lakes worldwide (O'Sullivan, 1983; Saarnisto, 1986). Bioturbation can deteriorate or destroy varves either syndepositionally at the sediment surface, or when animals burrow deeper into the deposited layers. Lakes containing large neustonic and psammonic communities are less likely to develop or retain thin laminations. Therefore, flat-bottomed lakes with low productivity are more likely to preserve thin deposits because of the decreased likelihood of sediment movement (Bradley, 1999).

Varves provide information on the biologic, geochemical, and sedimentological response of lake systems to the seasonal climate cycle. When undisturbed, the sediment record can be used to study the climate variability over longer time periods (Anderson and Dean, 1988), such as thousands of years or more. Variations in the amount and type of sediment accumulated in a lake is in some measure a reflection of the regional climate

variability (Anderson, 1964). This strengthens the usefulness of studying Arctic varved lake sediments because of the strong seasonality in the polar regions.

Varves are often comprised of a couplet of two different sedimentation units (Davis, 1992) although studies involving complex varved sediments, those containing two or more depositional units per year, have also been undertaken (Dean *et al*, 2001; for an example see Hambley and Lamoureux, 2006). The dominant sediment constituents arriving to the lake bottom fluctuate throughout the year in a cyclical pattern due to seasonal changes in hydroclimatic factors (Boggs, 2001). Throughout the sequence, one component of the couplet is deposited under similar conditions to the same unit from the previous year, due to the regularity of seasonal change each year. Thus, each component is a distinct sedimentation unit (Otto, 1938) that is qualitatively repeated in alternation down the sediment record. The biological, chemical, and/or sedimentological properties of the units allow them to be attributed to a specific period of time within a year. For example, a component that is organic-rich may be due to algal blooms that only occur during the spring and summer in arctic lakes, making a seasonal attribution for the unit possible. Following these types of properties, a general descriptive classification for lacustrine varved sediments has been developed.

Each varve represents one sedimentary bed and is often composed of two laminae, which are the two sediment units (a couplet). The repetitive varve sequence forms a bedset (Campbell, 1967). Alternatively, Saarnisto (1986) defines each couplet as a lamination, where varves are a special type, called “annually laminated.” In the study of varved sediments, it is critical that the annual nature of the layering be established as the first step, because nonannual rhythmitic lake deposits could be present.

Anderson and Koopmans (1963) developed a generalised classification of glacial, clastic lake, marine, and evaporite varves, based largely on environmental factors controlling varve formation (Anderson, 1964). Saarnisto (1986) proposed a more detailed classification based on seasonal or rhythmic changes of the biological, chemical, or sedimentological properties within a basin. According to this classification, organic-rich laminations result from seasonal changes in lake productivity, including algal or diatom blooms. Calcareous laminations result from seasonal variations of calcite precipitation from the lake water. Iron-rich laminations result from seasonal changes in the amount of dissolved oxygen available at the water-sediment interface, due, for example, to circulation changes associated with turnover, influencing chemical reactions in lakes where iron-rich sediments are rapidly deposited. Lastly, seasonal variations in mineral matter deposition can form varves, where the type and grain size of the deposited minerogenic sediment varies throughout the seasons. Varves can form in many aquatic environments, although some types of varves may be dominant within some regions. In a given lake, a combination of varving mechanisms may play an important role, which may change or evolve over time.

Sediments consisting of numerous units deposited in one year are known as complex varves (Hambley and Lamoureux, 2006). These subannual laminae or rhythmites are often caused by processes unrelated to the dominant seasonal cycles of deposition, which leads to the formation of varves, and are superimposed within the sediment stratigraphy. Subannual laminae can be identified visually or, for example, through a high-resolution visualization of the particle size distribution down core. Identifiable layers will often have characteristics that can be used to identify them based

upon the grain size and sorting that is exhibited. Once identified, the nonannual "signal" can be removed from the varve chronology, making it still useful for paleoclimatic study (Hambley and Lamoureux, 2006). Sedimentation caused by intense summer rainfall events, mass wasting, subaqueous slumping, sudden changes to the jets or plumes of inflows (Hambley and Lamoureux, 2006), and changes in snowmelt patterns are possible mechanisms for subannual rhythmite formation in varved sediments.

A new and distinct sediment bed is deposited each year in a lake when these sediments are not disturbed, and over time these deposits accrue chronologically, following the stratigraphic Principle of Superposition. This situation can be considered as similar to many trees in temperate regions, which add a new ring of cambial growth each growing season. Incremental dating is used to assess the age of the tree, which is possible by boring a tree core or cutting a cross section. Adapting this method to a varved lake-sediment core permits the construction of a chronology through incremental lamination counting (Zolitschka, 2003). Because the methods of dendrochronology are well established, this similarity warrants the application of dendrochronologic methods to varved lacustrine sediments. Some shared characteristics are 1) having a series of measurable annual increments, where each year is separated by a distinguishable edge, 2) the ability to crossdate sampled cores from within a single site, and 3) the potential to crossdate and relate core records between multiple sampling sites. Crossdating involves matching the annual increment for a given year with the same increment within another core from the same sampling site (Fritts, 1976). This is possible because of similar environmental conditions across the site influencing formation and preservation. Proper crossdating acts as a quality control check on the chronology, helping to identify partial,

missing, or locally absent layers, as well as the identification of nonannual banding or layering (Fritts, 1976). A confident site chronology can be created that will represent the average conditions at the site, and any non-annual layers will be properly identified. This also works to reduce the total dating error of the final chronology. In this study, the application of dendrochronological methods to the varved lake sediment from Lake DV09 aided in constructing a new varve chronology for this lake site that is over ten times longer than the previously published record.

1.1.2 Arctic Varved Lake Sediments as a Paleoclimate Proxy

Studies in Arctic Canada have shown relations between varve width fluctuations and several climate variables, such as spring or summer temperature, precipitation, winter storminess, catchment snowmelt, and others. These relations are based on observations of local and regional controls, as well as comparisons with other instrumental and proxy records (cf. Hardy *et al*, 1996; Lamoureux and Bradley, 1996; Braun *et al*, 2000a; Hughen *et al*, 2000; Lamoureux, 2000; Lamoureux and Gilbert, 2004; Smith *et al*, 2004; Lamoureux *et al*, 2006; Besonen *et al*, 2008). To study the varves, radiometric dating, sedimentologic, dendrochronologic, and digital image analysis techniques were employed, as well as a method for precisely and accurately measuring varve widths. The following summarizes much of the literature covering varved sediments of the Arctic.

Lead-210 dating was used to verify the annual nature of the recent, laminated sediments from Lake C2, Ellesmere Island (Zolitschka, 1996), and multiple cores were successfully crossdated, permitting the creation of a composite sequence (Lamoureux and Bradley, 1996). Thin sections were prepared of the resin-embedded sediment, and varve width measurements were made using the eyepiece graticule of a light microscope.

Multiple cores were crossdated into a composite record. Varve thickness measurements were correlated with Camp Century and Devon Island Ice Cap records, as well as other North American climate records, showing that the sedimentation in Lake C2 was responding to large-scale climatic variability over the past 600 years. Hardy *et al* (1996) demonstrated a relationship between air mass temperature and daily sediment discharge into Lake C2. A large portion of the sediment influx was shown to have occurred in a short time period within the summer season (Hardy *et al*, 1996; Bradley *et al*, 1996).

Varve width measurements from Lake Tuborg, Ellesmere Island, show more high-energy hydrologic discharge events from the mid-AD1800s to AD1962, corresponding with increased melting of the Agassiz Ice Cap (Smith *et al*, 2004). Embedded, polished, and scanned (1200dpi) sediment slabs were measured using digital image analysis software. Lead-210 dating was employed to document the annual nature of the youngest sediment. Braun *et al* (2000b) found that the hydrologic input to the lake was strongly influenced by regional-scale climate rather than local conditions. Correlations with meteorological data from Eureka suggested that the altitude of freezing temperatures in the atmosphere affected summer melt. The melt water carried water and sediment into the lake basin, and cores from various regions of the lake reflected differences in deposition. In addition, there were ubiquitous depositional events that could be used as marker years, and were found in multiple cores. The amount of melt was related to summer atmospheric temperatures, permitting a paleoclimatic interpretation of the varve sequence and showing that the period from ~AD1865-1962 was relatively warmer, with increased melt and thicker varves deposited.

A composite varve width chronology was used to create a 500-year paleotemperature record by crossdating three sediment cores taken from Upper Soper Lake, on southern Baffin Island (Hughen *et al*, 2000). Lead-210 dating suggested that the laminations were annual, and the dark lamina widths showed a strong correlation with average June temperature at nearby Kimmirut (Lake Harbour), Baffin Island. This correlation was then used to calibrate the dark lamina thickness measurements to mean June temperature to build a paleotemperature reconstruction covering the past 500 years. The reconstruction suggests that June temperatures were often between 3-5°C from AD1500-1700, then decreased to 2-4°C, with many troughs of lower temperatures between AD1700-1920, and show a dramatic increase after 1920 with temperatures often reaching 5-7.5°C. This study illustrates the usefulness in crossdating multiple varved sediment cores to create a composite that can be used to reconstruct paleoclimate variables, similar to dendrochronological studies of temperate latitudes.

In proglacial lakes, classic lamina couplets of coarse and then fine sediments can form (De Geer, 1934), which results from the seasonal changes in thermal conditions that control glacial melt and refreeze, controlling flow rates and sediment transport. A 1250-year clastic varved sediment record from Donard Lake, Baffin Island, reflects sediment influx variability largely controlled by the summer melt of Caribou Glacier (Moore *et al*, 2001). The laminae couplets were shown to be annual, based on the seasonal cycle of melt water energy and the presence of a coarse and fine lamina, representing the spring and summer season, and then the lower-energy winter period. A single radiocarbon date matched well with the varve count, supporting the annual nature of the couplets. The varve width chronology was highly correlated to summer temperatures from Cape Dyer,

only 19km east of Donard Lake. Summer temperatures appear to have been warmer between AD1200-1375, and cooler from AD1375-1820, interpreted as the Little Ice Age. The glacial varves of Donard Lake provide a robust record of past summer temperatures of eastern Baffin Island.

Bear Lake, located on northern Devon Island, is a proglacial lake largely fed by an outwash river from the Devon Island Ice Cap, and the varves were shown to be created by strong underflows (Lamoureux *et al*, 2002; Lewis *et al*, 2002; Lamoureux and Gilbert, 2004). The rhythmites were interpreted as annually laminated based upon the strong seasonality that controls sediment input to the lake, similar to proglacial Donard Lake. Lead-210 dating was problematic due to low levels of unsupported lead. The varve width chronology showed a low correlation but a general similarity to the Devon Island Ice Cap ice core records ($\delta^{18}O$ and ice melt percentage). A lower amount of coarse sand grains was observed from the beginning of the 750-year record until AD1850, and was interpreted as a long period of reduced winter storminess. Correlations between varve width and autumn temperature and snowfall were strongest for the instrumental period; however, the authors state that due to the many possible controls on sedimentation into the lake, the varve record likely contains a complex paleoclimatic signal (Lamoureux and Gilbert, 2004).

Annual sediment yield can be measured in varved lake sediment that can be used to interpret erosional and transport processes, which can then be used to infer hydroclimate variability over time (Lamoureux, 1999a; 1999b). Nicolay Lake, located in the north central coast of Cornwall Island, in the central Canadian High Arctic, is a small, deep, river-fed lake (Lamoureux, 2000), that contains laminated sediment shown to be

annual by lead-210 dating (Lamoureux, 1999a). Higher annual sediment yields were attributed to intense summer rainfall events, and subannual rhythmites were attributed to nival, slumping, or rainfall events, which allowed for studying the sedimentation response to various sedimentation processes. The author posits caution in interpreting varved sediment records from arctic lakes, as peaks in sediment yield may not necessarily be proportional to events, such as high summer rainfall, and how the system responds on decadal scales may be more representative of local geomorphology as opposed to an assumed prevailing climatic variable (Lamoureux, 2002). This notion is furthered by an exploration into lagged sedimentation responses to high yield events, especially to annual changes in suspended sediments. The intensive study of the subannual rhythmites permitted the identification of the laminae that reflected sediment arriving to the basin through nival processes. Once isolated, a significant correlation was shown between nival sediment yield and annual cumulative melting degree days from Isachsen and Resolute Bay, suggesting that the paleoclimatic signal reflects regional climate conditions (Hambley and Lamoureux, 2006).

Sawtooth Lake, located in central Ellesmere Island, contained annually-laminated sediments, yet the varve width chronology showed little variation through time (Francus *et al*, 2002). These laminations were showed to be annual by interpreting the lead-210 dating profile and the cesium-137 peak that corresponds to AD1963 (Perren *et al*, 2003; Francus *et al*, 2008). Paleoclimate inferences were made by measuring the median grain size for each varve year. Using these textural parameters, measured using image analysis, a correlation between median grain size and snowmelt intensity observed at Eureka was found. Snowmelt intensity influences the energy available to transport sediment to the

lake. The results showed strong decadal-scale variability, and a clear sediment coarsening during the twentieth century (Francus *et al*, 2002), which was also accompanied by a change in the diatom assemblages that suggested a decrease in summer ice cover (Perren *et al*, 2003). Strong co-variation between other records from the region, such as Lake Tuborg and Nicolay Lake, suggest that the High Arctic has a regional climate which influences these systems and could be observed elsewhere. The authors also suggest that a complex of processes likely affect the sedimentary profile of the lake and offer a word of caution when interpreting arctic varve sequences that are largely controlled by catchment snowmelt (Francus *et al*, 2008).

A study of the sediment input to Sanagak Lake, Boothia Peninsula, Nunavut, demonstrated that the bulk of sediment transport occurred over a short period of the summer (Lamoureux *et al*, 2006). The primary control was catchment snow water equivalent, varying substantially annually. This conclusion was strengthened by hydrometeorological measurements made within the catchment over previous field seasons (Forbes and Lamoureux, 2005). The laminations were shown to be annual through ^{210}Pb dating. Embedded thin sections were scanned at 2400dpi and varve width measurements taken using digital image analysis software. The varve width record showed a relationship with the duration of peak discharge of the river flowing into the lake since ~AD1550, which was controlled by snow water equivalent in the watershed, yet the author stated that more field measurements were needed to fully quantify the relationship.

A varve width chronology from Lower Murray Lake, Ellesmere Island, Nunavut, spanning the last millennium, demonstrated that the thickest varves were deposited from

~AD1100-1300, as well as during the most recent decades, and that the thinnest deposits dated from ~AD1700-1800s (Besonen *et al*, 2008). The chronology was verified by ^{210}Pb dating and a comparison of the paleomagnetic record of the lake to an independently-derived record from Sawtooth Lake. Using image analysis techniques the median apparent diameter of the sediment grains for each year was measured and included as a proxy for climate. The relationship to hydroclimate variables is due to the association between grain size and the amount of energy needed to entrain and transport the grain. They concluded that the millennium began relatively warmer, with more energy available to transport coarser sediment in higher quantities, which then cooled by the late AD1300s, and culminated during the AD1700s to mid AD1800s period. The most recent sediments seemed to support the notion of recent climate warming.

1.1.3 Studies of Lake DV09

A 14cm core from Lake DV09 was recovered on July 21, 1994 from the distal area of the lake (16m depth), and contained annually-laminated sediments covering the past 150 years (AD1993-1843) (Gajewski *et al*, 1997). Lead-210 dating, performed at the National Water Research Institute (NWRI) in Burlington, Ontario, supported the hypothesis that the laminations within the sediments from the deepest regions of the lake were varves (Turner, 1995). The varve width record was plotted along with the 5-year summer melt percentage of the Devon Island Ice Cap (Koerner, 1977), suggesting a broad relationship between summer temperature and sediment deposition in the lake. The results from this study provided the basis for recovering longer sediment cores for additional paleoclimatic investigation.

Water chemistry and limnological descriptions were originally reported by Gajewski *et al* (1997). Additional observations on trace metal scavenging and anthropogenic chemical inputs were published by Outridge *et al* (2005; 2007) and Stern *et al* (2005).

1.2 Study Site

1.2.1 Regional Setting

Jones Sound separates Ellesmere Island to the north and Devon Island to south, in the northern region of the Canadian Arctic Archipelago (Fig 1.1 inset map). A long peninsula protrudes north from the northwest of Devon Island encapsulating Bear Bay. The Thomas Lee Inlet extends inland from Bear Bay into the northern shore of the island. The shoreline is characterised by steep cliffs 200m in height, which rise up from a thin, rocky beach to the largely barren plateaus of western Devon Island, which are incised by ephemeral streambeds.

1.2.2 Quaternary History

The southeastern flank of the Innuitian Ice Sheet is thought to have covered the island during the last glacial maximum (Dyke, 1998). The deglaciation pattern over the island appears to have been dictated by initial ice thickness and elevation (Dyke, 1999), and the ice likely retreated inland from the coasts (Dyke *et al*, 2005). The site may have been free of the ice margin around 8500-8700 ^{14}C yrs (~9500-9700 cal yrs BP) (Dyke, 1999). The lake likely emerged from a maximum marine limit of 79-102m above current sea level (Dyke *et al*, 1991; Dyke, 1998) around 7500-8125 ^{14}C yrs (~7800-8350 cal yrs BP). This

was estimated from an exponential regression curve fitted to the relative sea level data of Thomas Lee Inlet (Dyke, 1998) (Fig 1.2; Table 1.1, uncalibrated data in Appendix 1). The lake may have been formed from glacial down cutting caused by narrowing of the valley opening, as evidenced by an eroded wall extending westward from west-facing cliffs of the valley and later dammed by till material.

1.2.3 Geological Setting

The local bedrock is Middle Ordovician Bay Fiord Formation, regionally composed of dolomite and gypsum with limestone, shale and siltstone. To the west and southwest of the lake are cliffs, made up of Cornwallis Group rocks consisting of limestones and dolomite (Thorsteinsson and Mayr, 1986) that overlay the Paleozoic rock in which the lake is situated. Soils are dominantly cryic regosols throughout the region (Maxwell, 1980). A till veneer surrounds most of the lake which contacts an alluvial terrace to the northeast that may have formed after isostatic rebound resulting in damming of the lake (Dyke, personal communication in Gajewski *et al*, 1997).

1.2.4 Climate and Vegetation

The nearest meteorological station with a relatively long record is Resolute Bay, Cornwallis Island (~180km; 74°43.2N, 94°59.4W, 65.50m elevation), where the mean annual temperature is –16.4°C with a standard deviation of 1.1°C. The mean annual total precipitation is 150mm, most of which falls as snow (Normals 1971-2000, Resolute Bay; Environment Canada, 2002). There is an average of 40 frost-free days per year.

The vegetation at the study site is classified as northern Arctic tundra (Elvebakk, 1999). Much of Devon Island is dry to wet, barren terrain with very sparse and very low-growing plant cover consisting of scattered herbs, lichens, mosses and liverworts (CAVM Team, 2003). The immediate vicinity of the lake has very sparse vegetation cover.

1.2.5 Lake DV09 - 75° 34'34"N, 89° 18'55"W

DV09 (Fig 1.3) is situated within a nonglaciated watershed that extends 12.5km inland, and covers an estimated catchment area of 55km^2 (Fig 1.4; for a summary of local conditions see Table 1.2). This freshwater lake is located within 1.5km of the northern coast of Devon Island at an elevation of roughly 35m m.a.s.l. (Gajewski *et al*, 1997). It is nearly rectangular in shape and is the largest (3ha) of a number of very small waterbodies within the watershed, yet it is largely closed, with no inflow channel and a single outflow at the north end, which connects to the main river and discharges northward into the Thomas Lee Inlet (part of Bear Bay). Sediment inputs to the lake may come from aeolian inputs, surface runoff, colluvium from the proximal cliffs, slopewash, and possible slushflows during the spring melt (Fig 1.5).

The lake is unnamed, but has the unofficial hydronym of Lake DV09 (Turner, 1995; Gajewski *et al*, 1997; Canadian Museum of Nature, 2006;) or DV-09 (Outridge *et al*, 2005; Stern *et al*, 2005; Outridge *et al*, 2007), and is known locally as Tasiq Ingiusilik, meaning "singing lake" in Inuktitut, after a natural audible phenomenon that occurs (Canadian Museum of Nature, 2006). This area is currently not within the boundaries of any Canadian Land Claim Settlements; however, there are Land Claims nearby that are locally important for freshwater fishing.

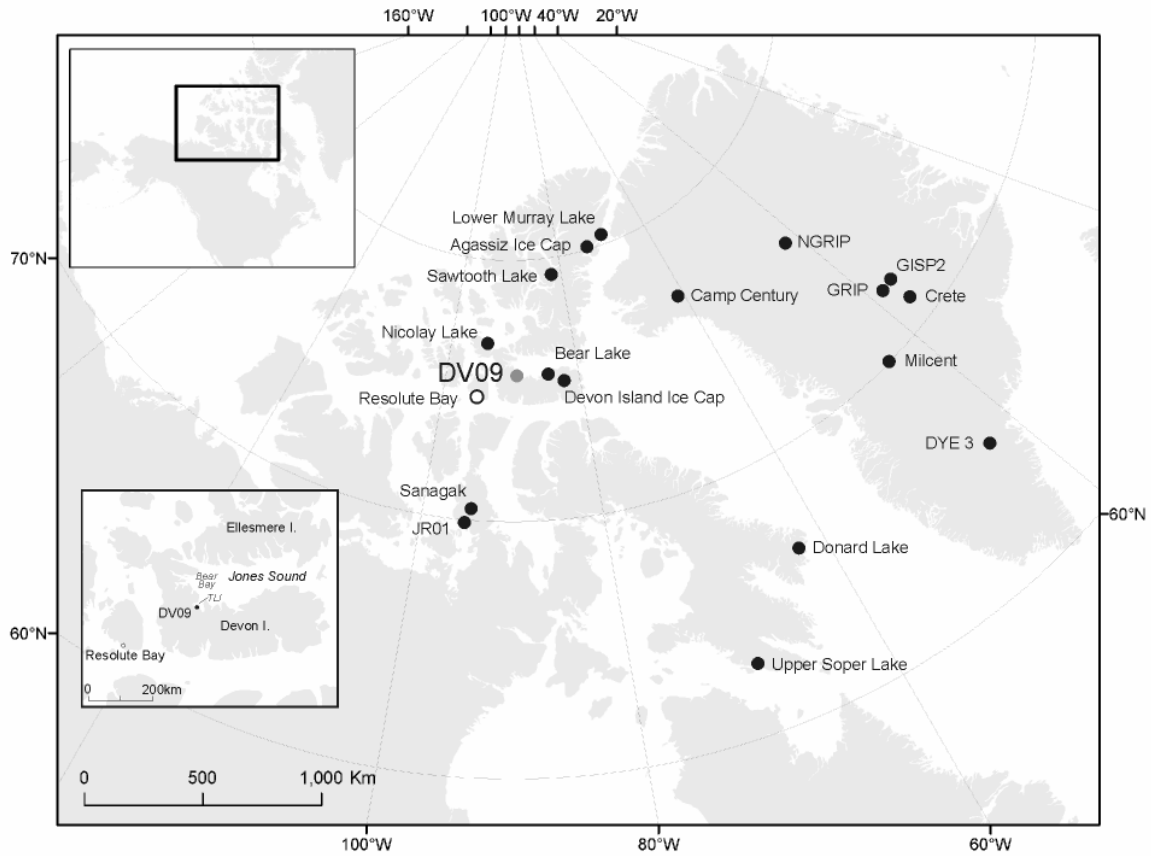

Fig 1.1: Arctic North America, grey dot shows the the study site, white dot shows the meteorological site, and black dots indicate other paleoclimate records discussed in the text. Inset Map: Devon Island region. TLI = Thomas Lee Inlet.

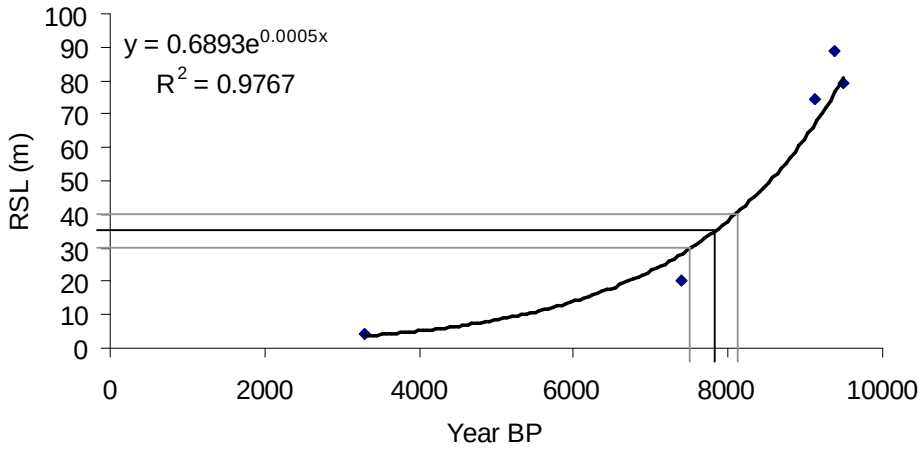

Fig 1.2: Relative sea level (RSL) exponential regression curve developed for the Thomas Lee Inlet, based on radiocarbon dates calibrated (IntCal04) from Dyke (1998). Grey lines represent the 30 and 40m contours from NTS maps, where Lake DV09 is approximately situated at 35m asl (black line). Appendix 1 lists the uncalibrated radiocarbon dates (Dyke, 1998).

Details	^{14}C Years	Cal. Years BP	References
Site is free of glacial ice margin	8500-8700	~9500-9700	Dyke *et al*, 1991; Dyke, 1999
Site emerges from marine inundation	7000-7500	~7800-8350	Dyke 1998; Dyke *et al*, 2005
Shell found above present lake level	7160 ± 80	7480-7800	This study Sample code: TO-7929

Table 1.1: Early Holocene deglaciation and uplift history of the study site.

Location	75° 34’34”N, 89° 18’55”W
Elevation	~35m asl (between 30-40m)
Surface area	3ha
Maximum lake depth	16m
Distance from coast	1.3km
Total watershed area (including DV09)	~55km
Water nutrients	Ultra-oligotrophic (Outridge *et al*, 2007)
pH	8.4
Bedrock	Middle Ordovician Bay Fiord Formation
Soil	Cryic regosols
Vegetation cover classification	Northern Arctic tundra
Mean annual temperature (Resolute Bay)	–16.4°C
Mean annual precipitation	150mm
Average annual frost free days	40

Table 1.2: Summary of local site conditions.

Fig 1.3: Lake DV09, view is looking south. Photo: K. Gajewski, June 1996.

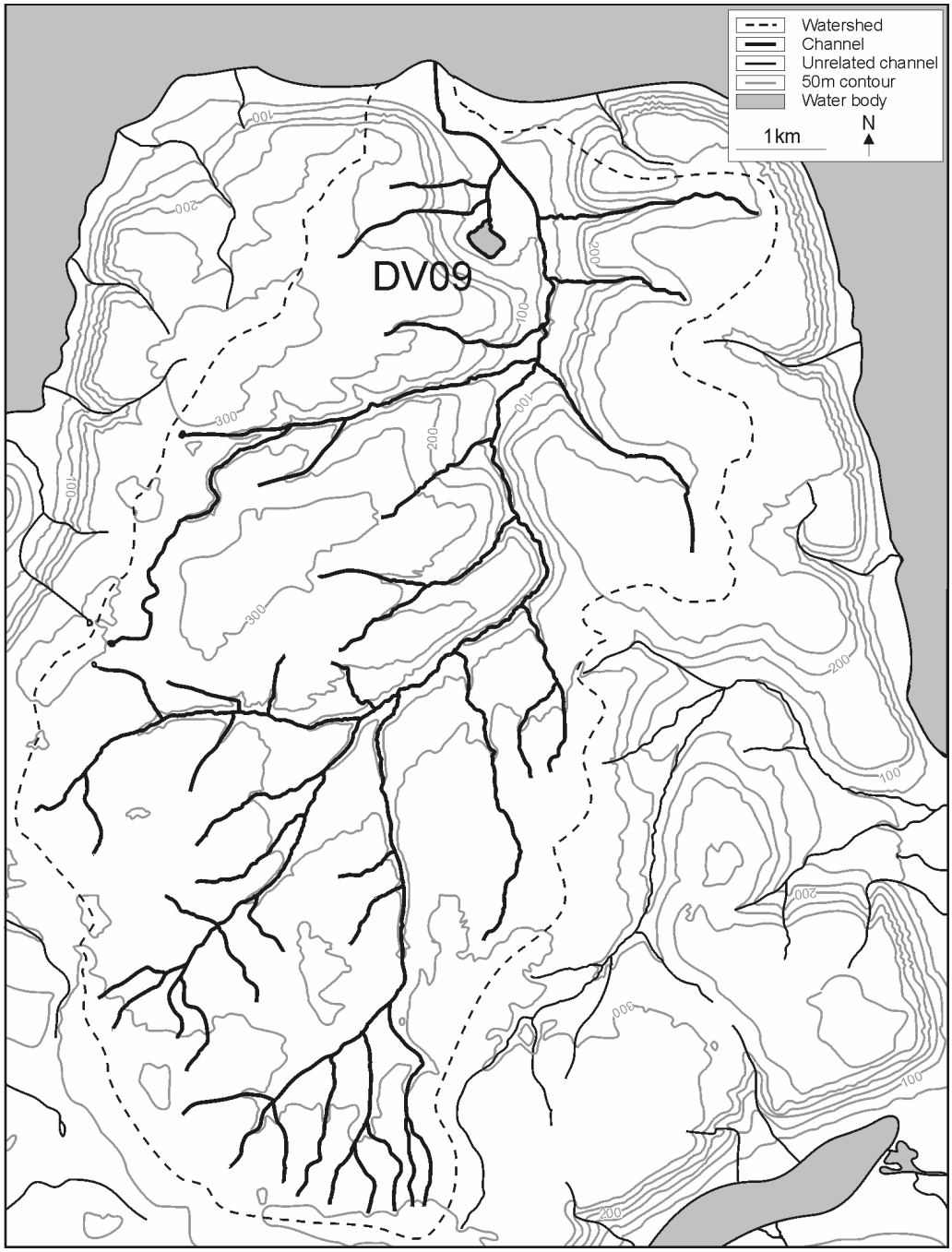

Fig 1.4: Map showing the drainage network that DV09 is a part of, yet has no direct input streams. Adapted from 1:50 000 NTS maps 58 H/07 and 58 H/10.

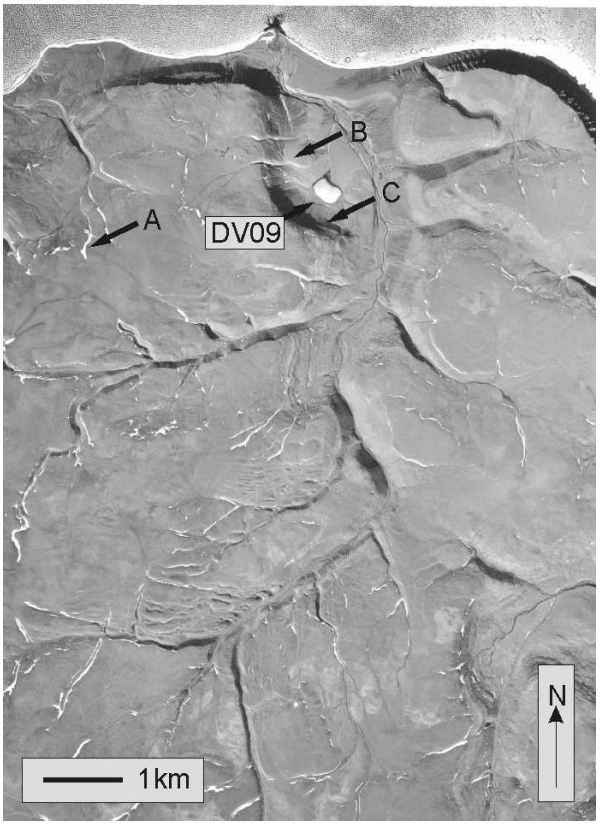

Fig 1.5: Air photo of the region, taken July 16, 1959, showing the lake with ice cover, as well as (A) ephemeral streams from the above plateau with some late lying snow accumulated in the depressions, (B) incised channels on the slopes with fans, and (C) the shaded cliff face where snow may remain into the summer months. Adapted from air photo A16752-177 with the permission of Natural Resources Canada (NRC), Earth Sciences Sector (ESS), courtesy of the National Air Photo Library (NAPL) (Appendix 2).

2 Methods

The overall purpose of the study was to characterize and quantify the nature of the sediments, to measure and create the varve chronology, and use the chronology to make paleoclimatic inferences. The methods can be divided into 1) Field methods employed to obtain the sediment cores, 2) The creation of a general sediment description, 3) Methods aimed at establishing a chronology, 4) Methods implemented to characterize the laminations, 5) Techniques for creating a composite varve chronology, and 6) Methods of comparing the chronology with other records.

2.1 Field Method

2.1.1 Core Collection

From June 15-26, 1996, eighteen lake sediment cores were collected using a 5cm-diameter Livingstone square-rod piston corer from the ice surface of Lake DV09 (core details listed in Appendix 3) (cf. Livingstone, 1955; Vallentyne, 1955; Rowley and Dahl, 1956; Wright *et al*, 1965). A small number of short cores were also obtained using a Glew gravity corer (Glew, 1991). An ice auger with handle extensions was used to manually drill a hole through the ~2m thick ice cover. A 1m-long clear plastic tube with a piston was lowered using metal extension rods through the water column to collect the uppermost sediments and to measure the water depth. Then, a series of PVC tubes were inserted into the hole to create a rigid casing. The Livingstone corer was lowered using the extension rods to collect additional meters of sediment. Each core was measured, wrapped in plastic wrap and aluminum foil, labeled, and then stored in a split PVC tube.

The cores were taken from the periphery and distal areas of the lake, and many cores were taken from one region (Fig 2.1). Core recovery lengths ranged from 25-648cm. The sediment base was not reached in all cores due to the presence of a hard sediment layer around 200-275cm depth, which was only penetrated in a few holes. In some cases only the surface sediment core (Drive 0) was taken. Some cores were collected with the water-surface interface intact and stored vertically, while the remainder were extruded (Glew, 1988) at the Polar Continental Shelf Project (PCSP) base at Resolute Bay, Cornwallis Island. All cores were then shipped to Ottawa and refrigerated at 4ºC at the Laboratory for Paleoclimatology and Climatology at the University of Ottawa.

2.2 Laboratory Methods

2.2.1 Non-Invasive Methods: General Sediment Description

2.2.1.1 Magnetic Susceptibility

Volume magnetic susceptibility (k) measures, in dimensionless units, the total magnetic attraction of the various constituents of the sediment when exposed to a magnetic field (Dearing, 1999; Snowball, 1999). It is defined as:

$$k = M \cdot H^{-1} \quad (1)$$

Where M is the magnetization per unit volume and H is the magnetic field strength or magnetizing force applied (Moskowitz, 1995).

Magnetic susceptibility is useful for correlating multiple sediment cores by comparing the variations in the susceptibility profiles, which reflect changes in the concentration of magnetic minerals within the deposits (Thompson, 1986). The concentration of iron-bearing minerals in the sediment is a dominant control on the ease at which it can be magnetized, and is measured by the sensor (Nowaczyk, 2001; Sandgren and Snowball,

2001; Smol, 2002). The variability in the magnetic susceptibility indicates changes over time in weathering, erosion, transport, and deposition processes within the basin (Nowaczyk, 2001; Zolitschka *et al*, 2001).

Whole-core logging of low frequency magnetic susceptibility was done using a Bartington Instruments Ltd. 60mm-diameter loop sensor (Type MS2C), with a precision of $1x10^{-5}$ SI ($1x10^{-6}$ CGS) (Dearing, 1999). The magnetic susceptibility was recorded at 1cm intervals for the length of each drive; this was repeated two or three times and the results averaged. Measurement values were corrected for an assumed linear measurement drift using the method developed by Dearing (1999). Although nonlinear drift is possible, the final data does not suggest that this may have occurred, and repeated measurements are highly correlated. Measurements made previously on some of the cores (Roch, 1999) in CGS units were converted to SI units using a standard equation. Conversion from dimensionless CGS units to dimensionless SI units:

$$\text{SI units} = (\text{CGS units})(0.4)(\pi) \qquad (2)$$

(Adapted from Moskowitz, 1995)

Some possible problems encountered include machine drift, and large anomalies within the profile created by the presence of an iron-rich clast within the sediment of a core that does not show up in adjacent sediment cores. Usually, the magnetic susceptibility measurements made for the uppermost 1-5cm and bottom 1-5cm of a sediment core are discarded because of the empty space above and below the core, decreasing the volume measured (Dearing, 1986). The values presented have 2-3cm removed from the ends to correct for the volume decreases.

2.2.1.2 Core Description

Cores were split longitudinally and a planar section was cut off and stored in a tray for x-raying and for varve width measurement. Each half core was stored in a split PVC tube and all portions were wrapped in plastic wrap and aluminum foil for protection from contamination and desiccation. The surface of the 1cm-thick slab was cleaned with a metal knife and deionized water, which is the most common method for working with varved sediments (Lamoureux, 2001). Immediately after splitting, a detailed core description was taken following Laboratory for Paleoclimatology and Climatology (LPC) protocol and various descriptive techniques (cf. Troels-Smith, 1955; Campbell, 1967; Dean *et al*, 1985; Mazzullo and Graham, 1988; Kershaw, 1997; Schnurrenberger, 2003). Simple stratigraphic diagrams were made for future reference. Notes were taken on colour, descriptions of sediment layering, presence or absence of organic matter, sediment type, core damage, and water content. Length measurements were also taken and occasionally spacers were inserted to monitor shrinkage.

2.2.1.3 Core Imaging

Digital photographs were taken of the open sediment cores so that the original condition, colour, and light reflectivity of the core were recorded. Light conditions were maintained by using lamps with 3200K bulbs and diffusion screens when needed to correct ambient light conditions (Lamoureux and Bollmann, 2004). Each image includes a section of the core, a colour card for calibration, a ruler for scale, and registration markers for aligning the pictures. Camera details:

Company: Sony Model: DSLR-A100 Year: 2007 Lens: 15mm, 18-70mm/F3.5-5.6 Resolution: 10.2 Megapixels	Company: Nikon Corporation Model: COOLPIX L15 Year: 2007 Lens: default lens on model Resolution: 8.0 Megapixels

2.2.1.4 X-radiography and Image Greyscaling

X-radiography provides a quick and inexpensive method that is non-destructive and useful for describing and analyzing a sediment core (Principato, 2004). Changes in the relative density of the sediments appear as visible white to black variations on the x-ray film or digital image, and can be used for qualitative and quantitative analysis using image analysis techniques (Ojala, 2004). Dense material absorbs x-rays more readily and shows up as a whiter shade on the film, while less dense material absorbs fewer x-rays and will appear blacker.

On November 13, 2007 and June 26, 2008, 1cm-thick slabs of the sediment were x-rayed at the Ottawa General Hospital. A Siemens Axiom Aristos MX x-ray machine was used set at 60.0kv, 2.00mAs, for 500ms, at source-to-image distance (SID) of 115cm. A metal caliper open to 10.0cm was placed beside each core for image calibration. The x-ray images were saved as 256 RGB TIF files (120dpi), and later converted to 8-bit greyscale TIF files (120dpi).

To extract the greyscale values, intensity profiles along the center of each core were plotted using the software NIS-Elements BR 3.0 and the data exported to Microsoft Excel. Each image was calibrated from pixels to $mm \cdot pixel^{-1}$ by using the 10.0cm calliper and values from overlapping images were averaged.

2.2.2 Invasive Methods: Sediment Analysis

2.2.2.1 Particle Size Distribution (PSD)

Measuring particle sizes and shapes can lead to an understanding of sediment sources and availability, transport energy, as well as mechanisms of transport and deposition (Folk and Ward, 1957; Visher, 1969; Briggs, 1977; Beierle *et al*, 2002). After samples were sieved with a 2mm sieve, a Lecotrac LT100 particle size analyzer was used to determine the grain size frequency distribution (Last, 2001). To reduce measurement inaccuracies caused by aggregated clay particles within the sediment samples (Beierle *et al*, 2002), a small amount of a dispersant, 15mL of 50g/L sodium hexametaphosphate $(NaPO_3)_6$, was added prior to measurement causing a cation exchange reaction on some clay minerals leading to disaggregation (Carver, 1971; Bamber, 1982; Griffiths and Holmes, 2000). From the distribution data, the percentage of clay, silt, and sand sized grains could be calculated and plotted down core.

2.2.2.2 Loss-on-Ignition Analysis (LOI)

The organic and inorganic carbon component of the sediment can be estimated using loss-on-ignition (Dean, 1974; Heiri *et al*, 2001). These measurements can indicate fluctuations of sediment water content, organic matter, and carbonate through time. Organic matter production should be directly proportional to lake temperature, if nutrient supply remains more or less constant. Carbonate input may indicate differences through time in clastic input from the watershed. The trophic level of the lake can impact the rates of calcium carbonate precipitation and concentration within the water column (Kelts and

Hsü, 1978; Dean, 1981; 1999; Boyle, 2001). Both production and carbonate precipitation influence the depositional characteristics of the sediments.

Subsampling at ~10cm intervals down the core, $1cm^3$ samples were weighed (W_{100}), then dried at 100°C overnight in an oven, weighed again (DW_{100}), and then ignited at 500°C for 3 hours in a muffle oven. After cooling in a desiccator, the weight was measured again (DW_{500}). Subsequently, the samples were reheated to 925°C for another 3 hours in the muffle oven, cooled in a desiccator, and reweighed (DW_{925}) (similar to Heiri *et al*, 2001).

Water content percentage was computed as follows:

$$\% \text{ water} = 100(W_{100} - DW_{100})(W_{100})^{-1} \quad (3)$$

The percent organic matter was calculated (Boyle, 2001):

$$\% \text{ organic} = 100(DW_{100} - DW_{500})(DW_{100})^{-1} \quad (4)$$

And the percent carbonate follows (Boyle, 2001):

$$\% \text{ carbonate} = 100(DW_{500} - DW_{925})(DW_{500})^{-1} \quad (5)$$

2.2.2.3 Biogenic Silica (BSi)

Biogenic silica reaches the lake bottom through the accumulation of diatoms and chrysophytes from the water column (Cohen, 2003). This biogenic silica is more chemically reactive than other sources, such as quartz, making it the most readily extractable form of silicate. Biogenic silica can be used as a proxy for diatom abundance, which can indicate variations in lake production over time (Conley and Schleske, 1993; 2001; Conley, 1998; Ohlendorf and Sturm, 2007).

Diatoms have been shown to be present within the recent sediments of Lake DV09 (Gajewski *et al*, 1997); however, it is possible that there has been dissolution and/or grazing of diatoms down core. In this case, there should be low quantities of BSi down core. For this study the wet-alkaline digestion technique was employed to extract the biogenic silica from the sediment (Conley, 1998). This documents changes in production, or potential changes in other environmental factors such as dissolution of diatom fossils caused by pH fluctuations over time.

Core T was subsampled for $0.5cm^3$ of sediment at 10cm intervals; the samples were dried at 105ºC for 27 hours in a VWR Scientific 1370FM oven, and subsequently crushed using a mortar and pestle. Using an electronic balance, 0.020 ± 0.002g of sediment from each sample was weighed and transferred into 125mL flat-bottomed Nalgene® bottles and labeled. Each batch of 26 samples included a reference sample as recommended by Conley (1998). To each sediment sample, 40mL of 1% sodium carbonate (Na_2CO_3) was added, the bottles were placed into an ~85ºC water bath and subjected to an oscillation of 70rpm. After increments of 2, 3, 4, and 5 hours, the samples were removed and placed in an ice-water bath to effectively stop the chemical reaction. Each time the bottles were stirred and a 1mL extraction of liquid from each sample was micropipetted into labeled graduated centrifuge tubes. Each sample was neutralized with 3.2mL of 0.06N hydrochloric acid (HCl) and diluted with 10mL of deionized water. A 1mL extraction from each of the 12 standard stock solutions (Table 2.1) were also treated and diluted in this way. All samples were stored in a refrigerator at ~5ºC for less than 24 hours.

An Ultrospec™ 2100 pro UV/Visible spectrophotometer, with a 0.001 ± 0.002 AU (absorbance unit) precision, was used to measure the absorbance of light at 660nm by the silicate ions present in each sample. Cleaned Hellma cell cuvettes with a 10mm light path were used. The following chemicals were added to each cuvette prior to measurement:

0.64mL of each sample/standard stock solution
0.84mL of ammonium molybdate reagent [$(NH_4)_6Mo_7O_{24}.4H_2O$ in 0.1N H_2SO_4]
0.64mL of oxalic acid reagent ($H_2C_2O_4$)
0.84mL of ascorbic acid ($C_6H_8O_6$)

The silicate concentration readings from the spectrophotometer were inputted into a spreadsheet to calculate the biogenic silica content based on the light absorbance values for each of the samples and standards.

2.2.2.4 Description of Subfossils

A number of small subfossils were found in the sediments of Core T while making observations under a light microscope and while picking datable radiocarbon material. This included plant detritus such as leaves and mosses, and a number of animal fossils, which were mounted on paleontological slides using tragacanth gum for identification.

2.2.2.4.1 Description of Fossils: Diatoms

Diatom extraction (following Battarbee *et al*, 2001 and Bouchard, 2004), which isolates fossil diatoms from the sediments, was done to gain qualitative insights on assemblage changes, which could indicate environmental changes within the lake. Subsamples of $0.5cm^3$ were taken at 40cm intervals down Core T. Fifteen mL of 10% hydrochloric acid (HCl) was added to dissolve the carbonate component of the sediments and left for 24

hours. The samples were then filled with deionized water to dilute the acid Samples were then centrifuged in an IEC Centra® GP8 centrifuge at 3000rpm for 6 minutes to concentrate the remaining sediment. The excess liquid was aspirated and the samples were refilled with deionized water. This was repeated four times, and the pH was assessed each time to track the dilution of the acid. After reaching near neutral pH, and on the final aspiration a 15mL mix of 50:50 molar ratio sulphuric (H_2SO_4) and nitric acid (HNO_3) was added and left for 19.5 hours. The samples were then heated in a water bath at 85 to 90ºC for 3 hours and stirred every 30 minutes. The samples were cooled at room temperature and left for 24 hours. Aspiration, dilution, and centrifugation were repeated 8 times, reaching a nearly neutral pH, allowing for serial dilutions to be made. This was done by adding 1mL of the stock solution to 20mL of deionized water, and a second serial dilution was made by adding 1mL of the first dilution to an additional 20mL of deionized water. Microscope slides were prepared using 1mL of these liquids.

2.2.3 Chronostratigraphic Techniques

2.2.3.1 Radiometric Dating

2.2.3.1.1 ^{210}Pb Dating of the Recent Sediments

Lead-210 dating utilizes fallout radionuclides, which makes use of the naturally occurring uranium-238 isotope, and subsequent decay series, to assess the change in erosion rates over the basin catchment (Appleby, 2001). Fallout of lead-210 from the atmosphere has been shown to be relatively constant on time scales of one year or higher, but does vary on shorter scales, while the geologic source of the isotope and decay series is a function of erosion and transportation to the lake. It is quickly scavenged by particulate matter in

the water column and is deposited, decaying at a known rate. Various studies from many different lakes around the world have shown that this is a viable dating technique for the uppermost lacustrine sediments (Krishnaswami *et al*, 1971; Pennington *et al*, 1976; Robbins, 1978; Appleby and Oldfield, 1983; Oldfield and Appleby, 1984; Binford *et al*, 1993; Blais *et al*, 1995).

The CRS (constant rate of supply) and CIS (constant initial concentration) models, as well as the lamination count of the upper sediment of lake DV09 (representing the past 150 years), are all in agreement, suggesting that the sediment is annually deposited (Turner, 1995; Gajewski *et al*, 1997). Lead-210 dating was determined using a variation of the polonium distillation procedure (Eakins and Morrison, 1978; Turner, 1990; 1995) at the National Water Research Institute, Burlington, Ontario.

2.2.3.1.2 Radiocarbon Dating

The radioactive decay of carbon-14 can be used to date organic material found in lake sediments and is useful for material from between a few hundred years and 45 000 years old (Björk and Wohlfarth, 2001). Organic material was manually taken out of sediment subsamples from the core using a light microscope and tweezers; care was taken to reduce contamination, which can cause erroneous dating when the average radiocarbon age of the sample is measured (Pilcher, 2003). Subsampling locations were chosen at approximately even intervals down core, or at levels where organic material could be seen. Attempts were made to pick enough organic detritus from the even interval subsamples, but in all cases there was not enough material to yield a date; an adequate amount of material was only found within thin coarse layers. Because of the small

quantities of organic material present, even within the coarse layers, the accelerator mass spectroscopy (AMS) radiocarbon dating technique was employed. Organic matter samples were subject to an acid/alkali/acid pretreatment prior to radiocarbon dating. The radiocarbon was measured by Beta Analytical Inc. (Miami, Florida), and IsoTrace Laboratory at the University of Toronto.

The results were calibrated from radiocarbon ages to calendar year ages, which is necessary due to historical fluctuations in the concentration of ^{14}C in the geosphere (Sewell, 1998; Reimer and Reimer, 2006). The calculations were done using CALIB Rev5.0.1 software (Stuiver and Reimer, 1993a and b), the marine shell was calibrated using the Marine04.14c curve (Hughen *et al*, 2004), and the terrestrial organic detritus samples were calibrated using the IntCal04.14c curve (Reimer *et al*, 2004). The lake water reservoir effect was assumed to be negligible.

2.2.3.2 Varve Chronology

2.2.3.2.1 Varve Delineation

The energy available to transport sediment to the lake basin in polar regions varies greatly over the seasonal cycle. During the winter freeze up, the lake is completely covered in ice up to 2m thick, the lake water stratifies and the finer sediments are able to settle. At this time, wind-blown sediments can be deposited on the lake ice, which may enter the lake after melting begins. During late spring/early summer, the snowpack melts and the high-energy runoff flows can transport larger sediments to the lake, which settle to the bottom more quickly, and should grade coarsest to finest from the shore to the central, deeper region (Stokes' Law). The summer period is also characterized by an

increase of biological activity that begins to deposit a thin organic-rich film at the sediment surface. As the temperature cools in autumn, the ice cover returns, and the finer sediments and organic matter can continue to settle.

Based on this inferred process of events, the varves preserved within the sediments of Core B were delineated using the organic lamina as the uppermost sediments and the clastic lamina as the basal sediments for each year, and continued this way down core. Thus, the sedimentation interval of each varve was defined from spring/early summer to the preceding spring/early summer.

2.2.3.2.2 Varve Counting and Identification of Marker beds

The very first varve was interpreted to have been deposited during 1996, because the cores were taken during the spring of that year, immediately following initiation of the spring/early summer thaw and the input of clastic material associated with the melt water. In this case, the upper organic-rich layer was not established yet, and does not represent one full year of sediment deposition. Following the method of delineation described above, each varve was counted down core. To aid in varve counting, 1.5cm-wide clear mylar plastic strips were placed along the open core face. This gave a clear and waterproof surface down core that could be written on with permanent markers. By writing on the plastic strip over the sediment core, varve counting and recounting was achieved similar to a method commonly employed in dendrochronological studies using cores from living trees (cf. Yamaguchi, 1991). Being waterproof also gave the added benefit of keeping the open core constantly moist so that shrinkage was reduced and the surface could be rinsed for better viewing.

Every five annual laminations were dotted with a single dot. Each 50-year count was marked with a double dot, while each 100-year count was marked with a triple dot. This made it easy to locate any particular varve year, and each lamination or any laminasets could be referenced to notes in a lab notebook.

Marker beds are the stratigraphic equivalent of marker rings employed in dendrochronology. Several qualitative descriptions of very distinct laminae acted as marker beds, which aided in verifying varve counts and eventually for crossdating multiple varve width measurement series. Thicker homogeneous layers, thicker normal-graded layers, conspicuous orange lamina, presence of intermittent sand grains or larger plant macrofossils, sand layers, distinct and thicker biolaminations, and series of discrete thin laminae were identified and used as markers.

2.2.3.2.3 Measuring the Varve Width Series

Once delineated and dot-counted, the laminae couplets were measured under a light microscope using an Acu-Rite Absolute Zero II bench micrometer with a precision of 0.001mm. MeasureJ2X software was used to record the digitized measurements.

2.2.3.2.4 Crossdating Multiple Measurement Series

Multiple varve measurement series can be cross-correlated, which is a dendrochronologic technique that can ensure accurate dating of the annual series (Lamoureux, 2001). Crossdating the sediment cores reduces the potential for chronological error and has long been employed in lacustrine varve studies (De Geer, 1912; 1934).

Crossdating of the series was done to create a composite series, which accounts for the missing or multiple varves in any measurement series. The method of crossdating addresses both counting errors as well measurement errors. Crossdating the multiple measurement series was done using Microsoft Excel by pattern matching and aided by the numerous identified marker beds. In general, thicker layers were the most useful property for identifying marker beds, and the high variability of varve widths throughout the core produced numerous marker beds. A spreadsheet was established with all the adjacent series and the marker beds were highlighted. In cases where one series showed a thick layer, while other series showed a number of laminae equalling the width of the thicker layer, a decision was needed to either interpret the one thicker layer as one varve or as multiple thinner varves. If a number of series agreed, the consensus was included in the composite series, and this was also aided with notes recording details about specific sections and laminae. This method of compiling a composite series allowed multiple measurement series to be reconciled. This method matched the annual increment for a given year with the same increment found within another series from the same sampling site (Fritts, 1976).

Once the series were crossdated the average values for each varve year in the composite could be determined. Varve widths that agreed across all records were averaged, varve layers that needed to be combined were added together first before averaging, and missing values from one series were supplemented by averaging the values from the other agreeing series. Appendix 4 contains the raw data values.

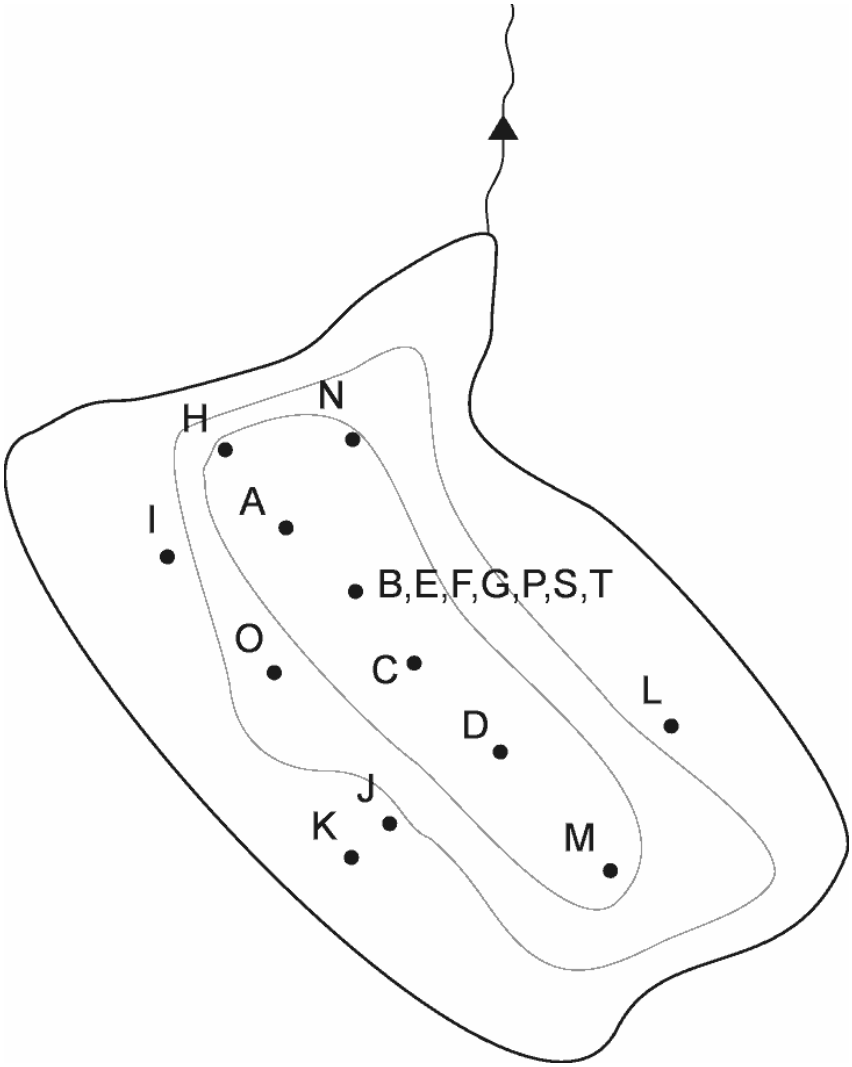

Fig 2.1: Relative position of holes drilled into the ice cover and corresponding sediment coring sites at Lake DV09. Note that B, E, F, G, P, S, T were all from the central region of the lake, two cores were recovered from hole D (D_i and D_{ii}) and that no sediment was recovered from hole K. Grey lines are estimated 5m bathymetric contours.

Silica Standard Stock	Silicate (SiO_2) Concentration ($mg \cdot L^{-1}$)
S0	0 + 1% Na_2SO_3
S1	10
S2	20
S3	30
S4	40
S5	50
S6	60
S7	80
S8	100
S9	125
S10	150
S11	200

Table 2.1: Silica standards used in the wet-alkaline digestion technique for measuring biogenic silica.

Results (Part 1)

Post-glacial sedimentology of Lake DV09, northern Devon Island, Nunavut, Canada

3.1 Introduction

Investigating the sedimentology of the laminated sediments from Lake DV09 gives an understanding of the evolution of the lake basin over time. The longest sediment cores recovered from the lake cover the entire sedimentary history of the lake, beginning during the early half of the Holocene.

This chapter reports the sedimentologic analyses conducted on a number of cores from the lake, and discusses these results within the context of a changing environment. The majority of the analyses were conducted on a long core from the deepest area of the lake, and other information was obtained from several other cores. The following section focuses on the annually deposited laminations of the most recent sediments.

Lake DV09 (unofficial name; 75°34'34"N, 89°18'55"W) is situated within a nonglaciated watershed that extends 12.5km inland, and drains an estimated catchment area of approximately 55km^2. This freshwater lake is located within 1.5km of the northern coast of Devon Island at an elevation of roughly 35m m.a.s.l., and has a maximum measured depth of 16m (Gajewski *et al*, 1997). It is nearly rectangular in shape (Fig 1.5) and covers an area of 3ha. The lake is largely closed, with no inflow channel and a single outflow at the north end, which connects to the main river and discharges northward into the Thomas Lee Inlet (part of Bear Bay). However, there may be ephemeral inputs from the slopes and plateau above.

The lake water is ultra-oligotrophic (Outridge *et al*, 2007) and water chemistry data has been published previously (Gajewski *et al*, 1997). Ice, up to 2m thick, covers the lake for most of the year. A moat of melt water develops during summer, and partial ice cover may persist throughout the summer months.

The local bedrock is Middle Ordovician Bay Fiord Formation, regionally composed of dolomite and gypsum with limestone, shale and siltstone. To the southwest and the west of the lake are steep cliffs, made up of Cornwallis Group rocks consisting of limestones and dolomite (Thorsteinsson and Mayr, 1986) that overlay the Paleozoic rock in which the lake is situated. A till veneer surrounds most of the lake which contacts an alluvial terrace to the northeast that may have formed after isostatic rebound resulting in damming of the lake (Gajewski *et al*, 1997). The vegetation cover is northern Arctic tundra (Elvebakk, 1999) with very sparse low-lying vegetation around the lake.

The sediment-source areas seem to be from the steep slopes and possibly from the plateau above during the rapid spring melt period where runoff and slushflows may enter the lake. Colluvial fans are present to the northwest of the lake. Water and sediment inputs to the lake may come from aeolian inputs, surface runoff, colluvium from the proximal cliffs, slopewash, and possible slushflows during the spring melt.

The southeastern flank of the Innuitian Ice Sheet is thought to have covered Devon Island during the last glacial maximum (Dyke, 1998). The deglaciation pattern over the island appears to have been dictated by ice thickness and elevation (Dyke, 1999), and the ice likely retreated inland from the coasts (Dyke *et al*, 2005). The study site may have been free of the ice margin around 8500-8700 ^{14}C yrs BP (~9500-9700 cal yrs BP) (Dyke, 1999). Driftwood and shell samples from raised beaches suggest that the lake

likely emerged from a maximum marine limit of 79-102m (Dyke *et al*, 1991; Dyke, 1998) around 7500-8125 ^{14}C yrs BP (~7800-8350 cal yrs BP) (Dyke, 1998).

The nearest meteorological station with a relatively long record is 180km away at Resolute Bay, Cornwallis Island. The mean annual temperature is –16.4°C with a standard deviation of 1.1°C. Mean annual total precipitation is 150mm, with most falling as snow, and an average of 40 frost-free days per year (1971-2000 climate normals; Environment Canada, 2002).

3.2 Methods

3.2.1 Field Methods and Sediment Description

From June 15-26, 1996, 18 lake sediment cores were collected using a 5cm-diameter Livingstone square-rod piston corer from the ice surface of DV09. Surface cores were shipped vertically with the water-sediment interface intact.

Whole-core logging of the magnetic susceptibility of all cores was done using a Bartington Instruments Ltd. 60mm-diameter loop sensor (Type MS2C) at 1cm intervals. This was repeated and the results averaged. The values were corrected for an assumed linear measurement drift (following Dearing, 1999). In the lab, Cores B, P, S, and T were split, and a 1cm-thick slab was cut off one of the half splits and stored in a metal tray, which was then photographed.

The 1cm-thick slabs of Core T were x-rayed using a Faxitron x-ray machine set at 100mA for 300ms, and the x-rays were printed on film. The 1cm-thick slabs of Cores B, P, and S were x-rayed at the Ottawa General Hospital using a Siemens Axiom Aristos MX x-ray machine set at 60.0kv, 2.00mAs, for 500ms at a source-to-image distance

(SID) of 115cm. A metal calliper open to 10.0cm was placed beside each core for image calibration. Digital x-ray images were saved as 256 RGB TIF files (120dpi), and converted to 8-bit greyscale TIF files (120dpi). To extract the greyscale values, intensity profiles along the center of each core was plotted using NIS-Elements BR 3.0 and the data exported to Microsoft Excel. Each image was calibrated from pixels to $mm \cdot pixel^{-1}$ using the calliper image and the values from overlapping images were averaged.

Lead-210 dating of the uppermost sediments was reported previously (Turner, 1995; Gajewski *et al*, 1997). Subsequently, other short cores from this lake, taken from 13.5m depth, were lead-210 dated and confirmed the annual nature of the uppermost laminae couplets from AD1854-1999 (Outridge *et al*, 2005; 2007; Stern *et al*, 2005).

Core T was subsampled for a number of additional sedimentologic analyses. Particle size distributions were measured using a Lecotrac LT100 particle size analyzer, and 15mL of $50g \cdot L^{-1}$ sodium hexametaphosphate was added as a dispersant to disaggregate the samples. Sediment water content was measured by drying $1cm^3$ samples at 100°C for 24 hours in a VWR Scientific 1370FM oven. Organic matter content was measured by loss-on-ignition at 500°C for 3 hours, and subsequently, carbonate content was measured by igniting the sample at 925°C for another 3 hours (similar to Heiri *et al*, 2001). Biogenic silica was separated from the sediments using the wet-alkaline digestion technique (Conley, 1998), and the dry weight percentage was calculated from the absorbance of light at 660nm measured using an Ultrospec™ 2100 pro UV/Visible spectrophotometer, with a 0.001 ± 0.002 AU precision. Ostracode fossils, picked and mounted during picking of material for radiocarbon, were identified by Joan Bunbury.

Limited amounts of small organic detritus were found throughout the sediment column; however, conspicuous coarse layers contained higher amounts of organic matter. The organic matter from a number of these coarse layers yielded AMS radiocarbon dates. The uppermost sample also includes material from Core B, because not enough material could be found in Core T alone. The sample contained mainly plant matter and mosses with occasional chironomid larvae head capsules. Additionally, a *Dryas* leaf found in Core E was also dated. A *Mya truncata* Linnaeus valve found on the ground surface just above the present lake level was dated to estimate when the lake was uplifted from marine inundation. The dating was performed by Beta Analytic Inc, Miami, FL, and the shell was dated by IsoTrace Laboratory, Toronto, ON. Radiocarbon years were calibrated using IntCal04.14c (Reimer *et al*, 2004) and the Marine04.14c curve (Hughen *et al*, 2004) for the shell date.

The varves of Core B were measured from the moist core surface under a stereomicroscope using an Acu-Rite Absolute Zero II bench micrometer with a precision of 0.001mm. A detailed methodology and discussion of these varves is presented in the next chapter.

3.3 Results

The majority of sedimentological analyses were conducted on the sediments of Core T, although some data were also obtained from other cores (Table 3.1).

3.3.1 General Sediment Stratigraphy (Fig 3.1)

From the sediment base to 550cm depth, the sediments are largely homogenous beige to grey in colour, and from 590-633cm, large, angular, dark grey clasts, often less than 1cm in size up to a few centimeters were found. From 490-530cm there is a transition from the beige and grey deeper sediments to an orange-tan colour, which dominates the colouration above 490cm. Chironomid head capsules and foraminifera fossils were found above and below this transition zone; whereas, ostracode fossils were only present above it. Note that these fossils were observed during various other sediment analyses and were not systematically studied down core. Layered sediments continue, and become increasingly thicker toward 350cm. From 350-275cm, the layers are thick, and there is a higher occurrence of visible organic detritus. Between 275-250cm is a massive layer of homogenous sediments. The thickness of this layer is variable across Cores P (18cm), S (20cm), and T (25cm). Above 250cm, the sediments are thinly layered, and in the next chapter are shown to be varved above 140cm. A decrease in the presence of chironomid, ostracode, and freshwater foraminifera fossils, and decreased presence of larger organic detritus was observed to a depth around 100cm. Above 150cm are thin organic-clastic laminations, with occasional more diffuse or massive layers of a few centimeters. These laminations were best preserved in Core B.

The magnetic susceptibility profiles from all of the cores are in good agreement, with Core T generally having slightly lower values throughout (Fig 3.1). The values increase from the basal sediments with occasional slight peaks. At 500cm depth, the values increase more rapidly to a depth of 350cm, where the variability significantly increases, although the amplitude is variable across cores, with Core T remaining less

variable. Above 225cm the values are relatively heightened, with lower variability than the previous section. Above 125cm the susceptibility values show a decrease, yet the depth of this occurrence is variable across cores. Around 50-25cm, there is a plateau of increased values, which decrease steadily toward the top of the cores, with a slight perturbation just above 10cm.

3.3.2 Sedimentology of Core T

The magnetic susceptibility of the sediments is relatively low, between 2 and $5x10^{-5}$ SI units, with little variation from 647 to ~300cm depth, but with a slight peak around 350cm (Fig 3.2). From 300-225cm depth, there are two sharp peaks, with a maximum of $16x10^{-5}$ SI units at 275cm, and an average value within this section that is also slightly elevated. Susceptibility values are low between 225-200cm, followed by a gradual increase peaking around 150cm. Values are decreasing until 50cm then remain at slightly increased values until 20cm, and then decrease steadily to the top of the core.

The biogenic silica content of the sediments remains extremely low and often measured less than 1% dry weight as biogenic silica). The highest value (1.5%) was measured within the final drive, with few values in the sediments of the middle of the core, and a small value (0.8%) found in the uppermost sediments. Given the low values, we assume that there are basically no diatoms in these sediments.

The particle size distributions suggests that silts (3.9-62.5μm) dominate the grain size at all levels in the core, consistently comprising 60% or more of the grain size distributions (not shown). Sands (62.5-2000μm) comprise between 0 and 35% of the distribution, but from 300-350cm depth, there are peaks up to 50%. Clays (1-3.9μm)

never comprise more than 5% of the distributions, and values are lowest around 300cm and highest near the end of the core.

Median grain size values are generally low (below 30µm) from 647 to close to 350cm depth, with few peaks up to 60µm, and slightly elevated values from 500-450cm (~50µm) (Fig 3.2). From 350-275cm, there are coarser layers, peaking with a median grain size over 100µm; however, the values are often between 30 and 60µm. The median grain size between 275-175cm remains around 40µm, and from 175-75cm remains higher, at 60-100µm. The uppermost sediments are finer.

Organic matter within the sediments is very low, remaining near or below 1% from 647-225cm depth, with a few higher values up to 2% around 250cm. The percent organic matter is between 1 and 3% from 225-75cm depth, and then returns to around 1% to the top of the core. Carbonate content, measured as loss on ignition at 925°C, remains below 4% throughout the sediments, with an extreme peak at 418cm (19%) and a smaller peak at 215cm depth (10%). The percent carbonate profile contains two erroneous (negative) values at 182 and 385cm that were removed. The sediment water percent is highly correlated (r=0.84) with percent organic matter. The values are very low, around 15% from 647-325cm depth. Water content is generally increased (~30%) from 325cm to the sediment surface, occasionally peaking above 40%; although, there is a decrease from 100-50cm to ~15%.

Fossil diatoms have been shown to be present in the uppermost sediments of DV09, with the highest concentration during the 1980s and 1990s, and significantly lower concentrations in the earlier part of the 20th century. Diatom identifications and concentrations for the period of AD1843-1993 were published by Gajewski *et al* (1997).

During radiocarbon picking various animal fossils were found. *Candona rectangulata* Alm, often found as juveniles, represented the only ostracode taxon found down to a depth of 481cm, with the exception of a single *Cytherissa lacustris* Sars specimen found at 331cm depth. In addition, a number of freshwater foraminifera were found and mounted on a paleontological slide, but remain unidentified.

3.3.3 Other Measurements

The relative sediment density profiles derived from the x-radiographs proved difficult to interpret, as there are both discrepancies and some similarities among the three cores analyzed. The mean values of the series are similar (Fig 3.3). Cores S and P are more parallel from the deeper portion up to 170cm, and show an increase in sediment density around 230cm. The deepest section of Core B, up to 100cm depth agrees with Core P.

3.3.4 Chronostratigraphy

The upper section of Core B was incrementally dated through varve counting, which is presented in detail in the following chapter. Six radiocarbon dates were obtained from Core T, with an additional date obtained from a *Dryas* leaf from Core E. In addition a shell, collected from the shore of Lake DV09, was dated to estimate uplift from marine inundation (Table 3.2). The shell of *Mya truncata* L., a littoral bivalve, can be used to estimate marine inundation within an approximate water depth from 0-20m, and this fits in with the lower dates on the sediment.

Although the lowermost 6 dates fall into a line, the date at 89-90cm appears too old. The varve date (AD1120; 830 years BP) of the layer containing the dated material is

4576 years younger than the radiocarbon date (median 2σ calibrated age: 5406 yrs BP), and is not included in the age-depth curve shown in Fig 3.4. Using this hypothesized chronology, this radiocarbon date is excluded, although the reason for the old date is not clear, perhaps it consists of reworked material. A curve was fitted to the radiocarbon dates, as well as the basal section of the varve-dated chronology to provide the chronology for this core (Fig 3.4).

We can explore an alternate hypothesis for the chronology of this core as well. The radiocarbon dates, including the one at 89-90 cm that we reject, do fall along a line. Thus, an alternative interpretation is explored in Fig 3.5. The intercept of a linear regression fit to all of the radiocarbon dates crosses 0 at just below 5000 cal yrs BP, possibly indicating that the dates are 5000 years too old. This is close to the 4576-year gap estimated using the varve dating. If the dates are 4576 years too old, then the age-depth curve remains linear, yet the slope suggests higher sedimentation rates than the cumulative varve width suggests, and the entire sediment column would be ~2500 yrs BP. There is little reason to believe that there was no sediment accumulation from 8000-2500 yrs BP, especially as this was supposedly the warmest part of the Holocene. We therefore do not accept this interpretation, but do present it as a possibility.

Another possibility is that all radiocarbon dates are unconformable material, due to heavy sediment reworking possibly during the mid Holocene. Because of the discrepancy between the predicted sedimentation rates and the young age of the entire sediment column estimated by the curve shown in Fig 3.5, subsequent results are discussed in the content of the age-depth curve of Fig 3.4. All of these dates and the varve chronology, except for the unconformable uppermost radiocarbon date from 89-90

cm, were used to create an age-depth curve for the sediments of the lake (Fig 3.1). This curve implies a rapid sediment accumulation in the early and mid Holocene and a rapid decrease in the late Holocene.

3.4 Discussion

3.4.1 Lake Ontology (Fig 3.1)

The site is estimated to have been deglaciated by 9500-9700 yrs BP (Dyke, 1999), and uplifted from marine inundation by 7480-8350 yrs BP, as indicated by the shell date and by Dyke (1998). After uplift, rapid sedimentation into the lake began, lasting until 6500 yrs BP. The sediment colour transition at 490-530cm (~7250 yrs BP) from greyer sediments to light orange sediments above may be due to freshening or deep water oxygenation, although further analyses are needed to confirm this hypothesis. An increased amount of organic detritus was deposited from 5000-6500 yrs BP, which may reflect increased biological production surrounding the basin or within the lake. Around 4500 yrs BP, a 15cm, homogenous, massive layer was deposited, corresponding with peaks in magnetic susceptibility, which was also difficult to core through (Gajewski, personal communication). A peak in the oxygen isotope record of Devon Island Ice Cap at this time suggests (Fig 3.6) warmer conditions on Devon Island. This may have affected precipitation regimes, which would affect erosion in the watershed, and/or affected the depth of penetration of summer overturning currents due to decreased ice cover and increased water temperatures. From 4500-1500 yrs BP, there is a decrease in the amount of visible macroscopic plant detritus, although the sediment organic content is higher (Fig 3.2), and there is a reduced presence of observed fossils, especially

foraminifera. Interpretation of this section is hampered by the lack of datable material; and the layered sediments were not extensively studied. Since at least ~1550 yrs BP, thin laminations have been continuously accruing, where the past 1600 organic-clastic laminae couplets have been interpreted as varves based on lead-210 dating and the apparent annual nature of the sediment deposition. The varves do not seem to be preserved to the same degree across the distal part of the lake, possibly due to bioturbation. The varves of Cores P and S are less discrete than within Core B. During the past century, changes in diatom abundance and assemblages suggest that significant environmental changes have been occurring (Gajewski *et al*, 1997), although the possibility of diatom dissolution cannot be discounted.

3.4.2 Interpretation of the Sedimentology

Core T magnetic susceptibility may be lower than the other cores because it is from the deepest portion of the lake (13.64m), where magnetic mineral-bearing sediment may have settled before reaching this distal region. The high variability in multiple cores between 200-350cm may be due to an increased presence of visibly larger clasts, either due to higher energy conditions or increased ice rafted debris from eroding shorelines. Both of which suggest warmer conditions during the mid Holocene, where the chronology is based on the radiocarbon dates.

The sediment throughout the core is dominantly silts, with some clay content, and some sandier layers, as well as occasional intermittent sand grains within some of the varves in the more recent sediments. The sand layers may be from sediment reworking or from colluvial inputs from the slope due to failures. The uppermost radiocarbon date

(5350-5470 yrs BP), which appears too old may be due to reworking of sediments from the mid Holocene period during the Medieval Warm Period possibly due to changes in overturn and exposure to wind turbation due to decreased ice cover.

Virtually every observed ostracode at all depths was found as a single valve, as opposed to intact carapaces (bivalve), which may be an indication of low sedimentation rates (Oertli, 1971; Brasier, 1980). The ostracodes identified represent two of the seven species reported in arctic lakes (Bunbury and Gajewski, submitted). The single *Cytherissa lacustris* Sars valve, found at 331cm depth, was heavily ornamented, which could be due to higher ion concentrations within the lake water (Bunbury, personal communication), although this observation is based on a single adult specimen.

The low sediment organic matter content and biogenic silica are indicative of low lake productivity. However, low BSi content may be due to post-depositional dissolution of the diatoms, while the low organic content may be due to grazing by chironomids, ostracodes, forams, and other organisms.

3.5 Conclusions

Following uplift from marine conditions (7480-8350 yrs BP) sedimentation into the lake was rapid, slowing by the mid Holocene where the sediment is layered, some of which contained higher amounts of plant detritus. The upper sediments have thin laminations, which are varved for at least the past 1600 years. The lake sediment has a low organic content, but the presence of subfossils indicate that the lake supports communities of organisms. The sediments of DV09 seem to have been affected by climate variability throughout the Holocene.

Core	Water Depth (m)	Length (m)	# of Drives	Analyses Conducted
B	13.2	1.47	2	Magnetic susceptibility, x-ray density, varve widths
E	13.4	6.26	7	Magnetic susceptibility, 1 radiocarbon date
P	13.01	2.65	4	Magnetic susceptibility, x-ray density
S	13.11	3.30	5	Magnetic susceptibility, x-ray density
T	13.64	6.48	10	Magnetic susceptibility, PSD, LOI, BSi, radiocarbon dating, fossil identification

Table 3.1: Summary information of cores used for sedimentologic analyses. Magnetic susceptibility was measured on all other cores.

Calibrated Age cal. yr BP						
Depth (cm)	Core	^{14}C yr BP	Sample ID	Mean 1σ range	Mean 2σ range	Material dated
89-90	Core T	4600 ± 40	Beta-242790	5422	5405.5	Plant fibers, mosses, Chironomidae head capsules
303-306	Core T	5870 ± 40	Beta-240752	6697	6702	Plant fibers, mosses, Chironomidae head capsules
329-332.5	Core T	5860 ± 40	Beta-236401	6687	6676	Plant fibers, mosses, Chironomidae head capsules
347	Core E	5730 ± 40	Beta-146688	6514.5	6536.5	*Dryas* sp. (L.) leaf
353-355	Core T	5910 ± 40	Beta-235291	6713	6726	Plant fibers, mosses, Chironomidae head capsules
394-398	Core T	6180 ± 50	Beta-236402	7069	7063.5	Plant fibers, mosses, Chironomidae head capsules
478-481	Core T	6500 ± 40	Beta-235292	7438	7401	Plant fibers, mosses, Chironomidae head capsules
-	-	7160 ± 80	TO-7929	7630.5	7639.5	*Mya truncata* (Linnaeus, 1758) valve

Table 3.2: AMS radiocarbon dates, calibrated using IntCal04 (Reimer *et* al, 2004) and Marine04 curve for the shell date (Hughen *et al*, 2004) (full details in Appendix 5).

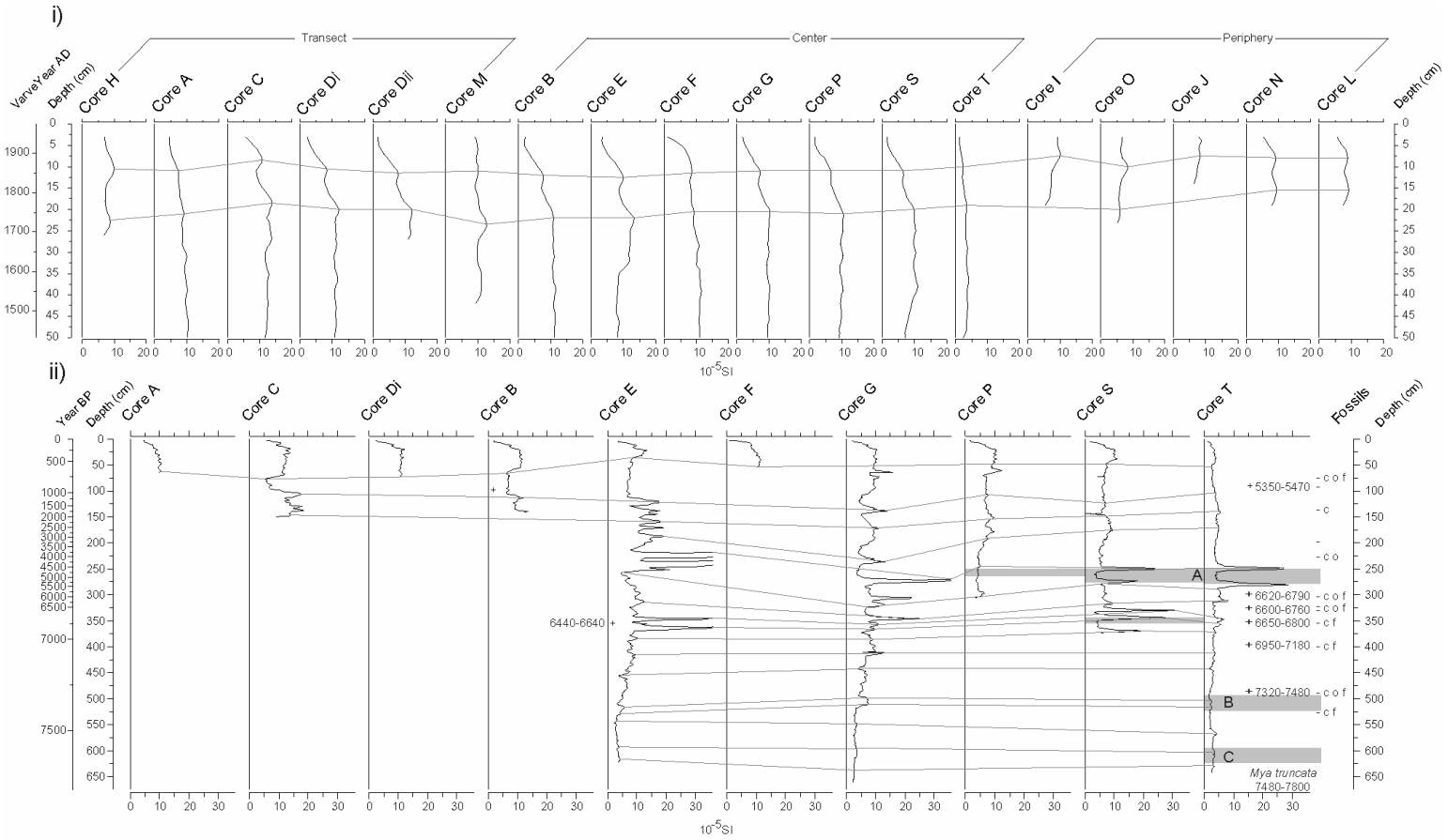

Fig 3.1: i) Magnetic susceptibility profiles of all cores, truncated at 50cm, and ii) "Wiggle-matched" magnetic susceptibility profiles (gray lines) of cores longer than 50cm. 2-sigma calibrated radiocarbon dates (+), subfossil presence at sampling sites (-), where c is chronomid head capsules, o is ostracode valves, and f is forams. Grey zones are A) a thick homogenous bed, B) a transition zone between deeper grey sediments and orange-tan sediments above, and C) a portion containing dark grey pebbles.

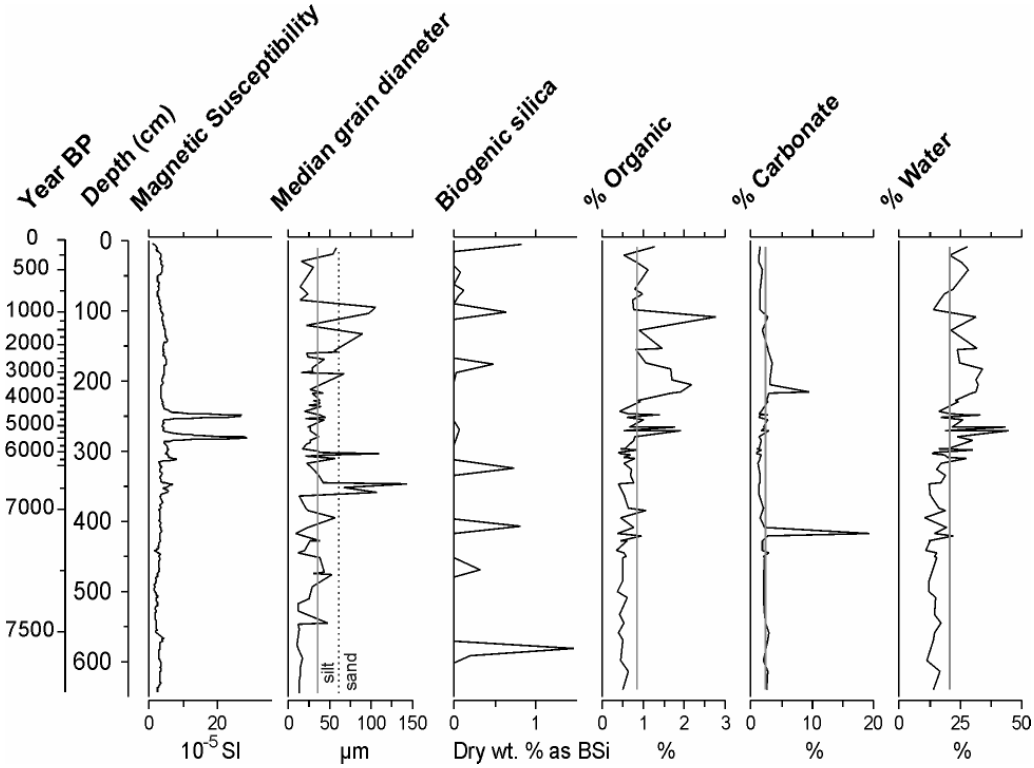

Fig 3.2: Core T sedimentologic measurements. The vertical grey line shows the respective series mean, equal to 35.11µm for the median grain size diameter, 0.844% for organic matter, 2.54% for carbonate content, and 20.88% for water content.

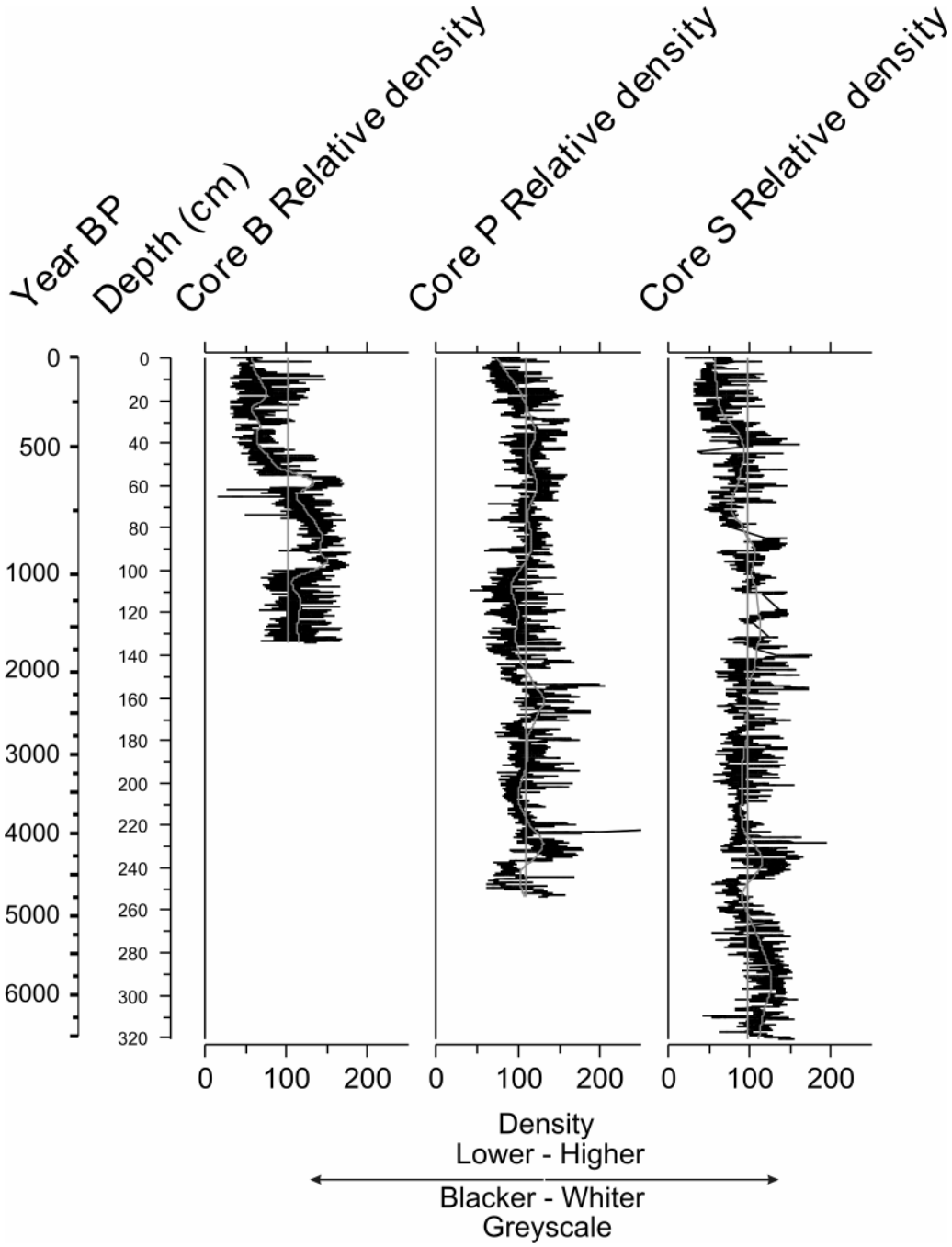

Fig 3.3: Relative sediment x-ray density profiles represented by greyscale values 0 (black) to 255 (white). The grey vertical lines are the respective mean values of 102.2, 101.0, and 96.3. The grey curves are 0.1 span, 0 iterations lowess splines.

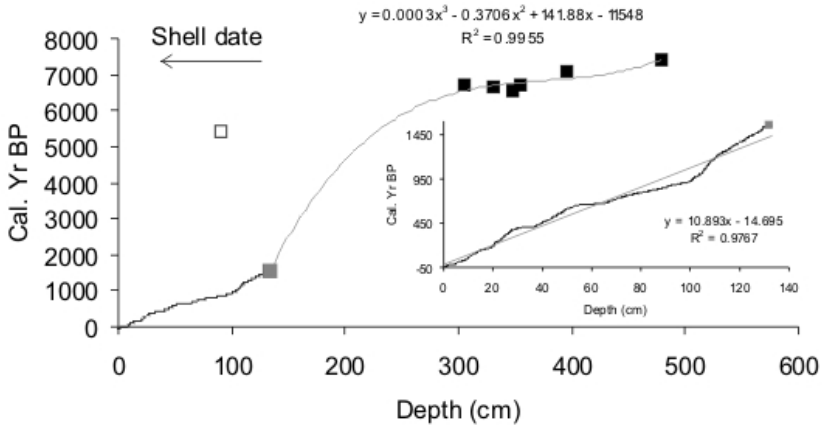

Fig 3.4: Chronostratigraphy, black curve is the cumulative varve depth, the grey square is the last known varve date, black squares are the median 2σ radiocarbon dates, the white square is the radiocarbon date interpreted as too old and is not included in the age-depth curve, and the shell date estimating uplift is included with an arrow. The inset graph shows the cumulative varve depth from Core B and a linear regression.

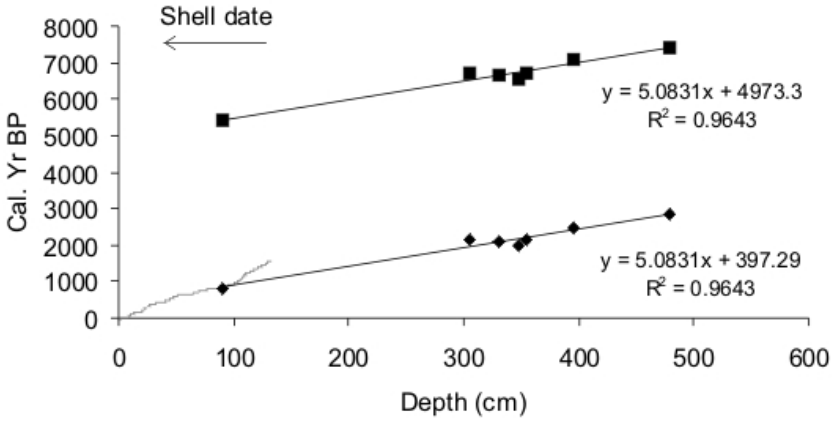

Fig 3.5: Chronostratigraphy assuming all radiocarbon dates are correct, and radiocarbon dates corrected for the difference between the varve age and radiocarbon age. Black squares are the median 2σ radiocarbon dates, black diamonds are varve-age adjusted radiocarbon dates, and the grey curve shows the cumulative varve depth.

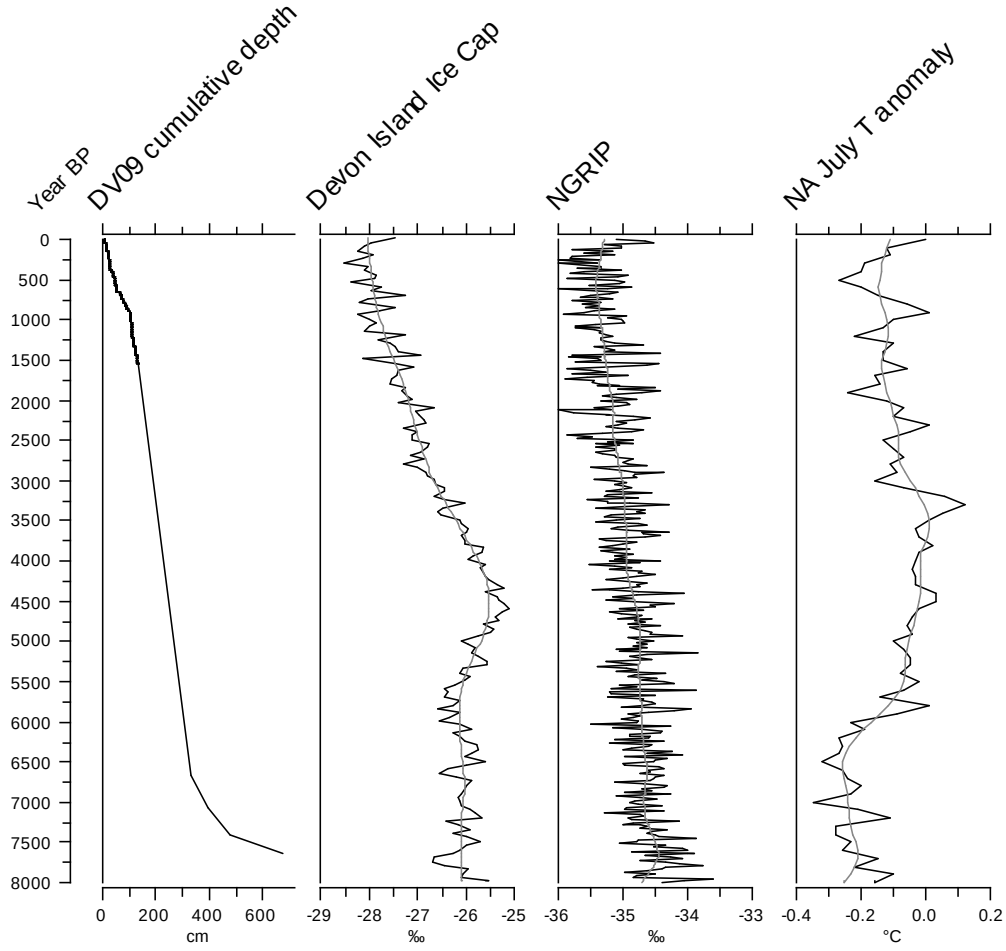

Fig 3.6: Age-depth curve of the sediments of DV09 (excluding the uppermost radiocarbon date), the 50-year $\delta^{18}O$ record from Devon Island Ice Cap (Fisher, 1979; Fisher *et al*, 1983), the NGRIP 20-year averaged $\delta^{18}O$ record (GICC05) (Vinther *et al*, 2006; Rasmussen *et al*, 2007), the pollen-based reconstructed mean July temperature anomaly of North America (100-year resolution) (Viau *et al*, 2006). Grey curves are 0.1 span, 0 iterations lowess splines.

Results (Part 2)

A 1600-year climate-proxy record inferred from the annually-laminated sediments of Lake DV09, northern Devon Island, Nunavut, Canada

4.1 Abstract

A 147cm sediment core from Lake DV09, northern Devon Island, Nunavut, Canada (75° 34'34"N, 89° 18'55"W) contains annually-laminated (varved) sediments, providing a 1600-year record of climate variability. A minerogenic lamina deposited during the annual thaw period and a thin deposit of organic matter during the summer, and through settling over winter, together form a clastic-organic couplet each year. The thinnest varves occur from AD800-1050, and are thickest from AD1100-1300, during the Medieval Warm Period. The relative sediment density is also highest during this period suggesting increased sediment transport energy. The coldest period of the Little Ice Age appears to be during the AD1600s. Varve widths over the past century indicate climate warming in the region.

Key words: varves, lake sediments, paleoclimate, Canadian Arctic, 'Medieval Warm Period', 'Little Ice Age'

4.2 Introduction

High-resolution climate records from the Arctic can be used to place the current observed global climate warming and subsequent environmental changes in a longer-term context. However, instrumental records largely span the latter half of the twentieth century, and meteorological stations are sparsely located. Many proxy-climate records of longer duration have only low temporal resolution (Atkinson and Gajewski, 2002). Many of the available annually-resolved climate-proxy records from the Canadian Arctic often only cover the past few centuries (Hughen *et al*, 2000; Lamoureux, 2000; Francus *et al*, 2002; Smith *et al*, 2004; Lamoureux *et al*, 2006) or up to the past millennium (Fisher and Koerner, 1994; Lamoureux and Gilbert, 2004; Besonen *et al*, 2008) or slightly longer (Moore *et al*, 2001), and longer records are limited (Paterson *et al*, 1977; Lamoureux and Bradley, 1996). These factors highlight the importance of studying more natural climate-proxies, such as varved lake sediments, to gain an understanding of past Arctic climate variability at a high resolution over a longer time period.

In this paper, we report the analysis of laminated sediments from Lake DV09, which provides a 1600-year record of climate variability of the northern coast of Devon Island, Nunavut, Canada. A previous study of the past 150 years of sedimentation indicated that the laminations are annually deposited, i.e. varves (Gajewski *et al*, 1997). In this study, we extend the record back in time, interpreting the sediment record as a proxy for past climatic change in the region.

Lake DV09 (unofficial name; 75°34'34"N, 89°18'55"W) is situated within a nonglaciated watershed that extends 12.5km inland, and drains an estimated catchment area of approximately 55km^2. This freshwater lake is located within 1.5km of the

northern coast of Devon Island at an elevation of roughly 35m asl, and has a maximum measured depth of 16m (Gajewski *et al*, 1997). It is nearly rectangular in shape and covers an area of 3ha. The lake is largely closed, with no inflow channel and a single outflow at the north end, which connects to the main river and discharges northward into the Thomas Lee Inlet (part of Bear Bay). However, there may be ephemeral inputs from the slopes and plateau above.

The lake water is ultra-oligotrophic (Outridge *et al*, 2007) and water chemistry data has been published previously (Gajewski *et al*, 1997). Ice, up to 2m thick, covers the lake for most of the year. A moat of melt water develops during summer, and partial ice cover may persist throughout the summer months. Freeze up likely begins in September and intensifies over the autumn and winter.

The local bedrock is Middle Ordovician Bay Fiord Formation, regionally composed of dolomite and gypsum with limestone, shale and siltstone. To the southwest and the west of the lake are steep cliffs, made up of Cornwallis Group rocks consisting of limestones and dolomite (Thorsteinsson and Mayr, 1986) that overlay the Paleozoic rock in which the lake is situated. A till veneer surrounds most of the lake which contacts an alluvial terrace to the northeast that may have formed after isostatic rebound resulting in damming of the lake (Gajewski *et al*, 1997). The vegetation cover is northern Arctic tundra (Elvebakk, 1999) with very sparse low-lying vegetation around the lake.

The sediment-source areas seem to be from the steep slopes and possibly from the plateau above during the rapid spring melt period where runoff and slushflows may enter the lake. Fans are present on the slopes to the northwest of the lake. Water and sediment

inputs to the lake may come from aeolian inputs, surface runoff, colluvium from the proximal cliffs, slopewash, and possible slushflows during the spring melt.

The study site may have been free of the ice margin around 8500-8700 ^{14}C yrs BP (~9500-9700 yrs BP) (Dyke, 1999). Driftwood and shell samples from raised beaches suggest that the lake likely emerged from a maximum marine limit of 79-102m (Dyke *et al*, 1991; Dyke 1998) around 7500-8125 ^{14}C yrs BP (~7800-8350 cal yrs BP) (Dyke, 1998).

The nearest meteorological station with a relatively long record is Resolute Bay, Cornwallis Island, where the mean annual temperature is –16.4°C with a standard deviation of 1.1°C, and the mean annual total precipitation is 150mm, most of which falls as snow, and an average of 40 frost-free days per year (1971-2000 climate normals; Environment Canada, 2002).

4.3 Methods

4.3.1 Field Methods and Sediment Description

From June 15-26, 1996, 18 sediment cores were recovered using a 5cm-diameter Livingstone square-rod piston corer from the ~2m thick ice surface of DV09. In this paper we will discuss the analysis of the laminated sediments preserved within Core B. Whole-core logging of the magnetic susceptibility was done using a Bartington Instruments Ltd. 60mm-diameter loop sensor (Type MS2C) at 1cm intervals. In the lab the cores were split, and a 1cm-thick slab was cut off, which was then x-rayed at the Ottawa General Hospital using a Siemens Axiom Aristos MX x-ray machine set at 60.0kv, 2.00mAs, for 500ms at a source-to-image distance (SID) of 115cm. A metal

calliper open to 10.0cm was also imaged for calibration. Greyscale values were extracted from digital x-ray images (8-bit greyscale TIF files 120dpi) along a transect at the center of each core using NIS-Elements BR 3.0 software.

Lead-210 dating of the uppermost sediments was reported previously (Turner, 1995; Gajewski *et al*, 1997). Subsequently, other short cores from this lake were dated using lead-210, confirming the annual nature of the uppermost laminae (Outridge *et al*, 2005; Stern *et al*, 2005).

A coarse layer at 86.9cm depth contained higher amounts of organic detritus, however additional material was needed and the sample was combined with material from the same layer identified in Core T (89cm), which together yielded enough material for AMS radiocarbon dating. The sample contained mainly plant matter and mosses with occasional chironomid larvae head capsules. Only one radiocarbon date was obtained within the varved sediments reported in this paper; several others were obtained from deeper within the sediment in other cores and are discussed in the previous section. The dating was performed by Beta Analytic Inc, Miami, FL, and calibrated using IntCal04 (Reimer *et al*, 2004).

4.3.2 Varve Chronology

An organic and a minerogenic layer together represented the sediment accumulation over one year, making these two units a varve couplet. The succession of these two identifiable units down core was the basis to creating the varve chronology. Varves were identified by inspecting the moist core surface under a stereomicroscope at 6.4 to 40x magnification. A thin strip of clear mylar plastic placed across the sediment made dot

counting with a permanent marker possible, similar to dot counting a tree core. Varve widths were measured under a stereomicroscope using an Acu-Rite Absolute Zero II bench micrometer with a precision of 0.001mm. MeasureJ2X software was used to record the digitized measurements.

Marker beds are the stratigraphic equivalent of marker rings used in dendrochronology. Distinct laminae, with readily identifiable qualitative characteristics, acted as marker beds that aided in varve counting and was used to crossdate the multiple varve width measurement series. Crossdating (Fritts, 1976) the varve width measurements created a single composite series, which was achieved by pattern matching in a spreadsheet, and aided by the identified marker beds. Creating a composite series acted to reduce the varve count error of any single measurement series. Once the series were crossdated, the average width values for each varve year for the composite series could be determined. Varve widths that agreed across all records were averaged, varve layers that needed to be combined were added together before averaging, and missing values from one series were supplemented by averaging the values from the other agreeing series.

4.5 Results

4.5.1 Sediment Stratigraphy

The core chosen for analysis, Core B, was 147cm long and recovered in 2 coring drives from a water depth of 13.2m. Fresh sediment was a solid black colour, with laminae difficult to discern. The sediments oxidized rapidly after splitting, tending toward an orange-beige and grey colouration, similarly observed in other Holocene-aged Arctic lake

sediments (Wohlfarth *et al*, 1995). The sediment consisted of lamina couplets down the length of the core. Each varve contained a minerogenic lamina of variable thickness, largely consisting of silts, with the thicker layers often visibly normally graded, and a thin, dark brown, organic-rich lamina, characterized by filamentous material and mat-like plates. The organic-rich layer was generally always thin and occasionally quite inconspicuous. In every varve, the minerogenic lamina dominated the varve width. This layer was commonly grey to a grey-orange colour, and often quite homogeneous. Coarser material and occasional very fine pieces of organic detritus were almost always deposited toward the base of the minerogenic lamina.

The sediments of Core B could be divided into 3 main sections based on the nature of the laminae (Fig 4.1). The top 52.4cm contained fine and discrete varves, with intermittent thicker varves, of orange-beige and grey colour, striped with brown organic laminae, and containing few to no larger clasts or organic matter. The second section begins at 52.4cm depth where the varves are consistently thicker, to a depth of 99.1cm depth. The clastic lamina often diffused into the darker organic lamina, which then ended abruptly and discreetly. Prominent within this section were two sand layers, each just over 1cm thick, containing higher amounts of organic detritus at 86.9 and 98.9cm, the latter of which ends this section. Following the second sand layer, to a depth of 133.3cm, are very fine varves, similar to those found in the first section, but accompanied by intermittent thicker varves that had a clastic component that was often more grey in colour. There were occasional varves containing isolated, rounded, quartz clasts within the minerogenic lamina, and organic matter remained extremely sparse in this section.

4.5.2 Chronology

The crossdated composite varve width series of Core B (Fig 4.1) was compiled using 8 measurement series (see Table 4.1). To a depth of 55.5cm, two transects were counted, measured and crossdated down the middle of the core, roughly covering the first sediment section outlined above. From 55.5-98.9cm, values from three transects were crossdated, covering the second section, and from 98.9-133.3cm, three series that cover the third section were crossdated. The counting error between the series to a depth of 55.5cm was 2.6% (based on 2 series), <0.01% from 55.5-98.9cm depth, and 5.1% from 98.9cm to the bottom of the core (based on 3 series each). The low counting error illustrates the coherency of the varved sequence within the sediments of Core B.

The varve record (Fig 4.2) begins with slightly elevated varve widths punctuated by intermittent thicker varves from AD399 until close to AD750, then the varve widths are thinner until AD1050 (Table 4.2). The widths are especially thin from AD750-950. Between AD800-1050, there is also a reduction in the number of thicker varves. Varve widths are generally thicker from AD1050 until approximately AD1350, reaching sustained maximum values between the AD1060s and AD1080s, as well as the AD1140s. Values remain generally higher yet decrease slowly until AD1250, then increase again until just after AD1300. From the 14th century until the AD1530s, varve widths show multi-decadal scale variability. The thickest varve in the record occurs during the mid-1540s and is followed by almost 3 decades of sustained thicker varves. The rest of the 16th century has generally lower varve widths, and there are consistently thinner varves during the AD1600s. There are some elevated values from AD1750-1850, although the

varve thicknesses during this period are highly variable. From AD1850 until AD1996 there is a slight trend toward slightly thicker varves.

The relative x-ray density of the sediments is represented by greyscale values per pixel, where the less dense sediments appear black (values near 0), and more dense sediments appear white (values near 255). The relative sediment density profile of a transect of pixels down the middle of the core largely parallels the broad pattern of the varve width measurements (Fig 4.1; Table 4.3). From AD399 to just after AD1000, the average value was around 115. The greyscale values are higher from around AD1050-1100, where they fall sharply and then increase again until another decrease around AD1150. The values remain above average (102.2) yet decrease until a peak at AD1275, then fall sharply to below average around AD1300. Sediment density continually decreases throughout the next few centuries, with a few short increases that parallel the intermittent thicker varve widths, and reach lowest values before the end of the 17th century. From AD1700 until the turn of the 20th century the density increases slightly, yet remains below average; however, there is an increased frequency of peaks above the mean. A peak centered on AD1980 is the only above-average peak during the 20th century.

A 14cm core from DV09 collected previously was ^{210}Pb dated, and CIS and CRS modeled dates fit well with the varve width record (Gajewski *et al*, 1997). The varve width chronology presented in this paper does show some discrepancy with the original varve width chronology (covering AD1843-1993); however, the overall trend of the two series is in agreement (Fig 4.3). The series presented here has generally lower varve width values than the 1997 record. From the late AD1880s until the AD1950s the records

are in good agreement, with some discrepancy between the mid 1950s to mid 1960s. The coherency of the varve records and the lead-210 dating is quite high, with a slight discrepancy between AD1954-1964 (Fig 4.4).

The AMS radiocarbon dating provided an age of 4600 ± 40 (2σ calibrated age: 5406 yrs BP). This is significantly older than the age estimated by varve counting (830 years BP; AD1120), a discrepancy of 4576 years.

4.5.3 Magnetic Susceptibility

From 141-122cm depth the magnetic susceptibility (Fig 4.1) remained at mean values ($8.7x10^{-5}$ SI), then slightly increased between 122-108cm (AD600-850). Following this peak, values remained very low from 105-60cm (~AD850-1275), then increased remaining above average until AD1750. Above 20cm, the values decreased toward the top of the core (from AD1750s-1996) with a slight perturbation around AD1900.

4.5 Discussion

4.5.1 Interpretation of the Varved Sediments of Lake DV09

The minerogenic lamina likely forms during late spring/early summer when increasing temperatures melt the snowpack, and the melt water transports clastic material to the lake. The presence of larger clasts as well as occasional organic detritus also suggest that minerogenic lamina is related to inwashing. There were occasional varves containing isolated, rounded, quartz clasts within the minerogenic lamina, which were never observed within the organic-rich lamina, suggesting that the minerogenic layers were related to the spring/summer period. The organic-rich lamina is interpreted as a

biolamination forming during the biologically-active summertime, or which has settled from the water column during the less turbid autumn and winter months. A similar annual cycle of sediment deposition forming clastic-organic couplets has also been described in varved sediments of Lake Lehmilampi, eastern Finland (Haltia-Hovi *et al*, 2007). Alternatively, the organic component may form as a mat at the water-sediment interface and may be deposited *in situ* as successive organisms die off and then are covered during the following inwashing during the thaw. Biolaminations have been have been described elsewhere in coastal lakes on Devon Island (Chutko and Lamoureux, 2008) and can be significant to sedimentary processes and to the sediment fabric (Noffke *et al*, 2001).

This cycle of deposition suggests that the varve widths of DV09 are largely controlled by the spring and summer temperatures, controlling the flow of snowmelt water and interflow from the active layer on the slope faces, which influences the energy available to transport clastic material to the lake. The organic material contributes only a minor amount to the overall varve thickness. Cooler polar summer phases lead to thinner varves; whereas, thicker varves are deposited during warmer polar summer conditions. Similar controls on varve thickness have also been reported at Lower Murray Lake, Ellesmere Island (Besonen *et al*, 2008) and Sawtooth Lake (Francus *et al*, 2008). In all cases, snow accumulation, summer precipitation, and slope stability may also influence sedimentation; however, polar summer temperature is likely a dominant control.

The relative sediment density does not seem to reflect variability over the course of one varve year. It is not clear whether this is due to a true lack of annual patterning in the density of deposited sediments, insufficient x-ray resolution, or x-ray scattering at the surface that could be overcome by epoxy impregnation and polishing of the sediment

slabs (cf. Lamoureux, 1994; Lotter and Lemcke, 1999). However, at a multi-annual and larger time scales, the relative sediment does show a relation with varve thicknesses (Fig 4.1; Table 4.2; 4.3). This is evidenced by the similarity in the overall trend of the varve widths and the relative sediment density. An interpretation of this similarity is that both varve widths and relative sediment density reflect changes in the energy available to transport material to the lake bottom. Both an increased amount of sediment as well as denser material are transported to the basin as a consequence of changes in the hydroclimate regime. Colder periods are characterised by the presence of thinner varves and a decrease in relative sediment density, whereas warmer periods show a tendency toward thicker varves and increased density. No analyses were performed to clarify if the density differences were due to variability in the number of grains per unit volume, from changes in the densities of individual grains (mineralogical differences), or a combination of both; however, the interpretation of relative density relating to the energy available to transport the material remains probable.

The magnetic susceptibility remains relatively low throughout the core, with low variability, possibly due to the nature of the sediment-source material. Decreases in the magnetic susceptibility may be related to changes in sedimentation rates, as a slightly increased rate may increase the randomness of magnetic domains during deposition, causing sections with thicker varves to have lower susceptibility. The higher susceptibility may be due to an ability for the less dense and fewer clastic particles to be aligned with the ambient geomagnetic field during and immediately following deposition and therefore have a slightly increased susceptibility when measured. The decrease in

magnetic susceptibility from 20cm to the surface may be due to an increase in sediment water content.

4.5.2 Climate and Varve Width Variability

Allochthanous sediments enter Lake DV09 through a number of mechanisms. Aeolian sediment can be deposited on the winter ice cover and enter during the spring and summer, and additional aeolian material can be deposited while the ice cover is reduced or absent during the summer season. The coarsest and most abundant sediments arrive during the rapid spring/summer thaw, likely during June in many years, when the melt water from the winter accumulation of snow is available to transport the sediments. Late lying snow, which may be stored on the shaded proximal cliffs (the north-facing slope) or in depressions on the plateau, may serve as a rapid or steady source of flowing water that can introduced material to the lake over the summer (Fig 1.3; 1.5), as may the occasional summer snow- or rainfall event. The region is a polar desert, so the spring deluge is likely the most significant source of transport energy for sediments; although, additional field measurements are necessary to investigate this.

Thawing of permafrost during warmer periods may act to free up sediments that can be entrained and transported to the lake. Thermokarst and failures on the cliff faces may rapidly input a large amount of sediment and possibly sustain increased sedimentation from the scar for a number of years after the event (Bowden *et al*, 2008) This may explain the pattern of a thick varve being followed by a number of moderately thick varves. Geomorphic processes such as these in cold environments may be largely controlled by climate, which supports the relevance of using this varve record to

understand paleoclimate. Additional field measurements would need to be conducted to understand this further.

4.5.3 Chronology

Some of the discrepancy between the new varve width series and previously published series may be due to the different water depths that the cores were recovered from, or due to some differences in varve interpretation. The overall trends are in agreement, suggesting that both cores record a common response to external forcing.

The discrepancy between the uppermost radiocarbon date and varve count suggests that this radiocarbon date is too old (see 3.3.4 Chronostratigraphy). This may be due to 1) reworking of sediment that was already deposited within the basin, which was then redeposited, 2) mass wasting of material stored in the permafrost of the proximal cliffs, 3) possible contamination of the sample, 4) a lake water reservoir effect, or 5) a terrestrial source of "old" carbon. Although the alternative – that the varves are not annual – is possible, this seems less likely, as the close correspondence of the lead-210 and varve counts in the upper 14cm suggests.

There are many instances of problematic dates in Arctic lake sediments (Gajewski *et al*, 1995), and this seems a more reasonable assumption for this site as well. In the remainder of this study, we assume the varves are annual. The discrepancy between the uppermost radiocarbon date and varve counts suggests that the radiocarbon date is too old. This has been observed in other Arctic lake sediments; although the discrepancy at DV09 is larger than most instances.

A hardwater effect causing a 1600-year age offset was estimated for the chronology of Lake MB01, southwest Victoria Island (Peros and Gajewski, 2008), and has been observed with an offset of up to 2000 years at other arctic lakes (Abbott and Stafford 1996; Child and Werner 1999; Fallu *et al,* 2004).

Picked material was dated from a varved sediment core from Lower Murray Lake, and one date was 915 years older than the varve-estimated date, while another date was over 46 000 ^{14}C yrs BP. The prior value was interpreted as likely reworked or redeposited material, while the latter date may have been Tertiary wood (Besonen *et al*, 2008).

Multiple humic acid radiocarbon dates did not conform to the tephrachronology established from the sediments of Haukadalsvatn, a lake in western Iceland. A maximum offset of just over 2000 years was found and interpreted as a possible terrestrial source of "aged" carbon (Geirsdóttir *et al*, 2008).

4.5.4 Interpretation of the DV09 Varve Record (Fig 4.2)

From the beginning of the record (AD399) until the late AD750s, the average varve widths are slightly lower than the series average, yet there is a high frequency of intermittent thicker varves (Table 4.2). Some varves within this period also contain intermittent quartz sand grains, which may reach the deeper basins of the lake through ice rafting. This is interpreted as a cooler climate, although the variability is high, and the average sediment density remains relatively high (greyscale value of 120±40). The intermittent thicker varves, and higher sediment density is indicative of increased energy available to transport sediment to the lake. The thicker layers may be due to years with increased snow, which melts over the summer, or increased summer precipitation. From

AD750-950, the average varve width is half that of the entire series (Table 4.2) and sediment density decreased, with fewer thick layers until after AD940. This is interpreted as the coldest period, due to a decrease in energy available to transport material into the lake during the thaw. There may have been extended ice cover at this time, resulting in thinner varves, and a reduction of the number of thicker varves. The lack of thicker varves and lower sediment density may be evidence of decreased winter snow cover, or a decrease in the rate of snowpack melt during the thaw.

From AD1000-1300, the varve widths are much thicker and the sediment density increases. Between AD1050-1200, the sediment density remains high and has reduced variability, although the widths and density decrease throughout the period. The increased varve widths and higher sediment densities may be indicative of higher energy available to transport clastic material into the lake basin. Sedimentation may have increased throughout the entire summer period, evidenced by the diffuse boundary between the minerogenic and organic laminae. Interestingly, throughout this period, the magnetic susceptibility remains lower (Fig 4.1).

Between AD1350-1600, the varve widths are just above the series average and the variability is high, yet sediment density falls below average values. There is a short period, from the AD1540s-1570, of increased varve widths that may be a period of warmer temperatures. From the end of the AD1500s-1850, the varves are thin and the sediment density is quite low, which may be the coldest phase of the Little Ice Age and, indeed, this time encapsulates the Maunder Minimum. The average varve width during the Maunder Minimum is very close to the previous cold period interpreted between

AD750-950 (Table 4.2). The varve widths increase after AD1850 to the present, which could be due to reduced sediment compaction in the uppermost sediments.

4.5.5 Comparison with Other Arctic Climate and Proxy Records

Lake DV09 varve widths, data from other Arctic lakes with varved sediments, and some other annual climate-proxy records were compared to attempt to determine the synoptic-scale climate of the past millennium. There are few arctic high-resolution climate records covering the entire DV09 varve record, and this record can be divided into three prominent phases (Fig 4.2). The beginning of the record shows thinner varves, and includes the thinnest varves between AD750-950, which is followed by thicker varves from AD1050-1315, and then thinner and more variable thicknesses from AD1316-1996.

A cold period between AD750-950 is also seen in the oxygen isotope records from the Greenland ice cores; although unlike DV09, the period is preceded and followed by higher oxygen-18 concentrations (Fig 4.5). The earliest few centuries of the varve record from Donard Lake (eastern Baffin Island) (Moore *et al*, 2001) also indicates relatively cool conditions during and slightly beyond this period. This indicates a large-scale response to cooler air temperatures across the eastern Arctic. These thin varves, interpreted as a cold period, are out of phase with the cold period of AD650-850 of a pollen-based reconstruction of North American July temperature anomalies (Viau *et al*, 2006). This reconstruction is dated by radiocarbon and has a resolution of 100 years; given this dating limitation, it may be possible that the cold period indeed lines up with the varve width record. Alternatively, it may be that the cold period was a local phenomenon. The cold phase does not appear at the hemispheric scale, based on

composite Northern Hemisphere land plus ocean temperature anomaly reconstruction (Mann *et al*, 2008). Some of this discrepancy may be due to the varve width record responding to summer temperatures, whereas the temperature anomaly reconstruction reflects annual temperatures at a larger geographical scale.

Over the past millennium, the varve width record of DV09 shows a warm period followed by a cooler period (Fig 4.6). From AD1050 until the 14th century the average varve width is double that of the entire varve record (Table 4.2), which may be due to a warmer climate producing a faster snowpack melt and leading to increased sediment input. This period is also characterised by an increase in relative sediment density, interpreted as a period of increased energy available for sediment transport (Fig 4.1; Table 4.3). The warm period at this time leads to an increase in available sediment transport energy at DV09, and has similarly been observed in the varved sediments of several lakes in the Canadian Arctic (Moore *et al*, 2001; Besonen *et al*, 2008); although, there appears to be temporal differences in the timing and duration (Fig 4.6).

Thicker varve widths in the sediments of Lake DV09 (Devon Island), Donard Lake (Baffin Island), Lower Murray Lake (LML) (Ellesmere Island), (Fig 4.6), as well as increased sediment density in DV09 (Fig 4.1), and increased apparent grain size diameter in LML, all occur during the latter half of a reconstructed continent-wide warmer summer interval from AD950-1300 (Viau *et al*, 2006) (Fig 4.6). At the hemispheric scale, the warm period occurs slightly earlier and seems to be shorter in duration. The increased varve widths and increase in apparent median grain size of the sediments of Lower Murray Lake (LML) during the 12th and 13th centuries were interpreted as warmer conditions (Besonen *et al*, 2008). Thicker varves between AD1200-1375 in the sediments

of Donard Lake were interpreted as warmer summer temperatures at this glacially-fed lake on Baffin Island (Moore *et al*, 2001). These warmer temperatures have been interpreted as the Medieval Warm Period (MWP) (Viau *et al*, 2006; Besonen *et al*, 2008), and this suggests that the climate variations at this time were sufficient to impact the surface hydroclimate at multiple sites across the Canadian Arctic. However, the timing and duration of this warmer period is different from Baffin Island (Moore *et al*, 2001) to the High Artic (DV09; Besonen *et al*, 2008), indicating either a variable geographical response to large-scale climate warming, or that the dating of this period at these sites is not precise enough.

This warm period is not evident in the $\delta^{18}O$ records from the Greenland glaciers (Fig 11; 12) as these records may be reflecting autumnal temperatures. However, it may have affected the melt records of Devon Island Ice Cap in the Arctic Archipelago, which reflect summer temperatures. The beginning of the 5-year melt percent record indicates heightened melt during the late AD1200s (Koerner, 1977) (Fig 4.6).

Within Lake JR01 on western Boothia Peninsula, floristic changes and increased diatom productivity occurred during the period of AD800-1350 (1150-600 cal. yrs BP) indicating warmer water temperatures, and was interpreted as the Medieval Warm Period (LeBlanc *et al*, 2004). Additionally, pollen percentages from the lake sediments indicate climate warming during this period. From AD1050-1200 (900-750 cal. yrs BP) the pollen percentages of *Alnus*, *Betula*, *Salix*, and Cyperaceae, increased, and *Pinus* pollen percentage decreased in this well-dated (radiocarbon) sediment core. This was interpreted as a short amelioration in the climate, which lead to an increase in the pollen production of the arctic-dwelling shrubs (Zabenskie, 2006; Zabenskie and Gajewski, 2007).

The beginning of this period (c.AD1000) marked the initiation of an eastward migration of the Thule culture from western Alaska. By the end of this period (AD1300s) the Thule had spread across the central, eastern and High Arctic, displacing much of the Dorset culture (Tuniit) peoples (McGhee, 1978; 1996). The Thule transportation technology, ability exploit sea mammal resources, an expanding trade economy, and a warmer climate in the central High Arctic may have facilitated this migration and significant societal change. The Thule may have capitalized upon a warmer climate by exploiting the improved waterway access throughout the summer, allowing for boat travel and a wider range for hunting of sea mammals. It should be noted that thinning sea ice could have been detrimental to boat and sled transport during the thaw, and that larger areas of open water could be of benefit to large sea mammals during pursuit. It also remains possible that other social or biological factors may also have played important roles in the demographic change of the Arctic that are unrelated to climate.

The average varve widths during the period following the Medieval Warm Period, from ~AD1300-1996, are nearly equal to the average varve width of the entire record although the variability is high (Table 4.2). The varve widths at DV09 are relatively thin from the AD1300s-1500s, with, however, a prominent peak around the AD1540s, which can also be seen in the melt percentages of the Devon Island Ice Cap record (Fig 4.7). There are also slight peaks within the varve width record of the sediments from LML and Bear Lake, and a peak in the total sediment yield of Nicolay Lake (Cornwallis Island) (Fig 4.7), as well as moderate melting in the Agassiz Ice Cap percent melt record. This may be due to a short warming interval and may suggest an abrupt and brief but consistently warmer climate across, at least, the eastern and central High Arctic, and

which may have been most pronounced around Devon Island. However this warmer period is not apparent in the Greenland ice core records, and this large peak in the DV09 varve width record coincides with a very strong average negative phase of the reconstructed winter North Atlantic Oscillation index (Fig 4.7).

The DV09 varve record shows very thin varves during the 17th century (Table 4.2) and the sediment density is also very low (Table 4.3), coincident with the Maunder Minimum, yet other arctic records remain variable at this time (Fig 4.7). Following the 17th century, varve widths are relatively low with intermittent peaks that show broad similarities with multiple varved sediment records from arctic lakes. Around AD1850, the varve records of DV09, Bear Lake, Lower Murray Lake (LML), and Sawtooth Lake, as well as melt percentages of both Agassiz and Devon Island Ice Caps, and the Northern Hemisphere temperature anomaly all suggest climate warming, with Upper Soper Lake showing this trend after the 1920s. Although the diatom record of DV09 showed assemblage changes and increases in concentration during the 20th century, with major increases in the 1920s and 1950s (Gajewski *et al*, 1997), it is difficult to determine if the concomitant increase in varve widths during this period is related to climate warming or to reduced compaction within the upper sediments. The magnetic susceptibility begins a steady decrease around AD1750, which continues to the top of the core (Fig 4.1), and may be due to the increased presence of water, which is diamagnetic, towards the core surface.

A Principal Components Analysis (PCA) was conducted on a correlation matrix of several annually resolved Arctic climate and proxy records, as well varve-based temperature reconstructions, and tree-ring-based atmospheric oscillation indices (Table

4.4). Due to the variable temporal ranges of many of the available datasets, the temporal range of the data was truncated to the AD1965-1700 period to maximise the number of variables kept within the matrix.

The total variance explained by the eigenvalues of the first 4 components is 34% (Table 4.4). Ice accumulation at Lomonosovfonna glacier on Svalbard Island, Devon Island and Agassiz Ice Cap oxygen-18 records, Upper Soper Lake and Lower Murray Lake varve widths, and the Atlantic Multidecadal Oscillation (AMO) index are all positively correlated with the first principal component, which accounts for 12% of the total variance (Table 4.4). The Greenland oxygen-18 records (Crete and Milcent) and the Pacific Decadal Oscillation (PDO) are negatively correlated with the second component, while Upper Soper and Donard Lakes (Baffin Island) are positively correlated. The Greenland records and Donard Lake are negatively correlated with the 3rd component, while Sawtooth Lake is positively correlated.

Lakes that are not near the eastern Arctic coast do not seem to be correlated with the first 3 components. All of the records that show positive correlations with the principal component may be related to the Atlantic Ocean and Baffin Bay temperatures, as they may relate to surface currents.

The scores of the first 4 components were plotted as a time series (Fig 4.8). The scores of the first component closely parallel (r=0.75) the composite Northern Hemisphere error-in-variables (EIV) temperature anomaly reconstruction which includes terrestrial and oceanic climate-proxy data (Mann *et al*, 2008). The greatest discrepancy is a slight warming during the 1830s, yet this peak appears in the scores of the 2nd component. Some of these data were used in developing the Northern Hemisphere

reconstruction, but the close relation of the first component of Canadian Arctic and Greenland records with the hemispheric curve indicates the structure of the atmospheric circulation and the importance of the North Atlantic-Greenland area in the hemispheric climate. The second through fourth components indicate regional differences in sedimentation or climate.

4.6 Conclusion

A 1600-year varve width and relative sediment density record has been created from a sediment core from Lake DV09, northern Devon Island. The varves are thin, averaging 0.7mm throughout the record, yet have a high variability with some varves up to ten standard deviations thicker. The varves consist of two distinct sedimentary units, a clastic lamina and an extremely thin organic-rich bio-lamina. Preservation of these fine structures seems to occur in the deepest basins of the lake bottom of DV09, and this has also been observed in other Arctic varved lake sediments (Besonen *et al*, 2008) and has been recognized in varved lakes worldwide (O'Sullivan, 1983; Saarnisto, 1986). Lead-210 has confirmed the annual nature of the surface sediments (Gajewski *et al*, 1997; Stern *et al* 2005). A single radiocarbon date was obtained; however, the date was much older than the varve-based age estimate, and due to the highly eroded nature of the organic matter this material was interpreted as unconformable.

The varve record of DV09 seems to record century-scale climate variability, and the record is consistent with other Arctic varve lake series, as well as ice melt and oxygen isotope data from Canadian Arctic Ice Caps and Greenland Ice Sheet records. High frequency variability is likely linked to local fluctuations in snow cover, rates of snow

melt, and possibly rare summer precipitation events. Given the proximity of the sedimentary rock cliffs, geomorphologic events, independent of climate, may influence the clastic inputs of sediment into the lake.

The varve width and relative sediment density record suggests relatively cool conditions from AD750-950s, followed by a rapid amelioration to warmer temperatures. This is concomitant with other Arctic lake records, yet seems to lag the continental temperature reconstructions. After AD1300 the record suggests cooler temperatures during the Little Ice Age, with high variability, and coldest conditions during the Maunder Minimum. An abrupt and short change to warmer conditions is observed around the mid AD1500s, which is also reflected in the Devon Island Ice Cap percent melt and to a lesser extent in the Agassiz Ice Cap percent melt. Recent climate warming seems to have begun after AD1850, yet it is uncertain whether some or this entire interpretation may be due to decreased sediment compaction.

4.7 Acknowledgements

This research program was funded by the Natural Sciences and Engineering Research Council of Canada (NSERC), and the Canadian Foundation for Climate and Atmospheric Sciences (CFCAS). Logistical support was provided by the Polar Continental Shelf Project (PCSP Contribution number 04508). We thank P.B. Hamilton and T. Malik for help in the field; M. Frappier, C. Prince, M.-C. Roch, B. O'Neil, T. Paull, and J. McGuinness for help in the laboratory; A. Trudel for supervising the x-radiography; and J. Bunbury for ostracode identifications. We would also like to thank the researchers who provided us with paleoclimatic datasets.

Stratigraphic Section			Varve Count			
Core	**Section**	**Depth (cm)**	**Transect 1**	**Transect 2**	**Transect 3**	**Counting Error (%)**
B0	roughly Section 1	0 - 55.5	719	700	-	2.64
Top of drive B1	Section 2	55.5 - 98.9	242	241	241	<0.01
Bottom of drive B1	Section 3	98.9 - 133.3	627	661	628	5.14

Table 4.1: Details of the 8 varve measurement series crossdated to create the composite varve width series. Sections are defined in 4.5.1: Sediment Stratigraphy (p.63).

Zone	Depth (cm)	Time Period (varve years AD)	Mean (mm)	Median (mm)	Std Dev (mm)	Max (mm)	Min (mm)	Kurtosis	Skewness
Full Record									
	0 - 133	399 - 1996	0.834	0.430	1.793	39.066	0.072	222.474	12.948
Zones									
LIA and recent	0 - 52.4	1316 - 1996	0.770	0.442	1.719	39.066	0.081	365.293	16.981
MWP	52.5 - 99.1	1050 - 1315	1.755	1.129	3.057	30.948	0.132	56.347	7.052
1st millennium	99.0 - 133.3	399 - 1049	0.526	0.332	0.744	8.513	0.072	32.900	4.949
Subzones									
Maunder Minimum	22.8 - 26.9	1600 - 1700	0.409	0.350	0.229	1.415	0.082	3.346	1.559
Pre-MWP	104.1 - 110.6	750 - 950	0.329	0.230	0.503	4.896	0.072	46.227	6.387

Table 4.2: Descriptive statistics of the varve record of DV09.

Zone	Depth (cm)	Time Period (varve years AD)	Mean (mm)	Median (mm)	Standard Deviation (mm)	Max (mm)	Min (mm)
Full Record							
	0 - 133	399 - 1996	102.247	104	36.373	178.5	16
Zones							
LIA and recent	0 - 52.4	1316 - 1996	67.862	63	22.031	149	30
MWP	52.5 - 99.1	1050 - 1315	132.612	137	23.770	178.5	16
1st millennium	99.0 - 133.3	399 - 1049	113.420	110.5	21.280	168	66
Subzones							
Maunder Minimum	22.8 - 26.9	1600 - 1700	50.740	47	13.775	101	31
Pre-MWP	104.1 - 110.6	750 - 950	107.280	102.75	22.181	165	71

Table 4.3: Descriptive statistics of the greyscale values of cores from DV09. Time periods estimated using the varve chronology.

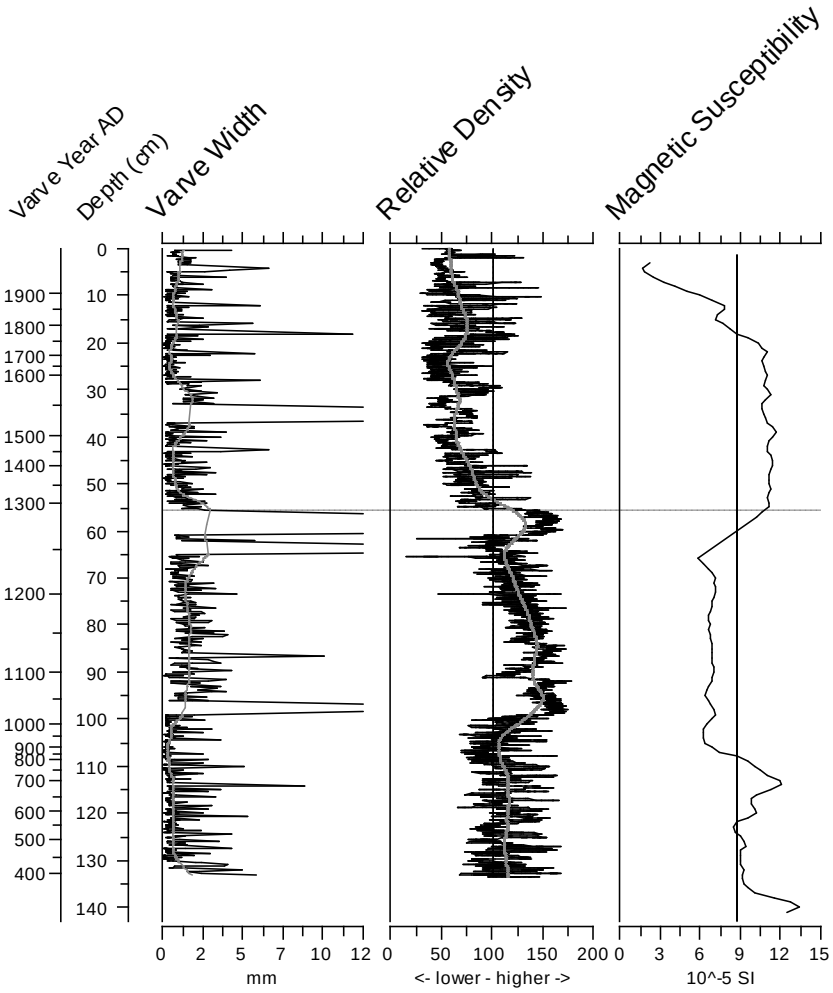

Fig 4.1: Sedimentological analyses of Core B: The varve width chronology, plotted versus core depth; the relative sediment density; and the magnetic susceptibility profile. The magnetic susceptibility values from the top and bottom 2cm of each sediment drive has been removed and have been interpolated. Dashed vertical lines show the mean of the respective variable (102.2 and 8.7) and the grey curves are 0.1 span, 0 iterations lowess spline. Dashed horizontal line is the division between drive 0 and 1 (at 55.5cm, AD1292).

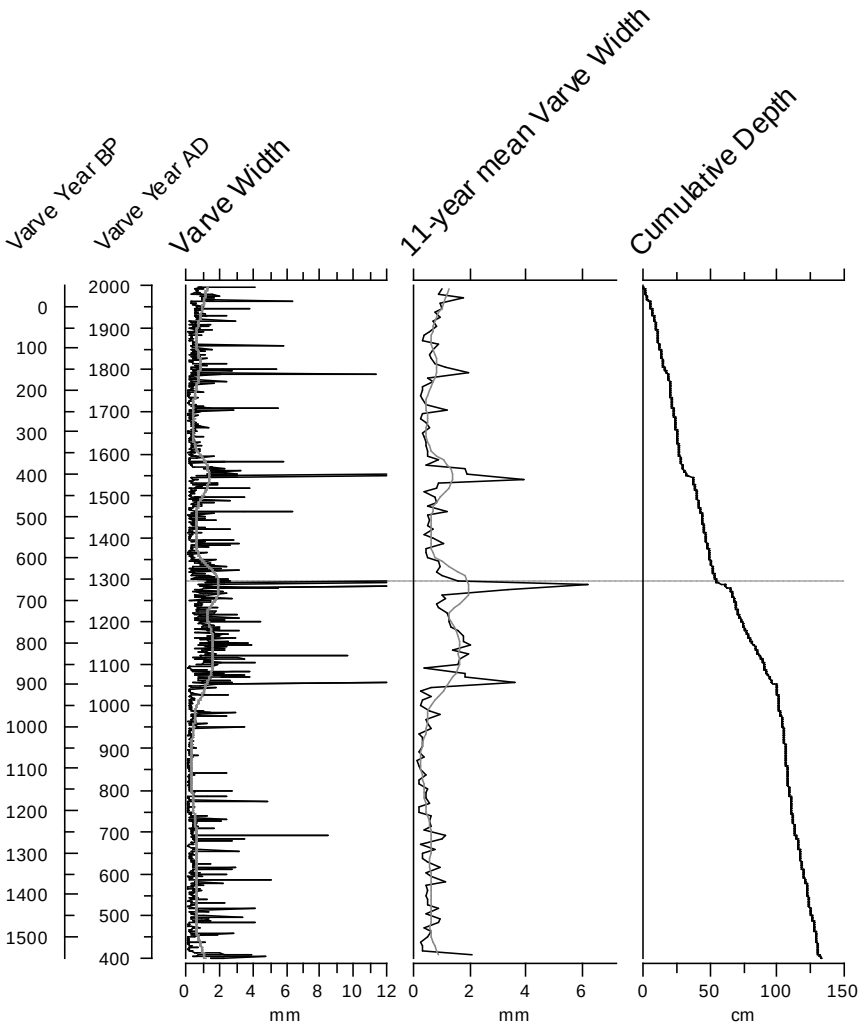

Fig 4.2: Varve width chronology of Core B, varve width smoothed with an 11-year running mean, and cumulative varve depth. Horizontal dashed line is the split between drives (at AD1292; 658 cal. yrs BP), and the grey curves are 0.1 span, 0 iterations lowess splines.

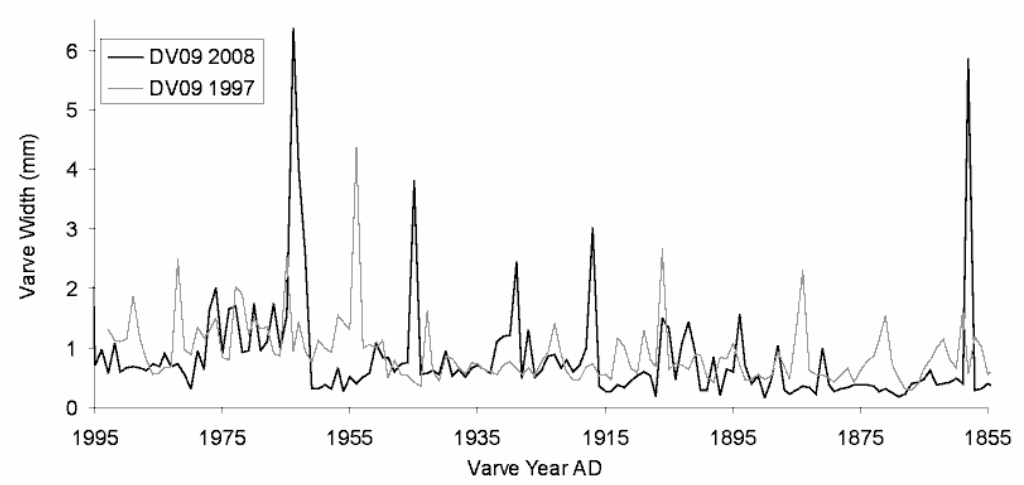

Fig 4.3: A comparison of the original varve width record (Gajewski *et al*, 1997) and the adjusted varve widths series from Core B.

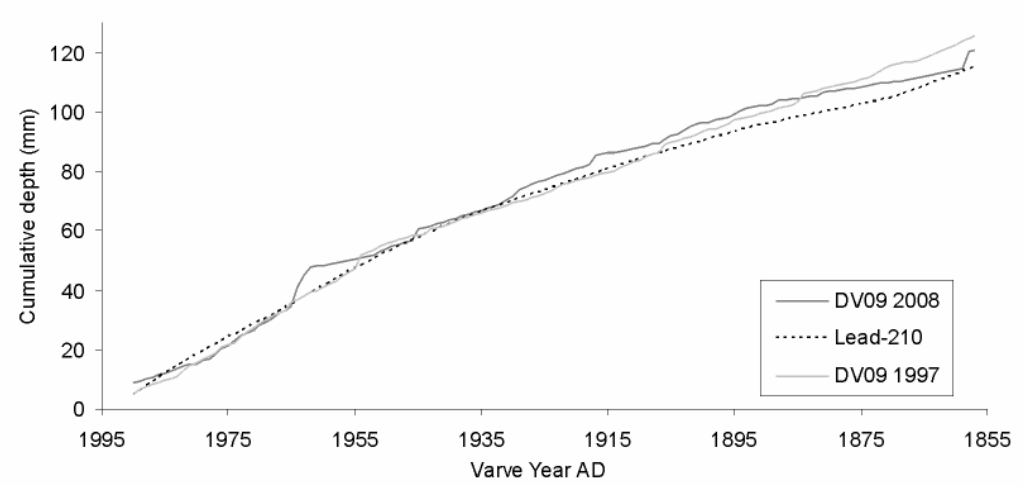

Fig 4.4: The varve record from this paper, and the lead-210 dates from a previously dated short core (Turner, 1995; Gajewsk i *et al*, 1997). Data was truncated to the CRS modeled dates (AD1990-1857).

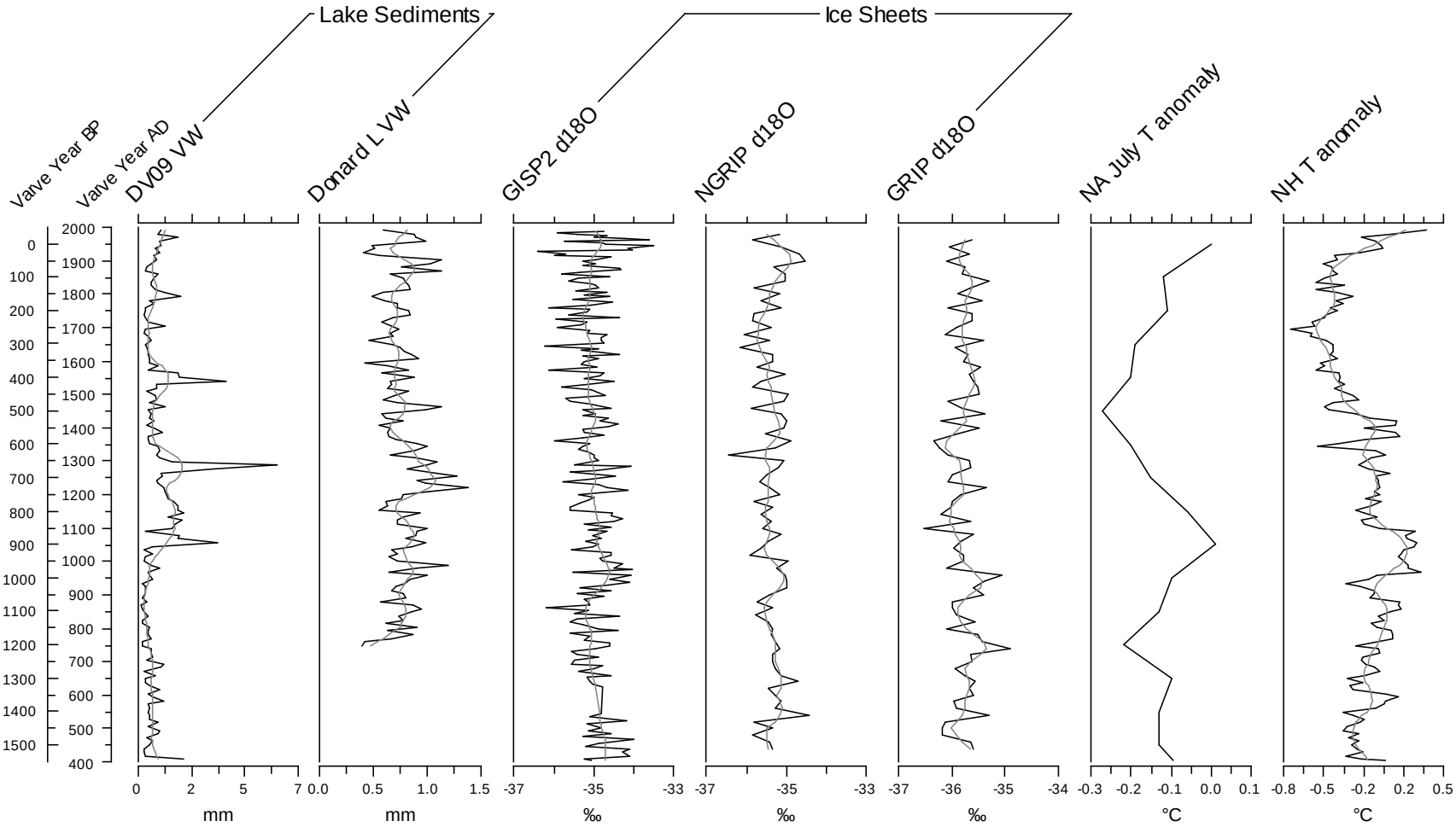

Fig 4.5: Past 1500 years. DV09 and Donard Lake varved width data (Moore *et al*, 2001) and the Northern Hemisphere (NH) temperature anomaly data is smoothed with 11-year running means. GISP2 oxygen isotope record (Grootes *et al*, 1993), the NGRIP and GRIP 20-year averaged oxygen isotope record (GICC05) (Vinther *et al*, 2006; Rasmussen *et al*, 2007), and the pollen-based reconstructed mean July temperature anomaly of North America (100 year resolution) (Viau *et al*, 2006). Composite Northern Hemisphere error-in-variables (EIV) land plus ocean temperature anomaly reconstruction (Mann *et al*, 2008). Grey curves are lowess splines with a span of 0.1 for all records except for the GISP2 data (0.025), all with 0 iterations.

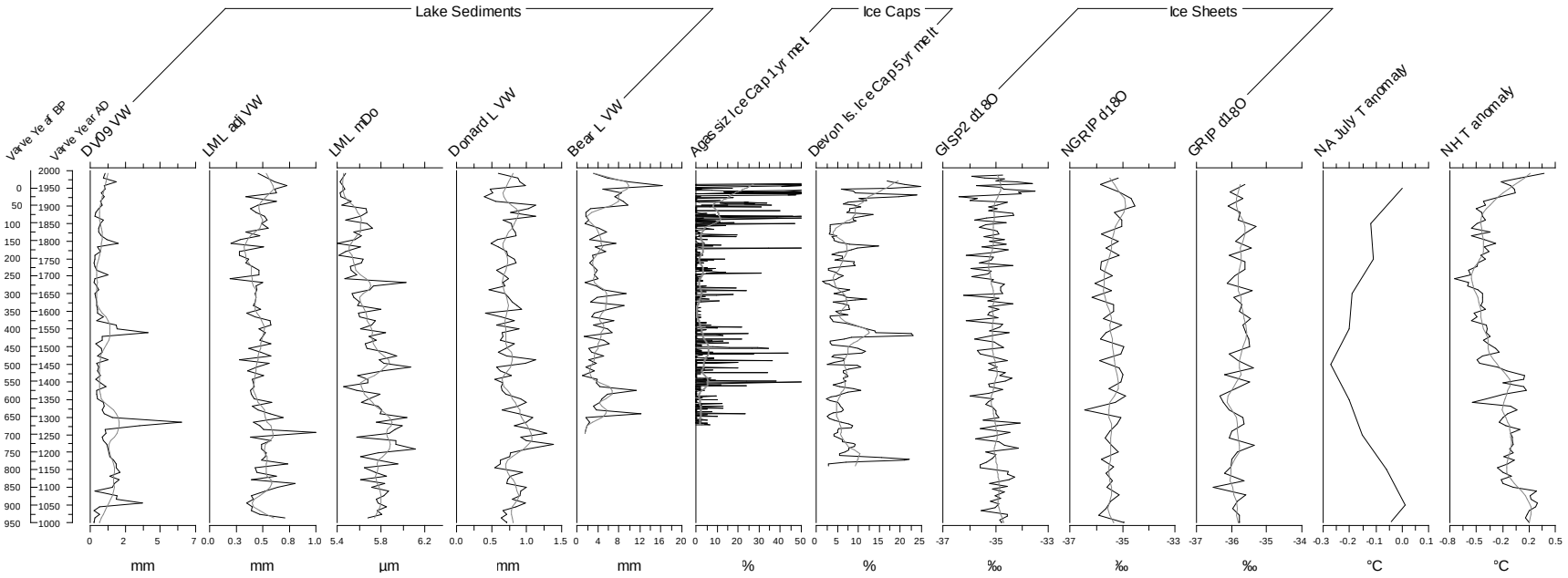

Fig 4.6: Past 1000 years. All varved lake and the Northern Hemisphere (NH) temperature anomaly data is smoothed with 11-year running means, Lower Murray Lake (LML) adjusted varve widths and apparent median grain size obtained through digital image analysis (Besonen *et al*, 2008), Donard Lake varve widths (Moore *et al*, 2001) and Bear Lake varve widths (Lamoureux and Gilbert, 2004). The Agassiz Ice Cap 1 year melt percentage (TIVOLI84) (Fisher and Koerner, 1994; Fisher *et al*, 1995), and the Devon Island Ice Cap 5 year melt percentage (Koerner, 1977), as well as the GISP2 (Grootes *et al*, 1993; Stuiver *et al*, 1995), NGRIP, and GRIP 20-year averaged oxygen isotope records (GICC05) (Vinther *et al*, 2006; Rasmussen *et al*, 2007), and the pollen-based reconstructed mean July temperature anomaly of North America (100 year resolution) (Viau *et al*, 2006). Composite Northern Hemisphere error-in-variables (EIV) land plus ocean temperature anomaly reconstruction (Mann *et al*, 2008). Grey curves are lowess splines with a span of 0.1 for all records except for the GISP2 data (0.025), all with 0 iterations.

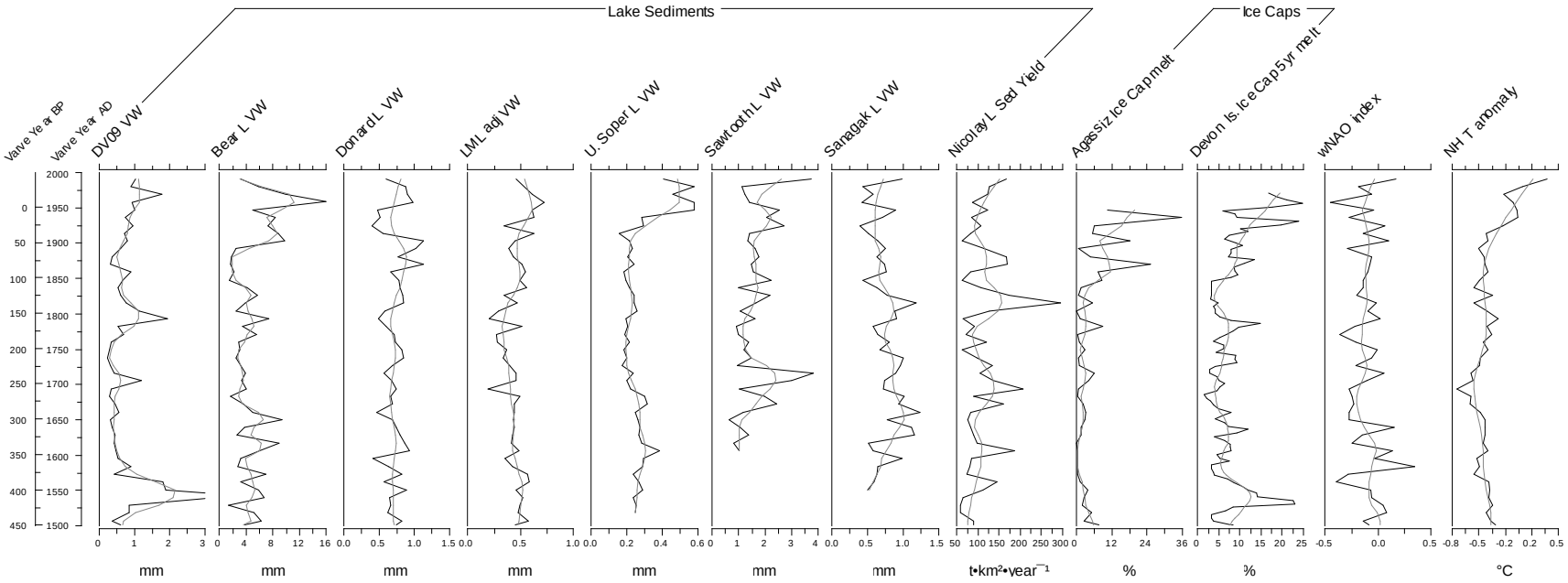

Fig 4.7: Past 500 years. All records except Devon Island Ice Cap 5-year melt percentage have been smoothed with an 11-year running mean. Bear Lake varve widths (Lamoureux and Gilbert, 2004), Donard Lake varve widths (Moore *et al*, 2001), Lower Murray Lake (LML) varve widths (Besonen *et al*, 2008), Upper Soper Lake varve widths (Hughen *et al*, 2000), Sanagak Lake varve widths (Lamoureux *et al*, 2006), Sawtooth Lake varve widths (Francus *et al*, 2002), Nicolay Lake annual sediment yield (Lamoureux, 2000), Agassiz Ice Cap 1 year melt percentage (TIVOLI84) (Fisher and Koerner, 1994; Fisher *et al*, 1995), Devon Island Ice Cap 5-year melt percentage (Koerner, 1977), reconstructed winter North Atlantic Oscillation (NAO) index (Cook *et al*, 2002), composite Northern Hemisphere error-in-variables (EIV) land plus ocean temperature anomaly reconstruction (Mann *et al*, 2008).
Grey curves are lowess splines with a span of 0.05 (DV09), 0.1 (Bear L, Donard, LML, Agassiz and Devon Island Ice Caps, and Northern Hemisphere temperature anomaly), and 0.2 (Upper Soper L, Sawtooth L, Sanagak L, Nicolay L, and reconstructed winter NAO index), all with 0 iterations.

Dataset or Site	Variable	Comp.1	Comp.2	Comp.3	Comp.4	References
DV09 2008	Varve width	0.04	-0.05	0.11	0.12	This Study
Crete	1yr $\delta^{18}O$	0.16	**-0.36**	**-0.22**	-0.02	Clausen *et al*, 1988
Crete A	1yr acc	0.11	**-0.22**	**-0.34**	0.19	Clausen *et al*, 1988
Milcent 1974	1yr acc	0.11	**-0.38**	**-0.37**	0.13	Dansgaard *et al*, 1975; Langway *et al*, 1985; Clausen *et al*, 1988
Milcent 1973	1yr acc	0.03	**-0.28**	**-0.29**	0.08	Dansgaard *et al*, 1975; Langway *et al*, 1985; Clausen *et al*, 1988
Lomonosov	1yr acc	**0.29**	0.02	0.13	**0.25**	Korotkevich and Kudriashov, 1974; Arkipov *et al*, 1987; Zagorodnov, 1988
Lomonosov	1yr acc corr	-0.06	-0.02	0.17	**0.22**	Korotkevich and Kudriashov, 1974; Arkipov *et al*, 1987; Zagorodnov, 1988
Eclipse IF	SO_4^{2-}	0.01	-0.02	0.10	**0.20**	Yalcin and Wake, 2001; Wake *et al*, 2002; Yalcin *et al*, 2003
CampCent	1yr $\delta^{18}O$	0.12	-0.07	-0.04	-0.12	Dansgaard *et al*, 1969; Hansen *et al*, 1966; Johnsen *et al*, 1970; 1972
Devon I. IC	1yr $\delta^{18}O$	**0.22**	0.06	0.09	-0.10	Paterson *et al*, 1977
Agassiz IC	1yr melt %	**0.24**	-0.01	-0.03	-0.06	Fisher and Koerner, 1994; Fisher *et al*, 1995
Bear L.	Varve width	0.13	-0.06	0.02	**0.23**	Lamoureux and Gilbert, 2004
U. Soper L.	Varve width	**0.35**	**0.23**	0.04	**0.35**	Hughen *et al*, 2000
U. Soper L.	Temp recon	**0.34**	**0.23**	0.01	**0.37**	Hughen *et al*, 2000
Sanagak L.	Varve width	-0.11	0.09	-0.10	0.11	Lamoureux *et al*, 2006
Nicolay L.	1yr sed yield	-0.07	0.09	-0.08	0.09	Lamoureux, 2000
L. Murray L.	Adj. VW	**0.29**	0.02	-0.01	-0.05	Besonen *et al*, 2008
L. Murray L.	mDo	-0.07	0.06	-0.05	-0.19	Besonen *et al*, 2008
Sawtooth L.	Varve width	0.02	-0.03	**0.24**	**-0.20**	Francus *et al*, 2002
Sawtooth L.	mDo	0.09	-0.01	**0.20**	-0.13	Francus *et al*, 2002
Donard L.	Varve width	-0.01	**0.44**	**-0.44**	-0.12	Moore *et al*, 2001
Donard L.	Temp recon	-0.01	**0.44**	**-0.44**	-0.12	Moore *et al*, 2001
AMO	Index	**0.41**	-0.05	-0.02	**-0.29**	Gray *et al*, 2004
AMO	SSTa recon	**0.37**	-0.06	-0.02	**-0.34**	Gray *et al*, 2004
wNAO	Index	-0.04	0.08	0.11	0.15	Cook *et al*, 2002
Nino3	index	-0.10	-0.03	-0.08	0.14	D'Arrigo *et al*, 2005
PDO	index	-0.16	**-0.23**	-0.05	-0.05	Biondi *et al*, 2001
Sunspots	1yr avg #	0.17	0.03	0.14	**-0.22**	SIDC-team, 2008
Eigenvalues						
Standard Deviation		1.85	1.50	1.47	1.34	-
Proportion of Variance		12%	8%	8%	6%	-
Cumulative Proportion		12%	20%	28%	34%	-

Table 4.4: Component loadings of a Principal Components Analysis (PCA) using a correlation matrix of annually resolved paleoclimate records from the Arctic (ice cores and varve width data) as well as climate oscillation reconstructions from tree ring series from the Northern Hemisphere, covering a period from AD1965-1700.

1yr = annual, VW = varve width data, Adj. VW = adjusted varve width data, IF = ice field, IC = ice cap, Temp recon = proxy-based temperature reconstruction, SSTa = sea surface temperature anomaly, mDo = mean sediment grain size, sed yield = sediment yield, SO_4^{2-} = sulphate micro-equivalents per Liter AMO = Atlantic Multidecadal Oscillation, wNAO = winter North Atlantic Oscillation index Nino3 = El Nino Southern Oscillation index, PDO = Pacific Decadal Oscillation index.

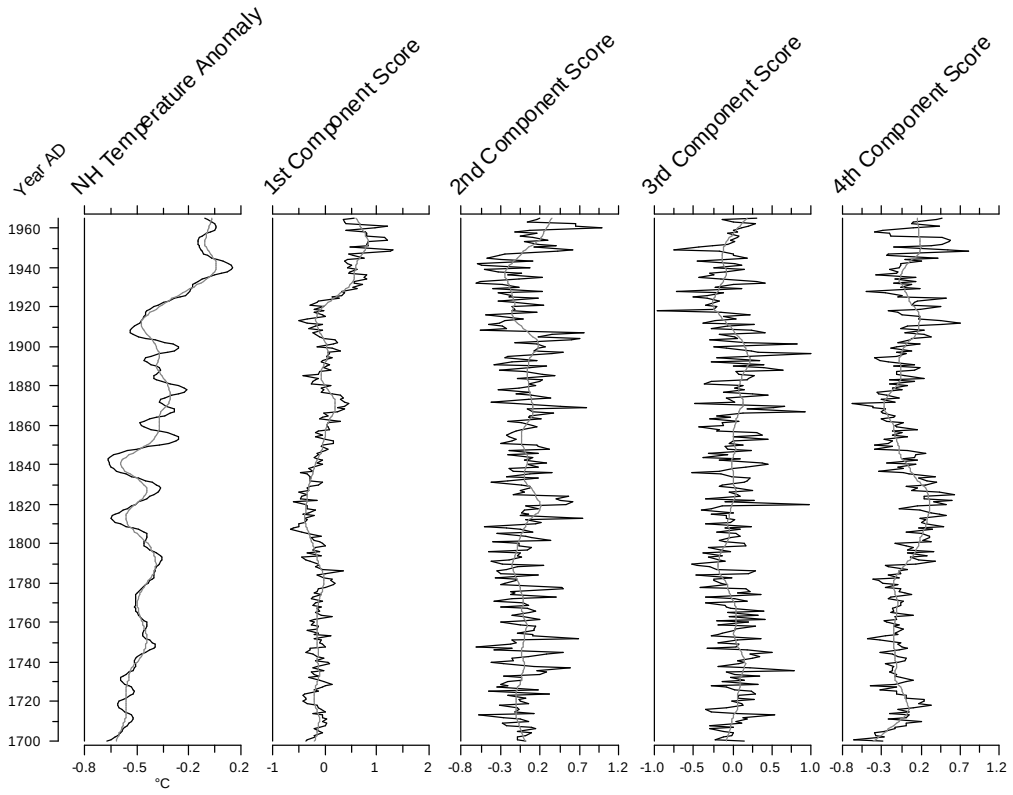

Fig 4.8: Composite Northern Hemisphere error-in-variables (EIV) land plus ocean temperature anomaly reconstruction (Mann *et al*, 2008) and sample scores of the first 4 components from a PCA analysis (AD1965-1700). Grey curves are 0.1 span, 0 iterations lowess splines.

Results (Part 3):

A preliminary exploration of the red-noise spectra of DV09 varve series in the context of other annual series from northern Canada and Greenland

5.1 Introduction

This section is an exploratory investigation into possible cycles in the varve width chronology in order to provide insight to potential relationships with climate variables, or commonalities across spatial scales with other paleoclimate records.

A continuous decline of spectral amplitude with increasing frequency in a time series, termed red noise, is common in paleoclimatic data (Schulz and Mudelsee, 2002), which is possibly due to temporal persistence in natural systems (Mann and Lees, 1996). The use of evenly spaced time series, i.e. the annually resolved varve width series, eliminates the need to interpolate between sampling intervals before estimating the red-noise spectrum, and therefore reduces any artificial red-shifting of the signal. The REDFIT program is designed for unevenly spaced time series data: however, the use of evenly spaced data (i.e. tree ring, varve width data) remains mathematically correct (Schulz, personal communication 2008). Amplitude peaks within the red-noise power spectra may suggest significant cyclical events within the varve width and other paleoclimate time series data, which can then be compared to known climate cycles.

5.2 Method and Data

The red-noise spectrum of the varve width series was estimated using the REDFIT v3.8 program (Schulz and Mudelsee, 2002). The raw paleoclimatic datasets (Table 5.1) were

run through the program using the following settings (for further details see Schulz and Stattegger, 1997; Schulz and Mudelsee, 2002):

1000 Monte-Carlo simulations 4.0 overspampling factor for Lomb-Scargle Fourier transform 1.0 maximum frequency analyzed 50 WOSA segments (with 50% overlap) Unused prescribed value for rho, ρ Rectangular window-type identifier (used to suppress sidelobes in spectral analysis)

5.3 Results

The red-noise bias-corrected spectrum of the Core B varve width series is shown in Fig 5.1. Periods ($1/f$) of ~511 to 213, 135-116, 88-82, and 11.5 years were estimated at the 99% confidence interval (Fig 5.2). Periods of 62, 52, 43, 13, and 5 years were also identified at confidence intervals above 80% (Fig 5.1; Table 5.2).

Significant peaks above the 80% confidence interval for other Arctic varved lake sediment records and ice core records are shown in Table 5.2. Datasets which did not show significant peaks include a decadally-averaged $\delta^{18}O$ record from Dunde Ice Cap, China (1000-1987 AD) (Thompson *et al*, 1989; 2003), the varve width series of the previously published DV09 study (1843-1993 AD) (Gajewski, 1997) and of Bear Lake, Devon Island (1250-1998 AD) (Lamoureux and Gilbert, 2004).

5.4 Discussion

5.4.1 Cycles in the DV09 Varve Width Data

Peaks at the high frequency end of the data are characteristic of red-noise spectra and likely do not reflect true cycles in the data. These were therefore disregarded. Although a peak around 120 years may be due to a solar cycle, the interval 135-116 is much too large

for any clear evidence of a response in the sediments of Lake DV09 to solar forcing at this cycle length.

The peaks between 78 and 88 years may be related to the Gleissberg solar cycle of 78 to 80 years (Pap *et al*, 1994). The signal reaches a peak at 85 years in the varve width series, yet remains at 95% for the years 77 to 79. The peaks surrounding the years 62, 52, 43, and 13 years are difficult to relate to known cycles, although the 4^{th} harmonic of the Suess solar cycle (~208 years) is 53 years (Pap *et al*, 1994). A cycle of 11.5 years is significant at the 99% confidence interval and may be related to the ~11 year sunspot cycle, which has been observed through historical sunspot counting at European and Chinese observatories over the past millennium and modern observations with ground-based telescopes and satellite measurements. The 5-year cycle may be a harmonic of this potential link with the sunspot cycle, which affects total solar irradiance.

Many peaks, and peaks covering broad ranges of years, make it difficult to clearly identify specific cycles in the data. This may be caused by some error in dating the varve width series, as well as white noise in the signal, and/or large portions of the variability being explained by non-cyclical climatic factors. Identifying true cycles is also hampered by the lack of strong evidence for physical mechanisms linking solar and other climate cycles to sedimentation in Lake DV09. These mechanisms are also difficult to identify in other varve records and the ice core records; but some observations of the results will be discussed in the next section.

5.4.2 Cycles in Other Arctic Paleoclimatic Datasets

The method was applied to a total of 17 other paleoclimatic datasets, with only 14 showing (15 including DV09) significant red-noise amplitude peaks, including other Arctic varved lake records, annual ice accumulations in glaciers, and glacier oxygen isotope records (Table 5.2). The most common cycles range between 8 and 12 years (9 of 15 records) and 42 and 52 years (7 records). This could be a response to the sunspot cycle for the prior and remains uncertain for the latter. All other intervals have 4 or fewer occurrences. There also seems to be no pattern between the type of record and the range of significant cycles. No cycles were identified in the varve width record of the sediments from Bear Lake, which is surprising given the proximity of Bear Lake and DV09 (~170km).

5.5 Conclusions

The results presented in Fig 5.1 and Table 5.2 reflect significant peaks in the red-noise power spectra of 18 paleoclimatic datasets. The results have been presented with some interpretation of suggestive links with known solar cycles; however, the uncertainties remain very high, with many significant peaks having no discernable connections with any real cycles. Even in the cases where cycles may be equal to known solar cycles, the physical mechanisms to make that possible remain poorly understood, speculative, or nonexistent. It is possible that future studies of natural systems, and how they respond to climate cycles, will allow for a better understanding of the possible physical mechanisms relating these processes and the possible impacts that may incur.

Data Set (Year AD)	Location	Data Range	References
DV09			
DV09 (2008)	Devon I.	1996-399	This document
DV09 (1997)	Devon I.	1993-1843	Gajewski *et al*, 1997
Varved Lake Sediments			
Bear L.	Devon I.	1998-1250	Lamoureux and Gilbert, 2004
Lower Murray L. (raw)	Ellesmere I.	2004-1013	Besonen *et al*, 2008
Donard L.	Baffin I.	1992-752	Moore *et al*, 2001
Sanagak L.	Boothia P.	1986-1550	Lamoureux *et al*, 2006
Upper Soper L.	Baffin I.	1992-1514	Hughen *et al*, 2000
Nicolay L. (annual sediment yield)	Cornwallis I.	1987-1493	Lamoureux, 2000
Ice Core Data			
Devon Island Ice Cap 1yr $\delta^{18}O$	Devon I.	1973-1512	Paterson *et al*, 1977
Camp Century 1yr $\delta^{18}O$	Greenland	1967-1242	Dansgaard *et al*, 1969; Hansen *et al*, 1966; Johnsen *et al*, 1970; 1972
DYE 3 1yr $\delta^{18}O$	Greenland	1872- -1899	Langway *et al*, 1985
GRIP 20yr $\delta^{18}O$ (GICC05)	Greenland	1980-460	Vinther *et al*, 2006
NGRIP 20yr $\delta^{18}O$ (GICC05)	Greenland	1980-440	Vinther *et al*, 2006
Devon Island Ice Cap 5yr melt %	Devon I.	1971-1161	Koerner, 1977
Agassiz Ice Cap 5yr melt % (TIVOLI87)	Ellesmere I.	1961-51	Fisher and Koerner, 1994; Fisher *et al*, 1995
Crete 1yr accumulation	Greenland	1974-553	Clausen *et al*, 1988
Lomonosovfonna 1yr accumulation	Svalbard	1973-1657	Korotkevich and Kudriashov, 1974; Arkipov *et al*, 1987; Zagorodnov, 1988
Dunde Ice Cap 10yr $\delta^{18}O$	Tibet, China	1987-1000	Thompson *et al*, 1989; 2003

Table 5.1: Data sets used for preliminary spectral analysis.

Data Set	Cycles (years)													
-	89-131	78-88	63-75	59-61	53-58	42-52	38-42	34-37	29-33	25-28	20-24	17-18	13-16	8-12
DV09														
DV09 (2008)	99	99				90							90	99
DV09 (1997)														
Varved Lake Sediments														
Bear L.														
Lower Murray L. (raw)							95					95		
Donard L.			90			90	99						95	
Sanagak L.														
Upper Soper L.														
Nicolay L. (annual sediment yield)						99								
Ice Core Data														
Devon Island Ice Cap 1yr $\delta^{18}O$														99
Camp Century 1yr $\delta^{18}O$													90	
DYE 3 1yr $\delta^{18}O$						95						90	95	
GRIP 20yr $\delta^{18}O$ (GICC05)					95	99								
NGRIP 20yr $\delta^{18}O$ (GICC05)			99			95								
Devon Island Ice Cap 5yr melt %						95					90			
Agassiz Ice Cap 5yr melt % (TIVOLI87)							90				95			
Crete 1yr accumulation	95													
Lomonosovfonna 1yr accumulation											90			90
Dunde Ice Cap 10yr $\delta^{18}O$														

Table 5.2: Significant cycles in the red-noise power spectra of some paleoclimate datasets estimated using Redfit3.8 (Schulz and Mudelsee, 2002). Peaks within the defined temporal ranges are identified at confidence intervals of 90, 95, and 99%; no value indicates no significance above the 89.9% confidence interval. See Table 5.1 for source of the series.

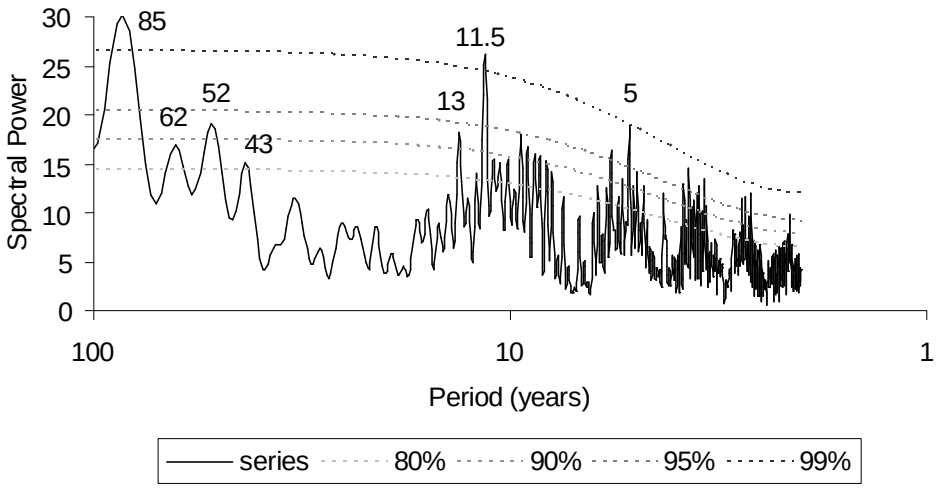

Fig 5.1: Red-noise bias-corrected spectrum of Core B varve width series, with estimated confidence intervals, showing significant cycles in the data (in varve years). X-axis shown at a logarithmic scale.

6 Summary and Conclusions

From at least 7500 cal. yrs BP until 6500 yrs BP sedimentation in Lake DV09 was rapid, with an increased amount of organic matter deposited in the deeper part of the lake from 6000-6500 cal. yrs BP, likely due to increased productivity during a warmer period. The latter half of the Holocene has a decreased sedimentation rate, and varves have been deposited for the past 1600 years. The varve record shows that sedimentation into the lake is likely due to variability in the energy available to transport sediments to the lake, which is controlled to some extent by climate. Varve widths during the first millennium are generally lower, reflecting cooler temperatures, especially from AD750-950. From AD1050-1300s the varve widths are thicker, responding to the warmer temperatures during the Medieval Warm Period. The coldest phase of the Little Ice Age appears to be during the AD1600s. The recent global climate warming can be seen in the slight increase in varve widths since the AD1850s.

Interpretations of the varve width series would benefit from longer-term local hydrological, sedimentologic, and meteorological measurements (cf. Lamoureux *et al*, 2002; Lewis *et al*, 2002; Lamoureux and Gilbert, 2004). Data from field monitoring could be used to closer investigate the processes and mechanisms leading to varve formation and preservation within the lake, and aid in understanding the linkages between climate change and the variability of varve characteristics. A focused effort studying the biology of the lake may yield insight into the processes that create the biolaminations within the sediments. The varve width record of DV09 may also be extended further back in time, yielding additional paleoclimatic information to at least the mid Holocene.

References

Abbott, M.B. and T.W. Stafford Jr. 1996. Radiocarbon geochemistry of modern and ancient Arctic lake systems, Baffin Island, Canada. Quaternary Research 45: 300–311.

Appleby, P.G. 2001. Chronostratigraphic techniques in recent sediments. In: Last, W.M. and J.P. Smol (eds.) Tracking Environmental Change Using Lake Sediments – DPER Volume 1: Basin Analysis, Coring, and Chronological Techniques. Kluwer Academic Publishers, Dordrecht, The Netherlands: 171-203.

Appleby, P.G. and F. Oldfield. 1983. The assessment of ^{210}Pb data from sites with varying sediment accumulation rates. Hydrobiologia 103: 29-35.

Anderson, R.Y. 1964. Varve Calibration and Stratification. In: Merriam, D.F. (ed.) Symposium on Cyclic Sedimentation. Kansas Geological Survey, Bulletin 169, Volume I: 1-20.

Anderson, R.Y. and W.E. Dean. 1988. Lacustrine Varve Formation Through Time. Palaeogeography, Palaeoclimatology, Palaeoecology 62: 215-235.

Anderson, R.Y. and L.H. Koopmans. 1963. Harmonic analyses of varve time series. Journal of Geophysical Research 68: 877-893.

Arkhipov, S.M., et al. 1987. Soviet glaciological investigations on Austfonna, Nordaustlandet, Svalbard in 1984 to 1985. Polar Geography and Geology 11:25-49.

Atkinson, D. and K. Gajewski. 2002. High-resolution estimation of surface air temperature in the Canadian High Arctic Journal of Climatology 15: 3601-3614.

Battarbee, R.W., V.J. Jones, R.J. Flowers, N.G. Cameron, H. Bennion, L. Carvalho and S. Juggins. 2001. Diatoms. In: Last, W.M. and J.P. Smol (eds.) Tracking Environmental Change Using Lake Sediments – DPER Volume 3: Terrestrial, Algal, and Siliceous Indicators. Kluwer Academic Publishers, Dordrecht, The Netherlands: 155-202.

Bamber, R.N. 1982. Sodium hexametaphosphate as an aid in benthic sample sorting. Marine Environmental Research 7: 251-255.

Beierle, B.D., S.F. Lamoureux, J.M.H. Cockburn and I. Spooner. 2002. A new method for visualizing sediment particle size distributions. Journal of Paleolimnology 27: 279-283.

Besonen, M.R., W. Partridge, R.S. Bradley, P. Francus, J.S. Stoner and M.B. Abbott. 2008. A record of climate over the last millennium from the Canadian High Arctic. The Holocene 18: 169-180.

Binford, M.W., J.S. Kahl and S.A. Norton. 1993. Interpretation of ^{210}Pb profiles and verification of the CRS model in the PIRLA project lake sediment cores. Journal of Paleolimnology 9: 275-296.

Biondi, F., A. Gershunov and D.R. Cayan. 2001. North Pacific decadal climate variability since AD 1661. Journal of Climate 14: 5-10.

Björk, S. and B. Wohlfarth. 2001. ^{14}C chronostratigraphic techniques in paleolimnology. In: Last, W.M. and J.P. Smol (eds.) Tracking Environmental Change Using Lake Sediments – DPER Volume 1: Basin Analysis, Coring, and Chronological Techniques. Kluwer Academic Publishers, Dordrecht, The Netherlands: 205-245.

Blais, J.M., J. Kalff, R.J. Cornett and R.D. Evans. 1995. Evaluation of ^{210}Pb dating in lake sediments using stable Pb, *Ambrosia* pollen, and ^{137}Cs. Journal of Paleolimnology 13: 197-178.

Boggs Jr., S. 2001. Continental Environments. In: Principles of Sedimentology. 3rd Ed. Prentice Hall, Upper Saddle River, NJ, USA: 267-320.

Bouchard, G. 2004. Freshwater Diatom Biogeography of the Canadian Arctic Archipelago. M.Sc. Thesis, Ottawa-Carleton Geoscience Centre and the University of Ottawa. 170pp.

Bowden, W.B., M.N. Gooseff, A. Balser, A. Green, B.J. Peterson and J. Bradford. 2008. Sediment and nutrient delivery from thermokarst features in the foothills of the North Slope, Alaska: Potential impacts on headwater stream ecosystems. Journal of Geophysical Research 113: G02026.

Boyle, J.F. 2001. Inorganic geochemical methods in paleolimnology. In: Last, W.M. and J.P. Smol (eds.) Tracking Environmental Change Using Lake Sediments – DPER Volume 2: Physical and Geochemical Techniques. Kluwer Academic Publishers, Dordrecht, The Netherlands: 83-142.

Bradley, R.S. 1999. Non-marine Geological Evidence. In: Paleoclimatology – Reconstructing Climates of the Quaternary. 2nd Ed. International Geophysics Series, Volume 68. Academic Press, San Diego, CA, USA: 285-334.

Bradley, R.S., M.J. Retelle, S.D. Ludlam, D.R. Hardy, B. Zolitschka, S.F. Lamoureux and M.S.V. Douglas. 1996. The Taconite Inlet Lakes Project: a systems approach to paleoclimatic reconstruction. Journal of Paleolimnology 16: 97-110.

Brasier, M.D. 1971. Microfossils. Chapman & Hall, London, UK. 193pp.

Braun, C., D.R. Hardy, R.S. Bradley and M.J. Retelle. 2000a. Streamflow and suspended sediment transfer to Lake Sophia, Cornwallis Island, Nunavut, Canada. Arctic, Antarctic, and Alpine Research 32: 456-465.

Braun, C., D.R. Hardy, R.S. Bradley and M.J. Retelle. 2000b. Hydrological and meteorological observations at Lake Tuborg, Ellesmere Island, Nunavut, Canada. Polar Geography 24: 83-97.

Brauer, A. and J.F.W. Negendank. 2002. The value of annually laminated sediments in Palaeoenvironment reconstruction. Quaternary International 88: 1-3.

Briggs, D.J. 1977. Sources and Methods in Geography – Sediments. Butterworths & Co. (Publishers) Ltd., London, England.

Bunbury, J. and K. Gajewski. 2008. Biogeography of freshwater ostracodes in the Canadian Arctic. Arctic – submitted September 10, 2008.

Campbell, C.V. 1967. Lamina, Laminaset, Bed and Bedset. Sedimentology 8: 7-26.

Canadian Museum of Nature (CMN). 2006. Sila – Clue into climate change – sifting clues from lake-bottom muck. Last updated: 2006-08-09. Last accessed: 2007-06-28. Available online: http://nature.ca/sila/dvtr/dtms_e.cfm http://nature.ca/sila/dvtr/dtms_f.cfm

Carver, R.E. 1971. Procedures in Sedimentary Petrology. Wiley-Interscience, New York, NY.

CAVM Team. 2003. Circumpolar Arctic Vegetation Map [map]. Scale 1:7 500 000. Conservation of Arctic Flora and Fauna (CAFF) Map No.1. USA Fish and Wildlife Service, Anchorage, Alaska.

Child J.K. and A. Werner. 1999. Evidence for a hardwater radiocarbon dating effect, Wonder Lake, Denali National Park and Preserve, Alaska, USA. Géographie physique et Quaternaire 53: 407–411.

Chutko, K.J. and S.F. Lamoureux. 2008. Stratigraphic analysis of a complex biolaminated sedimentary sequence from a coastal High Arctic lake. 38th International Arctic Workshop. March 5-7, 2008. University of Colorado at Boulder, Colorado, USA.

Clausen, H.B., N.S. Gundestrup, S.J. Johnsen, R. Bindschadler and J. Zwalley. 1988. Glaciological Investigations in the Crete area, central Greenland: A search for a new deep-drilling site. Annals of Glaciology 10: 10-15.

Cohen, A.S. 2003. Geochemical Archives in Lake Deposits. In: Paleolimnology. Oxford Press, New York: 241-272.

Conley, D.J. 1998. An interlaboratory comparison for the measurement of biogenic silica in sediments. Marine Chemistry 63: 39-48.

Conley, D.J. and C.L. Schleske. 1993. Potential role of sponge spicules in influencing the silicon biogeochemistry of Florida Lakes. Canadian Journal of Fish and Aqautic Sciences 50, 296-302.

Conley, D.J. and C.L. Schleske. 2001. Biogenic Silica. In: Smol, J.P, H.J.B. Birks and W.M. Last (eds.)Tracking Environmental Change Using Lake Sediments – DPER Volume 3: Terrestrial, Algal, and Siliceous Indicators. Kluwer Academic Publishers, Dordrecht, The Netherlands: 281-294.

Cook, E.R., R.D. D'Arrigo and M.E. Mann. 2002. A Well-Verified, Multiproxy Reconstruction of the winter North Atlantic Oscillation index since A.D. 1400. Journal of Climate 15: 1754-1764.

D'Arrigo, R., E.R. Cook, R.J. Wilson, R. Allan, M.E. Mann. 2005. On the variability of ENSO over the past six centuries. Geophysical Research Letters 32: L03711.

Dansgaard, W., S.J. Johnsen, J. Moller, and C.C. Langway. 1969. One thousand centuries of climatic record from Camp Century on the Greenland ice sheet. Science 166: 377-381.

Dansgaard, W., S.J. Johnsen, N. Reeh, N. Gundestrup, H.B. Clausen and C.U Hammer. 1975. Climatic changes, Norsemen and modern man. Nature 255: 24-28.

Davis Jr., R.A. 1992. Depositional Systems – An Introduction to Sedimentology and Stratigraphy. 2nd ed. Prentice-Hall, Inc., Englewood Cliffs, NJ, USA.

De Geer, G. 1912. A geochronology for the last 12,000 years. Proceedings of the XI International Geological Congress, Stockholm, 1910. Compte rendue 1: 241-258.

De Geer, G. 1934. Geology and geochronology. Geografiska Annaler 1: 1-52.

Dean, W.E. 1974. Determination of carbonate and organic matter in calcareous sediments and sedimentary rocks by loss on ignition: Comparison with other methods. Journal of Sedimentary Petrology 44: 242-248.

Dean, W.E. 1981. Carbonate minerals and organic matter in sediments of modern north temperate hard-water lakes. Society of Economic Paleontologists and Mineralogists Special Publication 31: 213-231.

Dean, W.E. 1999. The carbon cycle and biogeochemical dynamics in lake sediments. Journal of Paleolimnology 21: 375-393.

Dean, W.E., M. Leinen and D.A. Stow. 1985. Classification of deep-sea, fine-grained sediments. Journal of Sedimentary Petrology 55: 0250-0256.

Dean, J.M., A.E.S. Kemp and R.B. Pearce. 2001. Paleo-flux records from electron microscope studies of Holocene laminated sediments, Saanich Inlet, British Columbia. Marine Geology 174: 139-158.

Dearing, J.A. 1986. Core correlation and total sediment influx. In: Berglund, B.E. (ed.) Handbook of Holocene Palaeoecology and Palaeohydrology. John Wiley and Sons Ltd., Chichester, England: 247-270.

Dearing, J.A. 1999. Magnetic susceptibility. In: Walden, J., F. Oldfield and J. Smith (eds.) Environmental Magnetism: a practical guide. Technical Guide No. 6. Quaternary Research Association, London, UK: 35-62.

Dyke, A.S. 1998. Holocene delevelling of Devon Island, Arctic Canada: implications for ice sheet geometry and crustal response. Canadian Journal of Earth Science 35: 885-904.

Dyke, A.S. 1999. Last Glacial Maximum and deglaciation of Devon Island, Arctic Canada: support for an Innuitian Ice Sheet. Quaternary Science Reviews 18: 393-420.

Dyke, A.S., T.F. Morris and D.E.C. Green. 1991. Postglacial tectonic and sea level history of the central Canadian Arctic. Geological Survey of Canada Bulletin 397. Energy, Mines and Resources Canada, Minister of Supply and Services Canada, Ottawa.

Dyke, A.S., L.A. Dredge and D.A. Hodgson. 2005. North America deglacial marine- and lake-limit surfaces. Géographie physique et Quaternaire 59: 155-185.

Eakins, J.D. and R.T. Morrison. 1978. The calculation of ^{210}Pb dates assuming a constant rate of unsupported ^{210}Pb to the sediment. Catena 5: 1-8.

Elvebakk, A. 1999. Bioclimatic delimitation and subdivision of the Arctic. In: Nordal, I. and V.Y. Raahivin (eds.) The Species Concept in the High North – A Panarctic Flora Initiative. The Norwegian Academy of Science and Letters, Oslo, Norway: 81-112.

Energy, Mines and Resources Canada. July 16, 1959. A16752-177 [air photographs]. Scale 1:60 000. National Air Photo Library (NAPL), Ottawa, Canada.

Fallu, M.A., R. Pienitz, I.R. Walker, J. Overpeck. 2004. AMS ^{14}C dating of tundra lake sediments using chironomid head capsules. Journal of Paleolimnology 31: 11–22.

Fisher, D.A. 1979. Comparison of 100,000 years of oxygen isotope and insoluble impurity profiles from the Devon Island and Camp Century ice cores. Quaternary Research 11: 299-304.

Fisher, D.A., R.M. Koerner, W.S.B. Paterson, W. Dansgaard, N. Gundestrup and N. Reeh. 1983. Effect of wind scouring on climatic records from icecore oxygen isotope profiles. Nature 301: 205-209.

Fisher, D.A. and R.M. Koerner. 1994. Signal and noise in four ice-core records from the Agassiz Ice Cap, Ellesmere Island, Canada: details of the last millennium for stable isotopes, melt, and solid conductivity. The Holocene 4: 113-120.

Fisher, D.A., R.M. Koerner and N. Reeh. 1995. Holocene Climatic Records from Agassiz Ice Cap, Ellesmere Island, NWT, Canada. The Holocene. 5: 19-24.

Folk, R.L. and W.C. Ward. 1957. Brazos River bar, a study in the significance of grain-size parameters. Journal of Sedimentary Petrology 27: 3-27.

Forbes A.C. and S.F. Lamoureux. 2005. Climatic controls on streamflow and suspended sediment transport in three large middle arctic catchments, Boothia Peninsula, Nunavut, Canada. Arctic, Antarctic, and Alpine Research 37: 304-315.

Francus, P., R.S. Bradley, M.A. Abbott, W. Patridge and F. Keimig. 2002. Paleoclimate studies of minerogenic sediments using annually resolved textural parameters. Geophysical Research Letters, 29: 59 1-4.

Francus, P., R.S. Bradley, T. Lewis, M. Abbott, M. Retelle and J.S. Stoner. 2008. Limnological and sedimentary processes at Sawtooth Lake, Canadian High Arctic, and their influence on varve formation. Journal of Paleolimnology online.

Fritts, H.C. 1976. Tree Rings and Climate. Academic Press, London, England.

Fritts, H.C. 1991. Reconstructing Large-scale Climatic Patterns from Tree-Ring Data – A Diagnostic Analysis. The University of Arizona Press, Tucson, AZ, USA.

Gajewski, K., M. Garneau and J.C. Bourgeois. 1995. Paleoenvironments of the Canadian High Arctic derived from pollen and plant macrofossils: problems and potentials. Quaternary Science Reviews 14:609-629.

Gajewski, K., P.B. Hamilton and R. McNeely. 1997. A high resolution proxy-climate record from an arctic lake with annually-laminated sediments on Devon Island, Nunavut, Canada. Journal of Paleolimnology 17: 215-225.

Gale, S.J. and P.G. Hoare. 1991. Quaternary Sediments – Petrographic Methods for the Study of Unlithified Rocks. Halsted Press, New York, NY, USA.

Geirsdóttir, Á., G.H. Miller, T. Thordarson and K.B. Ólafsdóttir. 2008. A 2000 year record of climate variations reconstructed from Haukadalsvatn, West Iceland. Journal of Paleolimnology doi 10.1007/s10933-008-9253-z0.

Glew, J.R. 1988. A portable extruding device for close interval sectioning of unconsolidated core samples. Journal of Paleolimnology 1: 235-239.

Glew, J.R. 1991. Miniature gravity corer for recovering short sediment cores. Journal of Paleolimnology 5: 285-287.

Gray, S.T., L.J. Graumlich, J.L. Betancourt and G.D. Pederson. 2004. A tree-ring based reconstruction of the Atlantic Multidecadal Oscillation since 1567 A.D. Geophysical Research Letters 31: L12205.

Griffiths, H.I. and J.A. Holmes. 2000. Non-marine ostracods & Quaternary palaeoenvironments. Quaternary Research Association Technical Guide No. 8. Quaternary Research Association, London, England.

Grootes, P.M., M. Stuiver, J.W.C. White, S.J. Johnsen and J. Jouzel. 1993. Comparison of oxygen isotope records from the GISP2 and GRIP Greenland cores. Nature 366: 552-554.

Haltia-Hovi, E., T. Saarinen, M. Kukkonen. 2007. A 2000-year record of solar forcing on varved lake sediment in eastern Finland. Quaternary Science Reviews 26: 678-689.

Hambley G.W. and S.F. Lamoureux. 2006. Recent summer climate recorded in complex varved sediments, Nicolay Lake, Cornwall Island, Nunavut, Canada. Journal of Paleolimnology 35: 629-640.

Hansen, L.B., and C.C. Langway. 1966. Deep core drilling in ice and core analysis at Camp Century, Greenland, 1961-1966. CRREL Spec. Report 126, no. 5, p.207-208.

Hardy, D.R., R.S. Bradley and B. Zolitschka. 1996. The climatic signal in varved sediments from Lake C2, northern Ellesmere Island, Canada. Journal of Paleolimnology 16: 227-238.

Heiri, O., A. F. Lotter, and G. Lemcke. 2001. Loss on ignition as a method for estimating organic and carbonate content in sediments: Reproducibility and comparability of results. Journal of Paleolimnology 25: 101-110.

Hughen, K.A., J. Overpeck and R.F. Anderson. 2000. Recent warming in a 500-year palaeotemperature record from varved sediments, Upper Soper Lake, Baffin Island, Canada. The Holocene 10: 9-19.

Hughen, K.A., M.G.L. Baillie, E. Bard, A. Bayliss, J.W. Beck, C. Bertrand, P.G. Blackwell, C.E. Buck, G. Burr, K.B. Cutler, P.E. Damon, R.L. Edwards, R.G. Fairbanks, M. Friedrich, T.P. Guilderson, B. Kromer, F.G. McCormac, S. Manning, C. Bronk Ramsey, P.J. Reimer, R.W. Reimer, S. Remmele, J.R. Southon, M. Stuiver, S. Talamo, F.W. Taylor, J. van der Plicht and C.E. Weyhenmeyer. 2004. Marine04 marine radiocarbon age calibration, 0-26 cal kyr BP. Radiocarbon 46: 1059-1086.

Johnsen, S.J., W. Dansgaard, H.B. Clausen and C.C. Langway. 1970. Climatic oscillations 1200-2000 A.D. Nature 227: 482-483.

Johnsen, S.J., W. Dansgaard, H.B. Clausen, and C.C. Langway. 1972. Oxygen isotope profiles through the Antarctic and Greenland ice sheets. Nature 235: 429-434.

Kelts, K., and K.J. Hsü. 1978. Freshwater carbonate sedimentation. In: Lerman, A. (ed.) Lakes – Chemistry, Geology, Physics. Springer, New York, NY, USA.

Kershaw, P. 1997. A modification of the Troels-Smith system of sediment description and portrayal. Quaternary Australasia 15: 63-68.

Koerner, R.M. 1977. Devon Island ice cap: core stratigraphy and paleoclimate. Science 196: 15-18.

Korotkevich, Y.S. and B.B. Kudriashov. 1974. Ice sheet drilling by Soviet Antarctic expeditions. In Ice Core Drilling (J.F. Splettoesser, ed.). University of Nebraska, Lincoln, 28-30 August, 1974, 63-70.

Krishnaswami, S., D. Lal, J.M. Martin and M. Meybeck. 1971. Geochronology of lake sediments. Earth and Planetary Science Letters 11: 407-414.

Lamoureux, S.F. 1994. Embedding unfrozen lake sediments for thin section preparation. Journal of Paleolimnology 10: 141-146.

Lamoureux, S.F. 1999a. Spatial and interannual variations in sedimentation patterns recorded in nonglacial varved sediments from the Canadian High Arctic. Journal of Paleolimnology 21: 73-84.

Lamoureux, S.F. 1999b. Catchment and lake controls over the formation of varves in monomictic Nicolay Lake, Cornwall Island, Nunavut. Canadian Journal of Earth Sciences 36: 1533-1546.

Lamoureux, S.F. 2000. Five centuries of interannual sediment yield and rainfall-induced erosion in the Canadian High Arctic recorded in lacustrine varves. Water Resources Research 36: 309-318.

Lamoureux, S.F. 2001. Varve Chronology Techniques. In: Last, W.M. and J.P. Smol (eds.) Tracking Environmental Change Using Lake Sediments – DPER Volume 1: Basin Analysis, Coring, and Chronological Techniques. Kluwer Academic Publishers, Dordrecht, The Netherlands: 247-260.

Lamoureux, S.F. 2002. Temporal patterns of suspended sediment yield following moderate to extreme hydrological events recorded in varved lacustrine sediments. Earth Surface Processes and Landforms 27: 1107-1124.

Lamoureux, S.F. and J. Bollmann. 2004. Image acquisition. In: P. Francus (ed.) Image Analysis, Sediments and Paleoenvironments – DPER Volume 7. Springer, Dordrecht, The Netherlands: 11-34.

Lamoureux, S.F. and R.S. Bradley. 1996. A late Holocene varved sediment record of environmental change from northern Ellesmere Island, Canada. Journal of Paleolimnology 16: 239-255.

Lamoureux, S.F. and R. Gilbert. 2004. A 750-yr record of autumn snowfall and temperature variability and winter storminess recorded in varved sediments of Bear Lake, Devon Island, Arctic Canada. Quaternary Research 61: 134-147.

Lamoureux, S.F., R. Gilbert and T. Lewis. 2002. Lacustrine sedimentary environments in High Arctic proglacial Bear Lake, Devon Island, Nunavut, Canada. Arctic, Antarctic, and Alpine Research 34: 130-141.

Lamoureux, S.F., K.A. Stewart, A.C. Forbes and D. Fortin. 2006. Multidecadal variations and decline in spring discharge in the Canadian middle Arctic since 1550 AD. Geophysical Research Letters 33 (L02403): 1-4.

Langway, C.C., H. Oeschger and W. Dansgaard (eds.), 1985. Greenland ice core: Geophysics, geochemistry and environment: Geophysical Monographs, v. 33, American Geophysics Union, Washington D.C.

Last, W.M. 2001. Textural analysis of lake sediments. In: Last, W.M. and J.P. Smol (eds.) Tracking Environmental Change Using Lake Sediments – DPER Volume 2: Physical and Geochemical Techniques. Kluwer Academic Publishers, Dordrecht, The Netherlands: 41-82.

LeBlanc, M., K. Gajewski and P.B. Hamilton. 2004. A diatom-based Holocene palaeoenvironmental record from a mid-arctic lake on Boothia Peninsula, Nunavut, Canada. The Holocene 14: 417-425.

Lewis, T., R. Gilbert and S.F. Lamoureux. 2002. Spatial and temporal changes in sedimentary processes at proglacial Bear Lake, Devon Island, Nunavut, Canada. Arctic, Antarctic, and Alpine Research 34: 119-129.

Livingstone, D.A. 1955. A lightweight piston sampler for lake deposits. Ecology 36: 137-139.

Lotter, A.F. and G. Lemcke. 1999. Methods for preparing and counting biochemical varves. Boreas 28: 243-252.

Lowe, J.J. and M.J.C. Walker. 1997. Reconstructing Quaternary Environments. 2nd Ed. Pearson Education Ltd., Edinburgh Gate, England.

Mann, M.E. and J.M. Lees. 1996. Robust estimation of background noise and signal detection in climatic time series. Climatic Change 33: 409-445.

Mann, M.E., Z. Zhang, M.K. Hughes, R.S. Bradley, S.K. Miller, S. Rutherford and F. Ni. 2008. Proxy-based reconstructions of hemispheric and global surface temperature variations over the past two millennia. Proceedings of the National Academy of Sciences of the United States of America 105: 13252-13257.

Mazzullo, J. and A.G. Graham. 1988. Handbook for shipboard sedimentologists. Ocean Drilling Program Technical note No. 8, Texas A&M University.

Maxwell, J.B. 1980. The climate of the Canadian arctic islands and adjacent waters. Environnement Canada, Service de l'environnement atmosphérique, Ottawa, Canada.

McGhee, R. 1978. Canadian Arctic Prehistory. Toronto: Van Nostrand Reinhold Ltd. pp128.

McGhee, R. 1996. Ancient People of the Arctic. Vancouver, UBC Press. pp244.

Moore, J.J., K.A. Hughen, G.H. Miller and J.T. Overpeck. 2001. Little Ice Age recorded in summer temperature reconstruction from varved sediments of Donard Lake, Baffin Island, Canada. Journal of Paleolimnology 25: 503-517.

Moskowitz, B.M. 1995. Fundamental physical constants and conversion factors. In: Global Earth Physics – A Handbook of Physical Constants. AGU Reference Shelf 1. American Geophysical Union, Washington DC, USA: 346-355.

Noffke, N., G. Gerdes, T. Klenke and W.E. Krumbein. 2001. Microbially induced sedimentary structures: A new classification of the Primary Sedimentary Structures. Journal of Sedimentary Research 71: 649-656.

Nowaczyk, N.R. 2001. Logging of magnetic susceptibility. In: Last, W.M. and J.P. Smol (eds.) Tracking Environmental Change Using Lake Sediments – DPER Volume 1: Basin Analysis, Coring, and Chronological Techniques. Kluwer Academic Publishers, Dordrecht, The Netherlands: 155-170.

O'Sullivan, P.E. 1983. Annually-laminated sediments and the study of Quaternary paleoenvironmental changes – a review. Quaternary Science Reviews 1: 245-313.

Oertli, H.J. (ed.). 1971. Colloque sur la paléoecologie des ostracodes. Pau, France: Bulletin du Centre de Researches Pau – SNPA.

Ohlendorf, C. and M. Sturm. 2007. A modified method for biogenic silica determination. Journal of Paleolimnology published online may 30, 2007. 6pp.

Ojala, A.E. 2004. Application of X-ray Radiography and Densitometry in Varve Analysis. In: P. Francus (ed.) Image Analysis, Sediments and Paleoenvironments – DPER Volume 7. Springer, Dordrecht, The Netherlands: 187-202.

Oldfield, F. and P.G. Appleby. 1984. Empirical testing of ^{210}Pb dating models. In: Haworth, E.Y. and J.G. Lund (eds.) Lake sediments and environmental history. Leicester University Press: 93-124.

Otto, G.H. 1938. The sedimentation unit and its use in field sampling. Journal of Geology 46: 569-582.

Outridge, P.M., G.A. Stern, P.B. Hamilton, J.B. Percival, R. McNeely and L.W. Lockhart. 2005. Trace metal profiles in the varved sediment of an Arctic lake. Geochimica et Cosmochimica Acta 69: 4881-4894.

Outridge, P.M., H. Sanei, G.A. Stern, P.B. Hamilton and F. Goodarzi. 2007. Evidence for control of mercury accumulation rates in Canadian High Arctic lake sediments by variations of aquatic primary productivity. Environmental Science and Technology 41: 5259-5265.

Pap, J.M., C. Fröhlich, H.S. Hudson and W.K. Tobiska (eds.). 1994. The Sun as a Variable Star: Solar and Stellar Irradiance Variations – Proceedsings of the 143rd International Astronomical Union held in the Clarion Harvest House, Boulder, Colorado June 20-25, 1993. Cambridge University Press, Cambridge, England. 379pp.

Paterson, W.S., R.M. Koerner, D. Fisher, J. Johnsen, H.B. Clausen, W. Dansgaard, P. Bucher and H. Oeschger. 1977. An oxygen-isotope climatic record from the Devon Island ice cap, arctic Canada. Nature 266: 508-511.

Pennington, W., R.S. Cambray, J.D. Eakins and D.D. Harkness. 1976. Radionuclide dating of the recent sediments of Blelham Tarn. Freshwater Biology 6: 317-331.

Peros, M.C. and K. Gajewski. 2008. Pollen-based reconstructions of late Holocene climate from the central and western Canadian Arctic. Journal of Paleolimnology DOI 10.1007/s10933-008-9256-9.

Perren, B.B., R.S. Bradley and P. Francus. 2003. Rapid lacustrine response to recent High Arctic warming: a diatom record from Sawtooth Lake, Ellesmere Island, Nunavut. 2003. Arctic, Antarctic, and Alpine Research 35: 271-278.

Pilcher, J.R. 2003. Radiocarbon dating and environmental radiocarbon studies. In: Mackay, A., R. Battarbee, J. Birks and F. Oldfield (eds.) Global Change in the Holocene. Arnold Publishers, London, England: 63-74.

Principato, S.M. 2004. X-Ray Radiographs of sediment Cores: A Guide to Analyzing Diamicton. In: P. Francus (ed.) Image Analysis, Sediments and Paleoenvironments - DPER Volume 7. Springer, Dordrecht, The Netherlands: 165-186.

Rasmussen, S.O., I.K. Seierstad, K.K. Andersen, M. Bigler, D. Dahl-Jensen and S.J. Johnsen. 2007. Synchronization of the NGRIP, GRIP, and GISP2 ice cores across MIS 2 and paleoclimatic implications. Quaternary Science Reviews, INTIMATE special issue.

Reimer, P.J., M.G.L. Baillie, E. Bard, A. Bayliss, J.W. Beck, C.J.H. Bertrand, P.G. Blackwell, C.E. Buck, G.S. Burr, K.B. Cutler, P.E. Damon, R.L. Edwards, R.G. Fairbanks, M. Friedrich, T.P. Guilderson, P. Thomas, A.G. Hogg, K.A. Hughen, B. Kromer, G. McCormac, S. Manning, C.B. Ramsey, R.W. Reimer, S. Remmele, J.R. Southon, M. Stuiver, S. Talamo, F.W. Taylor, J. van der Plicht and C.E. Weyhenmeyer. 2004. IntCal04 Terrestrial Radiocarbon Age Calibration, 0–26 Cal Kyr BP Radiocarbon 46: 1029-1058.

Reimer, R.W. and P.J. Reimer. 2006. Marine reservoir corrections and the calibration curve. Pages News Past Global Changes 14: 12-13.

Robbins, J.A. 1978. Geochemical and geophysical applications of radioactive lead. In: Nriagu, J.O. (ed.) Biogeochemistry of lead in the environment. Elsevier Scientific, Amsterdam, The Netherlands: 285-393.

Roch, M-C. 1999. Susceptibilité Magnétique. Laboratory for Paleoclimatology and Climatology, Department of Geography, University of Ottawa. Undergraduate thesis, supervisor Dr. Konrad Gajewski.

Rowley, J.R. and A.O. Dahl. 1956. Modifications in design and use of the Livingston piston sampler. Ecology 37: 849-851.

Saarnisto, M. 1986. Annually laminated lake sediments. In: Berglund, B.E. (ed.) Handbook of Holocene Palaeoecology and Palaeohydrology. John Wiley and Sons Ltd., Chichester, UK: 343-370.

Sandgren, P. and I. Snowball. 2001. Application of mineral magnetic techniques to paleolimnology. In: Last, W.M. and J.P. Smol (eds.) Tracking Environmental Change Using Lake Sediments – DPER Volume 2: Physical and Geochemical Techniques. Kluwer Academic Publishers, Dordrecht, The Netherlands: 217-238.

Schnurrenberger, D., J. Russell and K. Kelts. 2003. Classification of lacustrine sediments based on sedimentary components. Journal of Paleolimnology 29: 141-154.

Schulz, M. and M. Mudelsee. 2002. REDFIT: estimating red-noise spectra directly from unevenly spaced paleoclimatic time series. Computers & Geosciences 28: 421-426.

Schulz, M. and K. Stattegger. 1997. SPECTRUM: spectral analysis of unevenly spaced paleoclimatic time series. Computers & Geosciences 23: 929-945.

Sewell, D.R. 1998. A note for novices. Radiocarbon 40: xi.

SIDC-team (Solar Influences Data Analysis Center). 2008. World Data Center for the Sunspot Index, Royal Observatory of Belgium, Monthly Report on the International Sunspot Number, online catalogue of the sunspot index: http://www.sidc.be/sunspot-data/

Smith Jr., S.V., R.S. Bradley and M.B. Abbott. 2004. A 300 year record of environmental change from Lake Tuborg, Ellesmere Island, Nunavut, Canada. Journal of Paleolimnology 32: 137-148.

Smol, J. 2002. Reading the records stored in sediments: the present is a key to the past. In: Pollution of lakes and rivers, a paleoenvironmental perspective. Oxford Press Inc., New York: 45-66.

Snowball, I. 1999. Electromagnetic units and their use in environmental magnetic studies. In: Environmental Magnetism: a practical guide. Technical Guide No. 6. Quaternary Research Association, London, UK: 89-97.

Stern, G.A., E. Brackevelt, P.A. Helm, T.F. Bidleman, P.M Outridge, W.L. Lockhart, R. McNeeley, B. Rosenberg, M.G. Ikonomou, P. Hamilton, G.T. Tomy and P. Wilkinson. 2005. Modern and historical fluxes of halogenated organic contaminants to a lake in the Canadian arctic, as determined from annually laminated sediment cores. Science of the Total Environment 342: 223-243.

Stuiver, M. and P.J. Reimer. 1993a. CALIB User's Guide Rev. 3.0. University of Washington, Quaternary Isotope Laboratory.

Stuiver, M. and P.J. Reimer. 1993b. Extended ^{14}C Data Base and Revised CALIB 3.0 ^{14}C Age Calibration Program. Radiocarbon 35: 215-230.

Stuiver, M., P.M. Grootes and T.F. Braziunas. 1995. The GISP2 18O climate record of the past 16,500 years and the role of the sun, ocean and volcanoes. Quaternary Research 44: 341-354.

Thompson, L.G., E. Mosley-Thompson, M.E. Davis, J.F. Bolzan, T. Yao, N. Gundestrup, X. Wu, L. Klein and Z. Xie. 1989. 100,000 year climate record from Qinghai-Tibetan Plateau ice cores. Science 246: 474-477.

Thompson, L.G., E. Mosley-Thompson, M.E. Davis, P.-N. Lin, K. Henderson and T.A. Mashiotta. 2003. Tropical glacier and ice core evidence of climate change on annual to millennial time scales. Climatic Change 59: 137-155.

Thompson, R. 1986. Palaeomagnetic dating. In: Berglund, B.E. (ed.) Handbook of Holocene Palaeoecology and Palaeohydrology. John Wiley and Sons Ltd., Chichester, UK: 313-327.

Thorsteinsson R. and U. Mayr. 1986. Geology of Bear Bay West and Baillie-Hamilton Island, District of Franklin, Northwest Territories. Geological Survey of Canada map 1614A [map]. Scale 1:250000.

Troels-Smith, J. 1955. Characterization of Unconsolidated sediments. Dansmarks Geologiske Undersogelse IV Series 3(10).

Turner, L.J. 1990. Laboratory determination of ^{210}Pb-^{210}Po using alpha spectronomy. 2nd ed. National Water Research Institute, Burlington, Ontario. Technical Note LRB-90-TN-07. 7p.

Turner, L.J. 1995. ^{210}Pb dating of lacustrine sediments from a Devon Island lake (Core 069, Station DV09), NWT. National Water Research Institute, Burlington, Ontario. NWRI Contribution 95-103, January, 1995. 23p.

Vallentyne, J.R. 1955. A modification of the Livingstone piston sampler for lake deposits. Ecology 36: 139-141.

Viau, A.E., K. Gajewski, M.C. Sawada and P. Fines. 2006. Millennial-scale temperature variations in North America during the Holocene. Journal of Geophysical Research 111 (D09102): 1-12.

Visher, G.S. 1969. Grain size distributions and depositional processes. Journal of Sedimentary Petrology 39: 1074-1106.

Vinther, B.M., H.B. Clausen, S.J. Johnsen, S.O. Rasmussen, K.K. Andersen, S.L. Buchardt, D. Dahl-Jensen, I.K. Seierstad, M.-L. Siggaard-Andersen, J.P. Steffensen, A.M. Svensson, J. Olsen and J. Heinemeier. 2006. A synchronized dating of three Greenland ice cores throughout the Holocene. Journal of Geophysical Research 111 (D13102).

Wake, C.P., K. Yalcin and N. Gundestrup. 2002. The climate signal recorded in the oxygen isotope, accumulation, and major ion time-series from the Eclipse Ice Core, Yukon Territory. Annals of Glaciology 35: 416-422.

Wohlfarth, B., G. Lemdahl, S. Olsson, T. Persson, I. Snowball, J. Ising and V. Jones. 1995. Early Holocene environment on Bjornoya (Svalbard) inferred from multidisciplinary lake sediment studies. Polar Research 14: 253-275.

Wright Jr., H.E., E.J. Cushing and D.A. Livingstone. 1965. Coring devices for lake sediments. P. 494- in Kummel, B. and Raup, D. Handbook of paleontological techniques. W.H. Freeman, San Francisco. 520.

Yalcin, K. and C.P. Wake. 2001. Anthropogenic signals recorded in an ice core from Eclipse Icefield, yukon Territory. Geophysical Research letters 28: 4487-4490.

Yalcin, K., C.P. Wake and M. Germani. 2003. A 100-year record of North Pacific volcanism in an ice core from Eclipse Icefield, Yukon Territory, Canada. Journal of Geophysical Research 108: 10.1029/2002JD00244.

Yamaguchi, D.K. 1991. A simple method for cross-dating increment cores from living trees. Canadian Journal of Forest Research 21: 414-416.

Zabenskie, S. 2006. Post-Glacial climatic change on Boothia Penisnula, Nunavut, Canada. MSc Thesis, University of Ottawa. 98pp.

Zabenskie, S. and K. Gajewski. 2007. Post-Glacial climatic change on Boothia Penisnula, Nunavut, Canada. Quaternary Research 68: 261-270.

Zagorodnov, V.S. 1988. Recent Soviet activities on ice core driling and core investigations in Arctic region. Bulletin of Glacier Research 6: 81-84.

Zolitschka, B. 1996. Recent sedimentation in a High Arctic lake, northern Ellesmere Island, Canada. Journal of Paleolimnology 16: 169-186.

Zolitschka, B. 2003. Dating based on freshwater- and marine-laminated sediments. In: Mackay, A., R. Battarbee, J. Birks and F. Oldfield (eds.) Global Change in the Holocene. Arnold Publishers, London, England: 63-74.

Zolitschka, B., J. Mingram, S. Van Der Gaast, J.H. Fred Jansen and R. Naumann. 2001. Sediment logging techniques. In: Last, W.M. and J.P. Smol (eds.) Tracking Environmental Change Using Lake Sediments – DPER Volume 1: Basin Analysis, Coring, and Chronological Techniques. Kluwer Academic Publishers, Dordrecht, The Netherlands: 137-154.

Appendix 1 – Study site relative sea level (RSL) regression curve

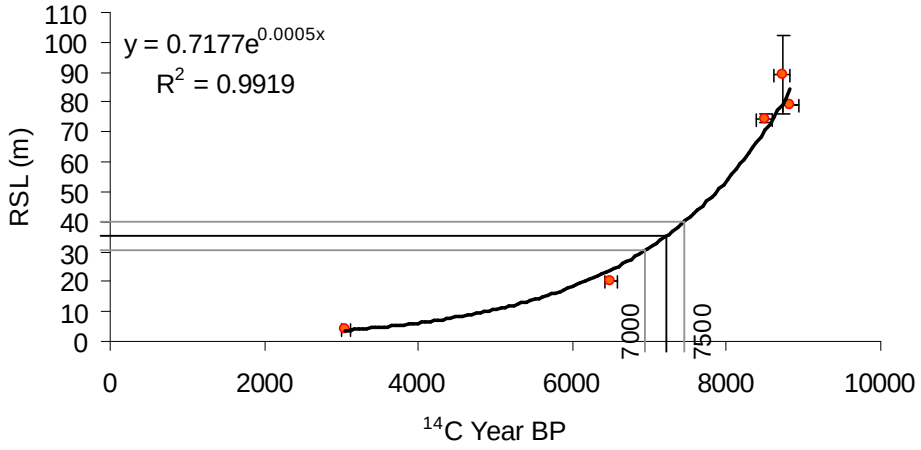

Relative sea level (RSL) exponential regression curve developed for the Thomas Lee Inlet, based on radiocarbon dates of material found on raised beaches (Dyke, 1998). Lake DV09 is situated at 35m (between 30 and 40m contour intervals on NTS map 58 H/10. Fig 2 contains the corresponding calibrated dates.

Appendix 2 – Copyright consent form for use of air photo

Natural Resources Canada | Ressources naturelles Canada

Earth Sciences Sector | Secteur des sciences de la Terre

Ottawa, Ontario K1A 0E8 | Ottawa (Ontario) K1A 0E8

September 19, 2008

Colin John Courtney Mustaphi
Laboratory for Climatology and Paleoclimatology
Department of Geography
University of Ottawa
60 University Private
Ottawa, ON K1N 6N5

Mr. Mustaphi,

Formal permission is granted to use on a one time basis (this purpose only) the following image. An adaptation of the aerial photograph will be reproduced in your university thesis.

ROLL NO.	PHOTO NO.	DATE
A16752	177	1959

The material should appear with an appropriate acknowledgement, for example "Reproduced with the permission of Natural Resources Canada 2008, courtesy of the National Air Photo Library."

Sincerely,

Joanne Tremblay
Copyright Office
Data Dissemination Division
Earth Sciences Sector

Canada

Appendix 3 – DV09 sediment core recovery information

Cores recovered from Lake DV09 July 15 – 26, 1996, by K. Gajewski, P. Hamilton, and T. Malik.

Number	Core	Date/Time	Water depth (m)	Length (m)	Number of drives	Notes
1	A	15-Jun-96	13	0.70	1	
2	B	15-Jun-96	13.2	1.47	2	
3	C	15-Jun-96	14.1	1.66	2	Glew core also taken
4	D_i	15-Jun-96	12.9	0.76	1	
5	D_{ii}	15-Jun-96	12.9	0.31	1	
6	E	16-Jun-96	13.4	6.26	7	
7	F	16-Jun-96	13.3	0.75	1	
8	G	16-Jun-96	13.3	6.75	8	
9	H	17-Jun-96	11.6	0.23	1	possible layer w/o laminations
10	I	17-Jun-96	3.48	0.25	1	
11	J	17-Jun-96	4.8	0.23	1	
-	K	17-Jun-96	1.8	0.00	0	mud layer at surface, no core recovered
12	L	17-Jun-96	4.2	0.29	1	
13	M	17-Jun-96	11.8	0.46	1	
14	N	17-Jun-96 - 15:50	10.7	0.42	1	
15	O	17-Jun-96	8.76	0.42	1	
16	P	22-Jun-96	13.01	2.65	4	Core P3 largely disturbed sediments
17	S	22-Jun-96	13.11	3.30	5	Core S4 largely disturbed sediments
18	T	26-Jun-96	13.64	6.48	10	Cores T4, T5, and T6 are parallel to main Core T hole

Summarized from the LPC field notebook labeled “Devon 1996”.

Appendix 4 – DV09 Core B crossdated varve width data values

Year AD	VW (mm)						
1996	4.135	1952	0.567	1908	0.527	1864	0.620
1995	0.705	1951	1.090	1907	0.167	1863	0.376
1994	0.967	1950	0.844	1906	1.509	1862	0.397
1993	0.562	1949	0.837	1905	1.321	1861	0.417
1992	1.083	1948	0.596	1904	0.458	1860	0.477
1991	0.601	1947	0.724	1903	1.088	1859	0.395
1990	0.669	1946	0.751	1902	1.422	1858	5.867
1989	0.677	1945	3.810	1901	0.924	1857	0.287
1988	0.661	1944	0.545	1900	0.294	1856	0.318
1987	0.607	1943	0.572	1899	0.278	1855	0.403
1986	0.717	1942	0.616	1898	0.841	1854	0.323
1985	0.690	1941	0.545	1897	0.203	1853	0.405
1984	0.901	1940	0.954	1896	0.638	1852	0.678
1983	0.676	1939	0.526	1895	0.605	1851	0.592
1982	0.731	1938	0.631	1894	1.571	1850	0.588
1981	0.542	1937	0.510	1893	0.705	1849	1.585
1980	0.312	1936	0.672	1892	0.403	1848	0.461
1979	0.952	1935	0.714	1891	0.526	1847	0.360
1978	0.638	1934	0.639	1890	0.152	1846	0.334
1977	1.632	1933	0.581	1889	0.460	1845	1.168
1976	2.015	1932	1.108	1888	1.031	1844	0.443
1975	0.894	1931	1.191	1887	0.292	1843	0.790
1974	1.663	1930	1.217	1886	0.215	1842	0.621
1973	1.703	1929	2.456	1885	0.295	1841	0.348
1972	0.923	1928	0.490	1884	0.348	1840	0.382
1971	0.942	1927	1.307	1883	0.325	1839	0.707
1970	1.749	1926	0.501	1882	0.220	1838	0.537
1969	0.954	1925	0.621	1881	0.993	1837	0.536
1968	1.096	1924	0.864	1880	0.377	1836	1.188
1967	1.744	1923	0.884	1879	0.273	1835	0.239
1966	0.995	1922	0.660	1878	0.316	1834	0.303
1965	1.537	1921	0.790	1877	0.333	1833	0.434
1964	6.365	1920	0.605	1876	0.371	1832	0.680
1963	4.040	1919	0.712	1875	0.380	1831	0.855
1962	2.584	1918	0.984	1874	0.383	1830	0.791
1961	0.315	1917	3.025	1873	0.350	1829	0.350
1960	0.319	1916	0.357	1872	0.264	1828	0.763
1959	0.365	1915	0.257	1871	0.309	1827	0.374
1958	0.314	1914	0.260	1870	0.246	1826	0.570
1957	0.660	1913	0.375	1869	0.181	1825	1.227
1956	0.272	1912	0.322	1868	0.210	1824	0.436
1955	0.511	1911	0.450	1867	0.406	1823	0.701
1954	0.394	1910	0.521	1866	0.408	1822	0.394
1953	0.514	1909	0.594	1865	0.458	1821	0.170

* VW = varve width

1820	0.237	1775	0.211	1730	0.329	1685	0.406
1819	0.426	1774	0.703	1729	0.508	1684	0.203
1818	0.335	1773	2.475	1728	0.285	1683	0.282
1817	0.294	1772	0.347	1727	0.316	1682	0.348
1816	0.422	1771	0.301	1726	0.231	1681	0.427
1815	0.461	1770	0.331	1725	0.334	1680	0.235
1814	0.679	1769	0.450	1724	0.261	1679	0.232
1813	2.391	1768	0.264	1723	0.245	1678	0.128
1812	0.878	1767	0.589	1722	0.187	1677	0.252
1811	1.248	1766	1.673	1721	0.157	1676	0.643
1810	0.995	1765	0.254	1720	0.156	1675	0.383
1809	0.716	1764	0.286	1719	0.194	1674	0.360
1808	0.518	1763	0.389	1718	0.248	1673	0.298
1807	0.774	1762	0.504	1717	0.574	1672	0.415
1806	0.713	1761	0.171	1716	0.500	1671	0.565
1805	0.381	1760	0.256	1715	0.605	1670	0.720
1804	0.287	1759	0.219	1714	0.390	1669	0.369
1803	0.339	1758	0.470	1713	1.012	1668	0.281
1802	0.302	1757	0.380	1712	0.326	1667	0.818
1801	5.441	1756	0.335	1711	0.543	1666	0.305
1800	2.271	1755	0.408	1710	1.464	1665	0.289
1799	0.689	1754	0.379	1709	0.658	1664	0.815
1798	2.694	1753	0.431	1708	5.507	1663	1.415
1797	2.780	1752	0.258	1707	0.477	1662	0.527
1796	0.907	1751	0.142	1706	0.414	1661	0.580
1795	0.426	1750	0.163	1705	0.677	1660	0.498
1794	0.604	1749	0.216	1704	0.181	1659	0.513
1793	0.880	1748	1.109	1703	0.304	1658	0.523
1792	0.381	1747	0.226	1702	2.889	1657	0.361
1791	0.326	1746	0.081	1701	0.320	1656	0.375
1790	11.314	1745	0.122	1700	0.257	1655	0.625
1789	0.333	1744	0.160	1699	0.513	1654	0.686
1788	0.563	1743	0.100	1698	0.888	1653	0.207
1787	2.152	1742	0.174	1697	0.282	1652	0.122
1786	0.203	1741	0.265	1696	0.207	1651	0.129
1785	0.417	1740	0.206	1695	0.153	1650	0.238
1784	0.416	1739	0.166	1694	0.159	1649	0.156
1783	0.321	1738	0.126	1693	0.229	1648	0.544
1782	0.231	1737	0.203	1692	0.082	1647	0.320
1781	0.330	1736	0.152	1691	0.289	1646	0.289
1780	0.400	1735	0.161	1690	0.260	1645	0.307
1779	0.590	1734	0.756	1689	0.691	1644	0.358
1778	0.528	1733	0.224	1688	0.345	1643	0.325
1777	0.317	1732	0.459	1687	0.255	1642	0.617
1776	0.344	1731	0.357	1686	0.226	1641	1.098

1640	0.269	1595	0.292	1550	2.416	1505	0.428
1639	0.272	1594	0.657	1549	1.264	1504	0.327
1638	0.207	1593	0.419	1548	1.862	1503	0.277
1637	0.189	1592	1.655	1547	3.043	1502	0.222
1636	0.355	1591	0.633	1546	1.355	1501	0.290
1635	0.169	1590	0.602	1545	0.623	1500	0.182
1634	0.263	1589	0.184	1544	39.066	1499	0.210
1633	0.528	1588	0.173	1543	0.332	1498	0.318
1632	0.341	1587	0.181	1542	0.317	1497	3.476
1631	0.207	1586	0.163	1541	0.305	1496	0.581
1630	0.264	1585	0.168	1540	0.397	1495	0.723
1629	0.198	1584	0.172	1539	0.393	1494	0.466
1628	0.500	1583	0.249	1538	0.754	1493	0.855
1627	0.443	1582	5.833	1537	0.528	1492	0.732
1626	0.889	1581	0.207	1536	0.380	1491	0.247
1625	0.544	1580	0.170	1535	0.269	1490	0.216
1624	0.590	1579	2.366	1534	0.238	1489	2.675
1623	0.466	1578	0.216	1533	0.298	1488	0.397
1622	0.350	1577	0.203	1532	0.348	1487	0.479
1621	0.389	1576	0.322	1531	0.445	1486	0.682
1620	0.943	1575	0.206	1530	0.640	1485	0.615
1619	0.403	1574	0.329	1529	1.885	1484	0.609
1618	0.330	1573	0.353	1528	0.782	1483	1.663
1617	0.529	1572	0.298	1527	1.418	1482	0.516
1616	0.399	1571	0.305	1526	0.419	1481	0.365
1615	0.402	1570	0.419	1525	1.887	1480	0.735
1614	0.266	1569	0.558	1524	1.061	1479	0.870
1613	0.267	1568	1.543	1523	0.952	1478	0.915
1612	0.314	1567	1.486	1522	0.642	1477	0.932
1611	0.264	1566	2.355	1521	0.974	1476	0.477
1610	0.798	1565	1.591	1520	0.732	1475	0.428
1609	0.777	1564	1.465	1519	0.514	1474	0.542
1608	0.826	1563	1.089	1518	3.786	1473	0.400
1607	0.397	1562	1.333	1517	0.265	1472	0.337
1606	0.266	1561	2.309	1516	0.354	1471	0.227
1605	0.449	1560	1.496	1515	0.313	1470	0.217
1604	0.146	1559	1.882	1514	0.302	1469	0.176
1603	0.563	1558	3.343	1513	0.496	1468	0.195
1602	0.483	1557	1.536	1512	0.673	1467	0.168
1601	0.317	1556	1.368	1511	0.454	1466	0.286
1600	0.359	1555	1.431	1510	0.430	1465	0.237
1599	0.265	1554	2.162	1509	0.497	1464	0.686
1598	0.442	1553	3.132	1508	0.206	1463	6.383
1597	0.185	1552	1.309	1507	0.174	1462	3.463
1596	0.307	1551	1.320	1506	0.504	1461	0.571

1460	0.510	1415	0.163	1370	0.499	1325	2.111
1459	0.371	1414	0.448	1369	0.220	1324	0.469
1458	0.383	1413	0.257	1368	0.289	1323	0.370
1457	1.683	1412	0.132	1367	0.143	1322	0.297
1456	0.498	1411	1.002	1366	0.496	1321	3.142
1455	0.159	1410	0.461	1365	0.481	1320	0.461
1454	0.195	1409	0.298	1364	0.631	1319	0.265
1453	0.180	1408	0.256	1363	1.283	1318	0.163
1452	0.393	1407	0.446	1362	0.394	1317	0.496
1451	1.122	1406	0.292	1361	0.139	1316	0.451
1450	0.251	1405	0.256	1360	0.361	1315	0.601
1449	0.199	1404	0.234	1359	0.297	1314	1.191
1448	0.280	1403	0.260	1358	0.446	1313	0.385
1447	0.293	1402	0.336	1357	0.256	1312	0.332
1446	1.168	1401	0.219	1356	0.364	1311	0.585
1445	0.227	1400	0.184	1355	0.427	1310	0.840
1444	0.231	1399	0.241	1354	0.285	1309	1.201
1443	0.414	1398	0.252	1353	0.514	1308	1.387
1442	1.781	1397	0.226	1352	0.466	1307	1.707
1441	0.606	1396	0.162	1351	0.452	1306	0.725
1440	0.439	1395	2.842	1350	0.366	1305	1.784
1439	0.538	1394	1.983	1349	0.902	1304	0.659
1438	0.404	1393	1.021	1348	1.107	1303	0.328
1437	0.395	1392	0.333	1347	1.792	1302	2.587
1436	0.188	1391	0.471	1346	1.290	1301	1.260
1435	0.186	1390	0.714	1345	0.238	1300	0.469
1434	0.469	1389	1.166	1344	0.394	1299	2.692
1433	0.388	1388	0.623	1343	0.882	1298	1.229
1432	0.479	1387	0.931	1342	0.534	1297	1.298
1431	0.340	1386	3.176	1341	0.497	1296	1.568
1430	0.378	1385	0.667	1340	0.902	1295	2.302
1429	0.511	1384	0.928	1339	0.746	1294	1.214
1428	0.644	1383	2.621	1338	1.477	1293	2.154
1427	0.596	1382	0.413	1337	0.816	1292	2.542
1426	0.721	1381	0.368	1336	1.715	1291	30.948
1425	1.176	1380	0.544	1335	1.340	1290	22.422
1424	0.261	1379	1.342	1334	1.186	1289	0.743
1423	0.188	1378	0.309	1333	2.442	1288	0.922
1422	0.748	1377	0.310	1332	1.253	1287	1.630
1421	1.418	1376	0.312	1331	0.455	1286	0.874
1420	1.211	1375	0.298	1330	0.398	1285	0.869
1419	2.618	1374	0.320	1329	0.393	1284	1.045
1418	0.195	1373	0.283	1328	0.213	1283	0.867
1417	0.241	1372	0.412	1327	0.414	1282	5.558
1416	0.206	1371	0.266	1326	0.448	1281	1.124

1280	26.831	1235	0.697	1190	1.025	1145	3.564
1279	1.049	1234	0.731	1189	0.922	1144	1.840
1278	0.909	1233	1.934	1188	1.230	1143	0.732
1277	0.798	1232	0.840	1187	1.747	1142	2.489
1276	0.952	1231	0.634	1186	2.011	1141	1.155
1275	0.566	1230	1.360	1185	1.518	1140	1.842
1274	2.219	1229	0.738	1184	1.284	1139	1.252
1273	0.411	1228	0.767	1183	0.827	1138	2.289
1272	0.629	1227	0.588	1182	1.994	1137	0.574
1271	1.606	1226	0.761	1181	0.549	1136	1.669
1270	0.611	1225	1.592	1180	2.022	1135	1.021
1269	0.825	1224	1.782	1179	3.202	1134	1.368
1268	1.132	1223	1.742	1178	1.250	1133	2.320
1267	1.307	1222	0.775	1177	1.606	1132	1.898
1266	2.461	1221	0.574	1176	1.731	1131	0.942
1265	1.353	1220	0.454	1175	1.356	1130	1.026
1264	1.026	1219	0.561	1174	0.552	1129	1.084
1263	0.483	1218	0.669	1173	0.780	1128	0.792
1262	0.547	1217	0.929	1172	2.383	1127	1.285
1261	1.138	1216	3.044	1171	2.556	1126	1.151
1260	0.505	1215	0.950	1170	1.700	1125	1.847
1259	0.690	1214	0.728	1169	2.190	1124	1.291
1258	1.009	1213	1.570	1168	1.851	1123	1.382
1257	2.768	1212	0.825	1167	1.254	1122	1.125
1256	0.960	1211	1.440	1166	2.039	1121	1.191
1255	1.016	1210	3.198	1165	1.935	1120	9.686
1254	1.876	1209	0.592	1164	1.723	1119	0.810
1253	1.315	1208	0.567	1163	0.542	1118	0.989
1252	0.333	1207	0.695	1162	0.902	1117	0.829
1251	0.256	1206	0.709	1161	2.986	1116	0.381
1250	0.494	1205	2.325	1160	2.767	1115	2.727
1249	1.455	1204	0.578	1159	0.867	1114	3.076
1248	1.520	1203	0.607	1158	1.296	1113	3.510
1247	0.772	1202	0.914	1157	1.602	1112	1.856
1246	0.730	1201	4.504	1156	1.307	1111	0.747
1245	0.705	1200	1.548	1155	1.368	1110	0.558
1244	0.932	1199	0.988	1154	1.742	1109	1.119
1243	0.924	1198	0.924	1153	1.627	1108	1.555
1242	0.553	1197	0.735	1152	2.507	1107	1.080
1241	0.768	1196	1.016	1151	0.892	1106	1.472
1240	0.612	1195	1.008	1150	3.692	1105	1.195
1239	0.485	1194	0.972	1149	0.841	1104	2.101
1238	0.904	1193	1.675	1148	3.074	1103	1.466
1237	0.760	1192	1.219	1147	1.418	1102	4.138
1236	0.547	1191	1.172	1146	3.963	1101	1.106

1100	0.972	1055	2.805	1010	0.367	965	0.365
1099	0.682	1054	0.393	1009	0.225	964	0.534
1098	1.624	1053	1.828	1008	0.282	963	0.591
1097	1.953	1052	13.956	1007	0.405	962	0.143
1096	1.645	1051	12.429	1006	0.248	961	0.633
1095	0.174	1050	1.931	1005	0.352	960	0.165
1094	0.176	1049	0.823	1004	0.344	959	0.213
1093	0.168	1048	0.209	1003	0.191	958	1.078
1092	0.193	1047	0.243	1002	0.245	957	1.265
1091	0.148	1046	0.275	1001	0.234	956	0.252
1090	0.132	1045	0.290	1000	0.173	955	0.381
1089	0.224	1044	0.410	999	0.369	954	0.366
1088	0.231	1043	0.397	998	0.342	953	0.509
1087	0.379	1042	1.824	997	0.318	952	0.745
1086	0.651	1041	0.231	996	0.236	951	0.793
1085	1.253	1040	0.198	995	0.272	950	0.594
1084	0.278	1039	0.224	994	0.274	949	3.528
1083	0.406	1038	0.196	993	0.287	948	0.348
1082	1.024	1037	0.241	992	0.230	947	0.231
1081	3.815	1036	0.226	991	0.315	946	0.249
1080	2.786	1035	0.204	990	0.297	945	0.221
1079	0.562	1034	0.216	989	1.028	944	0.166
1078	1.091	1033	0.212	988	0.727	943	0.445
1077	2.261	1032	0.335	987	0.404	942	0.279
1076	2.193	1031	0.269	986	1.456	941	0.225
1075	0.536	1030	0.384	985	0.737	940	0.233
1074	1.798	1029	0.343	984	1.246	939	0.202
1073	3.537	1028	0.951	983	3.014	938	0.184
1072	1.706	1027	0.881	982	0.446	937	0.164
1071	3.276	1026	2.506	981	0.407	936	0.186
1070	2.095	1025	0.342	980	0.330	935	0.253
1069	3.854	1024	0.162	979	0.664	934	0.315
1068	2.931	1023	0.193	978	0.898	933	0.348
1067	0.740	1022	0.232	977	0.371	932	0.257
1066	1.460	1021	0.353	976	0.303	931	0.149
1065	1.431	1020	0.432	975	2.467	930	0.126
1064	0.862	1019	0.554	974	0.440	929	0.170
1063	0.795	1018	0.444	973	0.502	928	0.452
1062	0.786	1017	0.368	972	0.505	927	0.357
1061	0.821	1016	0.417	971	0.466	926	0.359
1060	2.704	1015	0.486	970	0.405	925	0.379
1059	1.080	1014	0.241	969	0.386	924	0.364
1058	0.975	1013	0.213	968	0.328	923	0.290
1057	0.992	1012	0.292	967	0.332	922	0.187
1056	1.487	1011	0.329	966	0.306	921	0.240

920	0.319	875	0.221	830	0.167	785	1.259
919	0.358	874	0.158	829	0.210	784	0.123
918	0.330	873	0.129	828	0.238	783	0.165
917	0.402	872	0.091	827	0.277	782	0.150
916	0.385	871	0.072	826	0.243	781	0.132
915	0.323	870	0.128	825	0.268	780	0.137
914	0.264	869	0.230	824	0.250	779	0.182
913	0.291	868	0.210	823	0.161	778	0.168
912	0.320	867	0.156	822	0.168	777	0.190
911	0.311	866	0.203	821	0.155	776	0.199
910	0.351	865	0.181	820	0.209	775	0.232
909	0.397	864	0.134	819	0.177	774	4.896
908	0.231	863	0.151	818	0.148	773	0.238
907	0.258	862	0.123	817	0.229	772	0.203
906	0.203	861	0.139	816	0.220	771	0.124
905	0.223	860	0.141	815	0.175	770	0.098
904	0.197	859	0.217	814	0.231	769	0.138
903	0.212	858	0.148	813	0.160	768	0.169
902	0.232	857	0.146	812	0.150	767	0.140
901	0.676	856	0.169	811	0.174	766	0.130
900	0.379	855	0.151	810	0.185	765	0.169
899	0.339	854	0.212	809	0.193	764	0.102
898	0.447	853	0.364	808	0.212	763	0.123
897	0.273	852	0.273	807	0.194	762	0.104
896	0.167	851	0.254	806	0.255	761	0.214
895	0.145	850	0.235	805	0.264	760	0.179
894	0.239	849	0.230	804	0.292	759	0.494
893	0.199	848	0.199	803	0.261	758	0.115
892	0.177	847	0.185	802	0.313	757	0.106
891	0.192	846	0.239	801	0.224	756	0.137
890	0.211	845	0.237	800	0.241	755	0.097
889	0.243	844	0.297	799	0.695	754	0.157
888	0.231	843	0.273	798	2.731	753	0.243
887	0.190	842	0.424	797	0.564	752	0.116
886	0.267	841	2.436	796	0.539	751	0.085
885	0.245	840	0.289	795	0.463	750	0.099
884	0.184	839	0.310	794	0.541	749	0.129
883	0.753	838	0.249	793	0.315	748	0.138
882	0.498	837	0.253	792	0.383	747	0.171
881	0.470	836	0.231	791	0.388	746	0.316
880	0.329	835	0.486	790	0.379	745	0.431
879	0.404	834	0.186	789	0.396	744	0.363
878	0.343	833	0.169	788	0.391	743	0.245
877	0.426	832	0.165	787	0.572	742	0.249
876	0.285	831	0.151	786	2.452	741	0.276

740	0.288	695	0.369	650	0.344	605	0.206
739	1.298	694	0.381	649	0.176	604	0.371
738	0.280	693	0.405	648	0.204	603	0.898
737	0.344	692	8.513	647	0.506	602	0.334
736	0.405	691	0.582	646	0.244	601	0.393
735	0.418	690	0.384	645	0.280	600	0.412
734	0.329	689	0.367	644	0.295	599	0.593
733	0.256	688	0.486	643	0.236	598	2.452
732	2.466	687	0.492	642	0.318	597	0.269
731	0.319	686	0.382	641	0.284	596	0.937
730	0.185	685	0.394	640	0.217	595	1.003
729	0.205	684	0.495	639	0.270	594	0.137
728	0.233	683	3.459	638	0.261	593	0.154
727	2.137	682	0.425	637	0.267	592	0.182
726	0.532	681	0.570	636	0.457	591	0.200
725	0.366	680	2.794	635	0.288	590	0.339
724	0.336	679	0.676	634	0.313	589	0.401
723	0.576	678	0.742	633	0.403	588	0.164
722	0.476	677	0.613	632	0.567	587	5.053
721	0.658	676	0.299	631	0.307	586	0.789
720	0.657	675	0.316	630	0.301	585	0.606
719	0.455	674	0.312	629	0.376	584	0.734
718	0.435	673	0.394	628	0.496	583	0.568
717	0.468	672	0.410	627	0.386	582	0.537
716	0.596	671	0.392	626	0.587	581	0.578
715	0.416	670	0.302	625	1.461	580	0.722
714	0.392	669	0.199	624	0.489	579	2.276
713	0.691	668	0.149	623	0.430	578	0.447
712	0.540	667	0.133	622	0.482	577	0.713
711	0.464	666	0.158	621	0.461	576	0.276
710	1.664	665	0.114	620	0.518	575	1.012
709	0.363	664	0.309	619	0.471	574	0.347
708	0.390	663	0.439	618	0.473	573	0.772
707	0.259	662	0.648	617	0.405	572	0.503
706	0.446	661	0.631	616	0.409	571	0.457
705	0.504	660	0.423	615	0.458	570	0.395
704	0.456	659	0.604	614	2.936	569	0.361
703	0.334	658	0.597	613	0.825	568	0.145
702	0.317	657	0.889	612	0.723	567	0.136
701	0.278	656	3.220	611	2.776	566	0.151
700	0.385	655	0.496	610	0.414	565	0.854
699	0.377	654	0.463	609	0.427	564	0.403
698	0.434	653	0.369	608	0.451	563	0.624
697	0.320	652	0.415	607	0.468	562	0.432
696	0.366	651	0.422	606	0.334	561	0.597

560	0.651	515	0.604	470	0.377	425	0.711
559	1.003	514	0.795	469	0.365	424	0.239
558	0.272	513	0.666	468	0.348	423	0.262
557	0.202	512	1.402	467	0.211	422	0.143
556	0.277	511	0.682	466	0.213	421	0.162
555	0.486	510	0.378	465	0.207	420	0.154
554	0.376	509	0.339	464	0.660	419	0.292
553	0.306	508	0.231	463	0.204	418	0.183
552	0.276	507	0.491	462	0.227	417	0.338
551	0.248	506	0.350	461	0.354	416	0.434
550	0.386	505	0.433	460	0.361	415	0.369
549	0.493	504	0.280	459	0.473	414	0.505
548	0.493	503	0.597	458	2.853	413	0.659
547	0.470	502	0.630	457	0.998	412	0.629
546	0.696	501	0.672	456	0.371	411	1.984
545	0.396	500	1.055	455	0.874	410	2.351
544	0.613	499	3.396	454	1.869	409	3.892
543	0.331	498	0.366	453	0.744	408	3.729
542	0.242	497	0.515	452	0.561	407	0.703
541	0.621	496	0.312	451	0.115	406	0.621
540	1.275	495	0.352	450	0.135	405	0.425
539	1.089	494	0.368	449	0.142	404	1.341
538	0.305	493	0.926	448	0.204	403	4.815
537	0.120	492	1.383	447	0.138	402	2.208
536	0.278	491	1.057	446	0.199	401	1.438
535	0.303	490	0.709	445	0.115	400	2.346
534	0.276	489	0.438	444	0.100	399	5.676
533	0.364	488	1.512	443	0.243		END
532	0.329	487	0.533	442	0.146		
531	2.318	486	0.910	441	0.126		
530	0.612	485	4.100	440	0.164		
529	0.493	484	1.416	439	0.116		
528	0.312	483	0.185	438	1.207		
527	0.387	482	0.180	437	0.157		
526	0.424	481	0.137	436	0.110		
525	0.354	480	0.188	435	0.136		
524	0.167	479	0.177	434	0.175		
523	0.139	478	0.208	433	0.157		
522	0.141	477	0.115	432	0.177		
521	0.209	476	0.145	431	0.196		
520	0.517	475	0.350	430	0.297		
519	0.233	474	0.820	429	0.323		
518	0.249	473	0.403	428	0.322		
517	4.105	472	0.469	427	0.319		
516	0.788	471	0.489	426	0.229		

Appendix 5 - AMS Radiocarbon Dates Obtained. Calibration using Calib (Stuiver and Reimer, 1993a and b) Rev 5.0.1, IntCal04.14c curve (Reimer *et al*, 2004) and Marine04.14c curve (Hughen *et al*, 2004). Shell sample dated at IsoTrace Laboratory, University of Toronto, Department of Physics, 60 St. George Street, Toronto, Ontario, Canada M5S 1A7, Tel: (416) 978-2258 All others dated at Beta Analytic, Inc., 4985 S.W. 74th Court, Miami, FL, 33155, USA, Tel: (01) 305-667-5167.

Dated Specimen	Details	Sample ID	Measured Radiocarbon Age and Delta $^{13}C/^{12}C$ (‰)	Conventional Radiocarbon Age (years BP)	Calibration	Calibrated Calendar Age (years BP)
Mya truncata (Linnaeus, 1758) valve	Found on ancient beach above present lake level	TO-7929	---	7160 ± 80	Marine04 **One Sigma Ranges:** [7555 BP:7706 BP] 1 **Two Sigma Ranges:** [7481 BP:7798 BP] 1	7630.5 7639.5
Dryas sp. (L.) leaf	Core E, Drive 4, 18cm depth (347cm absolute core depth)	Beta-146688	5810 ± 40 -29.7	5730 ± 40	IntCal04 **One Sigma Ranges:** [6453 BP:6459 BP] 0.036521 [6463 BP:6566 BP] 0.893284 [6590 BP:6601 BP] 0.070194 **Two Sigma Ranges:** [6414 BP:6419 BP] 0.00782 [6424 BP:6425 BP] 0.002945 [6436 BP:6637 BP] 0.989235	6514.5 6536.5
Plant fibers, mosses, Chironomidae head capsules Acid/alkali/acid pretreatment	Core T, Drive 1, 34-35cm depth (89-90cm absolute depth) 2cm level With additional material from T1 archive, B1, and B1 archive	Beta-242790	4580 ± 40 -23.9	4600 ± 40	IntCal04 **One Sigma Ranges:** [5148 BP:5151 BP] 0.019683 [5289 BP:5326 BP] 0.462994 [5388 BP:5393 BP] 0.024965 [5398 BP:5446 BP] 0.492358 **Two Sigma Ranges:** [5067 BP:5110 BP] 0.074387 [5122 BP:5168 BP] 0.086958 [5173 BP:5181 BP] 0.00435 [5274 BP:5334 BP] 0.368277 [5345 BP:5466 BP] 0.466028	5422 5405.5
Plant fibers, mosses, Chironomidae head capsules Acid/alkali/acid pretreatment	Core T, Drive 6, 17-20cm depth (303-306cm absolute depth) 3cm level	Beta-240752	5870 ± 40 -25.2	5870 ± 40	IntCal04 **One Sigma Ranges:** 6656 BP:6738 BP 1 **Two Sigma Ranges:** 6567 BP:6588 BP 0.031803 6603 BP:6610 BP 0.007539 6616 BP:6788 BP 0.960658	6697 6702

Dated Specimen	Details	Sample ID	Measured Radiocarbon Age and Delta $^{13}C/^{12}C$ (‰)	Conventional Radiocarbon Age (years BP)	Calibration	Calibrated Calendar Age (years BP)
Plant fibers, mosses, Chironomidae head capsules Acid/alkali/acid pretreatment	Core T, Drive 6, 43-46.5cm depth (329-332.5cm absolute depth) 3.5cm level	Beta-236401	5940 ± 40 -29.8	5860 ± 40	IntCal04 **One Sigma Ranges:** [6643 BP:6731 BP] 1 **Two Sigma Ranges:** [6562 BP:6594 BP] 0.063805 [6596 BP:6756 BP] 0.908828 [6762 BP:6779 BP] 0.027366	6687 6676
Plant fibers, mosses, Chironomidae head capsules Acid/alkali/acid pretreatment	Core T, Drive 6, 67-69cm depth (353-355cm absolute depth) 2cm level	Beta-235291	5970 ± 40 -28.5	5910 ± 40	IntCal04 **One Sigma Ranges:** [6674 BP:6752 BP] 0.867621 [6764 BP:6777 BP] 0.132379 **Two Sigma Ranges:** [6645 BP:6646 BP] 0.001016 [6651 BP:6801 BP] 0.94957 [6814 BP:6847 BP] 0.049414	6713 6726
Plant fibers, mosses, Chironomidae head capsules Acid/alkali/acid pretreatment	Core T, Drive 7, 24-28cm depth (394-398cm absolute depth) 4cm level	Beta-236402	6200 ± 50 -26.2	6180 ± 50	IntCal04 **One Sigma Ranges:** [7008 BP:7130 BP] 0.866962 [7142 BP:7162 BP] 0.133038 **Two Sigma Ranges:** [6948 BP:7179 BP] 0.938932 [7195 BP:7243 BP] 0.061068	7069 7063.5
Plant fibers, mosses, Chironomidae head capsules Acid/alkali/acid pretreatment	Core T, Drive 8, 14-17cm depth (478-481cm) 3cm level	Beta-235292	6510 ± 40 -25.4	6500 ± 40	IntCal04 **One Sigma Ranges:** [7332 BP:7355 BP] 0.235571 [7372 BP:7389 BP] 0.133555 [7415 BP:7461 BP] 0.630874 **Two Sigma Ranges:** [7319 BP:7483 BP] 1	7438 7401